



Calhoun: The NPS Institutional Archive
DSpace Repository

NPS Scholarship

Theses

2005-09

Performance analysis of variable code rate
signals transmitted over
frequency-nonselctive, slowly fading
channels in a pulse-interference environment

Shih, Wan-Chun

Monterey, CA; Naval Postgraduate School

<https://hdl.handle.net/10945/2090>

Downloaded from NPS Archive: Calhoun



Calhoun is the Naval Postgraduate School's public access digital repository for research materials and institutional publications created by the NPS community. Calhoun is named for Professor of Mathematics Guy K. Calhoun, NPS's first appointed -- and published -- scholarly author.

Dudley Knox Library / Naval Postgraduate School
411 Dyer Road / 1 University Circle
Monterey, California USA 93943

<http://www.nps.edu/library>



**NAVAL
POSTGRADUATE
SCHOOL**

MONTEREY, CALIFORNIA

THESIS

**PERFORMANCE ANALYSIS OF VARIABLE CODE RATE
SIGNALS TRANSMITTED OVER FREQUENCY-
NONSELECTIVE, SLOWLY FADING CHANNELS IN A
PULSE-INTERFERENCE ENVIRONMENT**

by

Wan-Chun Shih

September 2005

Thesis Advisor:

Second Reader:

Clark Robertson

Frank Kragh

Approved for public release, distribution is unlimited

THIS PAGE INTENTIONALLY LEFT BLANK

REPORT DOCUMENTATION PAGE			<i>Form Approved OMB No. 0704-0188</i>
Public reporting burden for this collection of information is estimated to average 1 hour per response, including the time for reviewing instruction, searching existing data sources, gathering and maintaining the data needed, and completing and reviewing the collection of information. Send comments regarding this burden estimate or any other aspect of this collection of information, including suggestions for reducing this burden, to Washington headquarters Services, Directorate for Information Operations and Reports, 1215 Jefferson Davis Highway, Suite 1204, Arlington, VA 22202-4302, and to the Office of Management and Budget, Paperwork Reduction Project (0704-0188) Washington DC 20503.			
1. AGENCY USE ONLY (Leave blank)	2. REPORT DATE September 2005	3. REPORT TYPE AND DATES COVERED Master's Thesis	
4. TITLE AND SUBTITLE: Performance Analysis of Variable Code Rate Signals Transmitted over Frequency-Nonselective, Slowly Fading Channels in a Pulse-Interference Environment			5. FUNDING NUMBERS
6. AUTHOR(S) Wan-Chun Shih			
7. PERFORMING ORGANIZATION NAME(S) AND ADDRESS(ES) Naval Postgraduate School Monterey, CA 93943-5000			8. PERFORMING ORGANIZATION REPORT NUMBER
9. SPONSORING /MONITORING AGENCY NAME(S) AND ADDRESS(ES) N/A			10. SPONSORING/MONITORING AGENCY REPORT NUMBER
11. SUPPLEMENTARY NOTES The views expressed in this thesis are those of the author and do not reflect the official policy or position of the Department of Defense or the U.S. Government.			
12a. DISTRIBUTION / AVAILABILITY STATEMENT Approved for public release, distribution is unlimited			12b. DISTRIBUTION CODE
13. ABSTRACT (maximum 200 words) Wireless systems, including wireless local area networks (WLAN) and cellular networks, are increasingly being used for both commercial and military applications. For military applications, it is important to analyze the effect of interference on wireless communications systems. The objective of this research is to investigate the performance of variable code rate signals transmitted over frequency-nonselective, slowly fading channels in a worst case, pulse-noise interference environment. Both binary phase-shift keying (BPSK) and noncoherently detected binary frequency-shift keying (NCBFSK) are considered. System performance with both Viterbi hard decision decoding (HDD) and soft decision decoding (SDD) is analyzed for additive white Gaussian noise (AWGN) alone and for AWGN plus pulse-noise interference for various receiver types and conditions of channel fading. The effect of varying the code rate, both for HDD and SDD, is examined. The amplitude of the signal power a_c^2 is modeled as a random variable, and the channel is modeled as either Rayleigh fading or Ricean fading, depending on the modulation under consideration.			
14. SUBJECT TERMS WLAN, BPSK, NCBFSK, Hard Decision Decoding, Soft Decision Decoding, FEC, Convolutional Code, Rayleigh Fading, Ricean Fading, Pulse-Noise Interference, Noise-Normalization			15. NUMBER OF PAGES 117
			16. PRICE CODE
17. SECURITY CLASSIFICATION OF REPORT Unclassified	18. SECURITY CLASSIFICATION OF THIS PAGE Unclassified	19. SECURITY CLASSIFICATION OF ABSTRACT Unclassified	20. LIMITATION OF ABSTRACT UL

THIS PAGE INTENTIONALLY LEFT BLANK

Approved for public release, distribution is unlimited

**PERFORMANCE ANALYSIS OF VARIABLE CODE RATE SIGNALS
TRANSMITTED OVER FREQUENCY-NONSELECTIVE, SLOWLY FADING
CHANNELS IN A PULSE-INTERFERENCE ENVIRONMENT**

Wan-Chun Shih
Captain, Taiwan Army
B.S.E.E., Taiwan National Defense University Chung Cheng Institute of Technology, 1998

Submitted in partial fulfillment of the
requirements for the degree of

MASTER OF SCIENCE IN ELECTRICAL ENGINEERING

from the

**NAVAL POSTGRADUATE SCHOOL
September 2005**

Author: Wan Chun Shih

Approved by: Clark Robertson
Thesis Advisor

Frank Kragh
Second Reader

Jeffrey B. Knorr
Chairman, Department of Electrical and Computer Engineering

THIS PAGE INTENTIONALLY LEFT BLANK

ABSTRACT

Wireless systems, including wireless local area networks (WLAN) and cellular networks, are increasingly being used for both commercial and military applications. For military applications, it is important to analyze the effect of interference on wireless communications systems. The objective of this research is to investigate the performance of variable code rate signals transmitted over frequency-nonselctive, slowly fading channels in a worst case, pulse-noise interference environment. Both binary phase-shift keying (BPSK) and noncoherently detected binary frequency-shift keying (NCBFSK) are considered. System performance with both Viterbi hard decision decoding (HDD) and soft decision decoding (SDD) is analyzed for additive white Gaussian noise (AWGN) alone and for AWGN plus pulse-noise interference for various receiver types and conditions of channel fading. The effect of varying the code rate, both for HDD and SDD, is examined. The amplitude of the signal power a_c^2 is modeled as a random variable, and the channel is modeled as either Rayleigh fading or Ricean fading, depending on the modulation under consideration.

THIS PAGE INTENTIONALLY LEFT BLANK

TABLE OF CONTENTS

I.	INTRODUCTION.....	1
	A. BACKGROUND	1
	B. OBJECTIVE	1
	C. RELATED RESEARCH.....	1
	D. THESIS ORGANIZATION.....	2
II.	PERFORMANCE OF BPSK IN AN AWGN ENVIRONMENT	3
	A. INTRODUCTION.....	3
	B. FORWARD ERROR CORRECTION CODING	3
	C. BPSK IN AWGN WITHOUT FADING	4
	1. Without Forward Error Correction Coding	4
	2. With FEC – Using Convolutional Codes	5
	a. <i>Hard Decision Decoding.....</i>	<i>6</i>
	b. <i>Soft Decision Decoding.....</i>	<i>10</i>
	D. DESCRIPTION OF MULTIPATH FADING CHANNELS.....	13
	1. The Ricean Fading Channel.....	14
	2. The Rayleigh Fading Channel	15
	3. Average Probability of Bit Error.....	15
	E. BPSK IN AWGN IN A FADING ENVIRONMENT.....	16
	1. Without Forward Error Correction Coding	16
	2. With FEC Coding and HDD	17
	3. With FEC Coding and SDD	23
	F. CHAPTER SUMMARY.....	29
III.	PERFORMANCE OF BPSK IN AN PULSE-NOISE INTERFERENCE ENVIRONMENT.....	31
	A. INTRODUCTION.....	31
	B. PULSE-NOISE INTERFERENCE	31
	C. WITH CONVOLUTIONAL CODING AND HDD	32
	1. Without Fading	32
	2. With Rayleigh Fading and Continuous Jamming.....	37
	D. WITH CONVOLUTIONAL CODING AND SDD.....	38
	1. Using a Linear Combining Receiver in a Non-Fading Channel....	38
	2. Using a Linear Combining Receiver in a Rayleigh Fading.....	44
	3. Using a Noise-Normalized Receiver in a Non-Fading Channel....	45
	E. CHAPTER CONCLUSION.....	51
IV.	PERFORMANCE OF NCBFSK IN AN AWGN ENVIRONMENT	53
	A. INTRODUCTION.....	53
	B. NCBFSK IN AWGN WITHOUT FADING	53
	1. Without Forward Error Correction Coding	53
	2. With FEC – Using Convolutional Codes	54
	a. <i>Hard Decision Decoding.....</i>	<i>54</i>

	<i>b. Soft Decision Decoding</i>	57
C.	NCBFSK IN AWGN IN A FADING ENVIRONMENT	60
	1. Without FEC Coding.....	60
	2. With FEC Coding and HDD	61
	3. With FEC Coding and SDD.....	67
D.	CHAPTER SUMMARY.....	73
V.	PERFORMANCE OF NCBFSK IN AN PULSE-NOISE INTERFERENCE ENVIRONMENT.....	75
	A. INTRODUCTION.....	75
	B. WITH CONVOLUTIONAL CODING AND HDD.....	75
	1. Without Fading	75
	2. With Rayleigh Fading and Continuous Jamming ($\rho = 1$).....	80
	C. WITH CONVOLUTIONAL CODING AND SDD COMBINED WITH A LINEAR COMBINING RECEIVER.....	81
	1. Using a Linear Combining Receiver in a Non-Fading Channel....	81
	2. Using a Linear Combining Receiver in a Rayleigh Fading Channel.....	86
	3. Using a Noise-Normalized Receiver in a Non-Fading Channel....	88
	D. CHAPTER CONCLUSION.....	93
VI.	CONCLUSIONS	95
	A. INTRODUCTION.....	95
	B. FINDINGS.....	95
	C. FUTURE WORK.....	96
	LIST OF REFERENCES.....	97
	INITIAL DISTRIBUTION LIST	99

LIST OF FIGURES

Figure 1.	A simple communication system model.....	4
Figure 2.	BPSK without FEC coding.....	5
Figure 3.	BPSK HDD with $r = 1/3$ and different values of constraint length.....	8
Figure 4.	BPSK HDD with $r = 1/2$ and different values of constraint length.....	8
Figure 5.	BPSK HDD with $r = 2/3$ and different values of constraint length.....	9
Figure 6.	BPSK HDD with $r = 3/4$ and different values of constraint length.....	9
Figure 7.	BPSK SDD with $r = 1/3$ and different values of constraint length.....	11
Figure 8.	BPSK SDD with $r = 1/2$ and different values of constraint length.....	11
Figure 9.	BPSK SDD with $r = 2/3$ and different values of constraint length.....	12
Figure 10.	BPSK SDD with $r = 3/4$ and different values of constraint length.....	12
Figure 11.	BPSK without FEC.....	17
Figure 12.	BPSK with FEC and HDD when $r = 1/3$	18
Figure 13.	BPSK with FEC and HDD when $r = 1/2$	19
Figure 14.	BPSK with FEC and HDD when $r = 2/3$	20
Figure 15.	BPSK with FEC and HDD when $r = 3/4$	21
Figure 16.	BPSK with FEC and SDD when $r = 1/3$	23
Figure 17.	BPSK with FEC and SDD when $r = 1/2$	24
Figure 18.	BPSK with FEC and SDD when $r = 2/3$	25
Figure 19.	BPSK with FEC and SDD when $r = 3/4$	26
Figure 20.	BPSK with FEC and HDD when $r = 1/3$ in a jammed channel.....	33
Figure 21.	BPSK with FEC and HDD when $r = 1/2$ in a jammed channel.....	34
Figure 22.	BPSK with FEC and HDD when $r = 2/3$ in a jammed channel.....	35
Figure 23.	BPSK with FEC and HDD when $r = 3/4$ in a jammed channel.....	36
Figure 24.	BPSK with FEC and HDD in a jammed channel with Rayleigh fading.....	38
Figure 25.	BPSK with FEC and SDD using a linear combining receiver when $r = 1/3$...40	40
Figure 26.	BPSK with FEC and SDD using a linear combining receiver when $r = 1/2$...41	41
Figure 27.	BPSK with FEC and SDD using a linear combining receiver when $r = 2/3$...42	42
Figure 28.	BPSK with FEC and SDD using a linear combining receiver when $r = 3/4$...43	43
Figure 29.	BPSK with FEC and SDD using a linear combining receiver in Rayleigh fading.....	45
Figure 30.	BPSK with FEC and SDD using a noise-normalized receiver when $r = 1/3$...47	47
Figure 31.	BPSK with FEC and SDD using a noise-normalized receiver when $r = 1/2$...48	48
Figure 32.	BPSK with FEC and SDD using a noise-normalized receiver when $r = 2/3$...49	49
Figure 33.	BPSK with FEC and SDD using a noise-normalized receiver when $r = 3/4$...50	50
Figure 34.	NCBFSK without FEC coding.....	53
Figure 35.	NCBFSK HDD with $r = 1/3$ and different values of constraint length.....	54
Figure 36.	NCBFSK HDD with $r = 1/2$ and different values of constraint length.....	55
Figure 37.	NCBFSK HDD with $r = 2/3$ and different values of constraint length.....	55
Figure 38.	NCBFSK HDD with $r = 3/4$ and different values of constraint length.....	56
Figure 39.	NCBFSK SDD with $r = 1/3$ and different values of constraint length.....	58
Figure 40.	NCBFSK SDD with $r = 1/2$ and different values of constraint length.....	58

Figure 41.	NCBFSK SDD with $r = 2/3$ and different values of constraint length.	59
Figure 42.	NCBFSK SDD with $r = 3/4$ and different values of constraint length.	59
Figure 43.	NCBFSK without FEC.	61
Figure 44.	NCBFSK with FEC and HDD when $r = 1/3$	62
Figure 45.	NCBFSK with FEC and HDD when $r = 1/2$	63
Figure 46.	NCBFSK with FEC and HDD when $r = 2/3$	64
Figure 47.	NCBFSK with FEC and HDD when $r = 3/4$	65
Figure 48.	NCBFSK with FEC and SDD when $r = 1/3$	68
Figure 49.	NCBFSK with FEC and SDD when $r = 1/2$	69
Figure 50.	NCBFSK with FEC and SDD when $r = 2/3$	70
Figure 51.	NCBFSK with FEC and SDD when $r = 3/4$	71
Figure 52.	NCBFSK with FEC and HDD when $r = 1/3$ in a jammed channel.	77
Figure 53.	NCBFSK with FEC and HDD when $r = 1/2$ in a jammed channel.	78
Figure 54.	NCBFSK with FEC and HDD when $r = 2/3$ in a jammed channel.	79
Figure 55.	NCBFSK with FEC and HDD when $r = 3/4$ in a jammed channel.	80
Figure 56.	NCBFSK with FEC and HDD in a jammed channel with Rayleigh fading.	81
Figure 57.	NCBFSK with FEC and SDD combined with linear combining receiver when $r = 1/3$	83
Figure 58.	NCBFSK with FEC and SDD combined with linear combining receiver when $r = 1/2$	84
Figure 59.	NCBFSK with FEC and SDD combined with linear combining receiver when $r = 2/3$	85
Figure 60.	NCBFSK with FEC and SDD combined with linear combining receiver when $r = 3/4$	86
Figure 61.	NCBFSK with FEC and SDD combined with linear combining receiver in Rayleigh fading.	87
Figure 62.	NCBFSK with FEC and SDD combined with noise-normalized receiver when $r = 1/3$	89
Figure 63.	NCBFSK with FEC and SDD combined with noise-normalized receiver when $r = 1/2$	90
Figure 64.	NCBFSK with FEC and SDD combined with noise-normalized receiver when $r = 2/3$	91
Figure 65.	NCBFSK with FEC and SDD combined with noise-normalized receiver when $r = 3/4$	92

LIST OF TABLES

Table 1.	Information weight structures for $r = 1/3$ and $r = 1/2$. [11].....	6
Table 2.	Information weight structures for $r = 2/3$ and $r = 3/4$. [11].....	7
Table 3.	Summary of coding gains for BPSK HDD.....	10
Table 4.	Summary of coding gains for BPSK SDD.....	13
Table 5.	Summary of coding gains for BPSK HDD with $r = 1/3$ in fading environment.....	18
Table 6.	Summary of coding gains for BPSK HDD with $r = 1/2$ in fading environment.....	19
Table 7.	Summary of coding gains for BPSK HDD with $r = 2/3$ in fading environment.....	20
Table 8.	Summary of coding gains for BPSK HDD with $r = 3/4$ in fading environment.....	21
Table 9.	Summary of coding gains for BPSK HDD in Rayleigh fading.....	22
Table 10.	Summary of coding gains for BPSK HDD in Ricean fading with $\zeta = 10$	22
Table 11.	Summary of coding gains for BPSK HDD in Ricean fading with $\zeta = 20$	22
Table 12.	Summary of coding gains for BPSK SDD with $r = 1/3$ in fading environment.....	24
Table 13.	Summary of coding gains for BPSK SDD with $r = 1/2$ in fading environment.....	25
Table 14.	Summary of coding gains for BPSK SDD with $r = 2/3$ in fading environment.....	26
Table 15.	Summary of coding gains for BPSK SDD with $r = 3/4$ in fading environment.....	27
Table 16.	Summary of coding gains for BPSK SDD in Rayleigh fading.....	27
Table 17.	Summary of coding gains for BPSK SDD in Ricean fading with $\zeta = 10$	28
Table 18.	Summary of coding gains for BPSK SDD in Ricean fading with $\zeta = 20$	28
Table 19.	Summary of coding gains for NCBFSK HDD.....	56
Table 20.	Summary of coding gains for NCBFSK SDD.....	60
Table 21.	Summary of coding gains for NCBFSK HDD with $r = 1/3$ in fading environment.....	63
Table 22.	Summary of coding gains for NCBFSK HDD with $r = 1/2$ in fading environment.....	64
Table 23.	Summary of coding gains for NCBFSK HDD with $r = 2/3$ in fading environment.....	65
Table 24.	Summary of coding gains for NCBFSK HDD with $r = 3/4$ in fading environment.....	66
Table 25.	Summary of coding gains for NCBFSK HDD in Rayleigh fading.....	66
Table 26.	Summary of coding gains for NCBFSK HDD in Ricean fading with $\zeta = 10$	66

Table 27.	Summary of coding gains for NCBFSK HDD in Ricean fading with $\zeta = 20$	67
Table 28.	Summary of coding gains for NCBFSK SDD with $r = 1/3$ in fading environment.	68
Table 29.	Summary of coding gains for NCBFSK SDD with $r = 1/2$ in fading environment.	69
Table 30.	Summary of coding gains for NCBFSK SDD with $r = 2/3$ in fading environment.	70
Table 31.	Summary of coding gains for NCBFSK SDD with $r = 3/4$ in fading environment.	71
Table 32.	Summary of coding gains for NCBFSK SDD in Rayleigh fading.	72
Table 33.	Summary of coding gains for NCBFSK SDD in Ricean fading with $\zeta = 10$	72
Table 34.	Summary of coding gains for NCBFSK SDD in Ricean fading with $\zeta = 20$	72

ACKNOWLEDGMENTS

First and foremost, I would like to express my sincere appreciation to my advisor Professor Clark Robertson. This thesis would not have been completed without his initial ideas, continuous guidance and in depth explanations. Also, I would like to thank my second reader Professor Frank Kragh for his clear teaching and assistance.

I also want to thank my American sponsor Randyll Fernandez and Greek friend Spyridon Dessalermos for their friendship and helping me get through both courses and overseas life. Besides, I would like to thank Hannah Kriewaldt, Beth Summe, Barbara Young and Francy Maring for their encouragement and for helping me with my English in my American life.

Finally, I want to thank my family for their support and my country for providing this opportunity for me to pursue my postgraduate studies at the Naval Postgraduate School.

THIS PAGE INTENTIONALLY LEFT BLANK

EXECUTIVE SUMMARY

Wireless local area networks and cellular networks are increasingly being used for commercial and military applications. Wireless communications over multipath fading channels are increasingly important, especially for military operations, where the various wireless communication signals can suffer from fading due to multipath or/and from pulse-noise interference, either benign or hostile. The objective of this thesis is to investigate the performance of variable code rate signals transmitted over frequency-nonselective, slowly fading channels in a worst case, pulse-noise interference environment.

The performance of BPSK and NCBFSK in an AWGN only environment are examined in Chapters II and IV, respectively. Both non-coded and convolutionally coded signals transmitted over different types of channels (non-fading, Ricean fading, and Rayleigh fading) combined with either hard or soft decision Viterbi decoding are examined. Comparing the coding gains, we conclude that the performance of communications improves as the code rates decreases and/or as the number of memory elements increases. The exception is a NCBFSK modulated signal transmitted over a non-fading channel, where the optimum code rate is $r = 1/2$. In addition, for a non-fading channel, the coding gain obtained by implementing SDD is higher than that obtained by implementing HDD for the same conditions.

The performance of BPSK and NCBFSK in an AWGN plus pulse-noise interference environment are examined in Chapters III and V, respectively. A signal which is affected by multipath fading and jammed by the enemy is assumed. The results for the probability of bit error for BPSK and NCBFSK modulated signals encoded with different code rates and number of memory elements, transmitted over either a non-fading or a Rayleigh fading channel, jammed with fixed duty cycles, and decoded with either hard or soft Viterbi decision algorithms are analytically determined and plotted. The signal-to-interference ratio (SIR) vs. signal-to-noise ratio (E_b/N_o) at the threshold probability of bit error of 10^{-5} are plotted to visualize the areas of successful and

unsuccessful communication. The analysis of the soft Viterbi decision algorithm in a non-fading channel case involved two types of receivers: the linear combining receiver and the noise-normalized receiver. When using a linear combining receiver, the interference with $\rho = 0.01$ is the most efficient regardless of the number of memory elements. However, when using a noise-normalized receiver, the best performance is obtained from interference with $\rho = 0.01$ and the worst is obtained when ρ approaches one. In other words, the use of a noise-normalized receiver negates the effect of the pulse-noise interference.

I. INTRODUCTION

A. BACKGROUND

Wireless systems, including wireless local area networks (WLAN) and cellular networks, are increasingly being used for both commercial and military applications. Also, wireless communications over multipath fading channels are increasingly important, especially for military operations, which take place in many different types of environments, and the various wireless communication signals can suffer from fading due to multipath or/and from pulse-noise interference, either benign or hostile. Therefore, it is important to analyze the effect of interference and fading on wireless communications systems.

B. OBJECTIVE

The objective of this research is to investigate the performance of variable code rate signals transmitted over frequency-nonselctive, slowly fading channels in a worst case, pulse-noise interference environment. The interference signal is assumed to be turned on and off systematically (i.e., pulsed) with constant mean power, which makes the instantaneous interference power inversely proportional to the interference duty cycle. Both binary phase-shift keying (BPSK) and noncoherently detected binary frequency-shift keying (NCBFSK) are considered. System performance with both Viterbi hard decision decoding (HDD) and soft decision decoding (SDD) is analyzed, first in presence of additive white Gaussian noise (AWGN) alone and then in the presence of AWGN plus pulse-noise interference for various receiver types and conditions of channel fading. The amplitude of the signal power a_c^2 is modeled as a random variable, and the channel is modeled as either Rayleigh fading or Ricean fading, depending on the modulation under consideration.

C. RELATED RESEARCH

A number of works have dealt with the performance of coherent receivers under different environments. The performance of the signal combined with FEC and SDD transmitted over a frequency-selective, Nakagami fading channel with AWGN and non-fading interference was investigated in [1]. Then this work was extended in [2] which examined the performance of the signal transmitted over a Nakagami fading channel with

AWGN and interference for a range of fading conditions. Also, the performance of the *IEEE 802.11a* standard optimum and sub-optimum receiver in Nakagami fading channels with AWGN plus pulse-noise interference is examined in [3]. The performance of WLAN PSK signals transmitted over a Ricean fading channel with AWGN and interference (both non-fading and fading cases) was investigated in [4].

In this thesis, both coherent and noncoherent modulations are considered, and a number of different parameters are taken into account. A signal which is affected by multipath fading and jammed by the enemy is assumed. The results of probability of bit error (P_b) for BPSK and NCBFSK modulated signals encoded with different code rates and number of memory elements and transmitted over either a Ricean or a Rayleigh fading channel, jammed with different duty cycles, and decoded with hard or soft Viterbi decision algorithms are analytically determined and plotted. Also, for the case when interference is present, the signal-to-interference ratio (SIR) vs. signal-to-noise ratio (E_b/N_o) at the threshold P_b of 10^{-5} are plotted to visualize the areas of successful and unsuccessful communication. The results for the different circumstances are then compared.

D. THESIS ORGANIZATION

This thesis is divided into six chapters. After this introduction, the performance of BPSK in an AWGN only environment is evaluated in Chapter II. Both non-coded and convolutionally coded signals transmitted over different types of channels (non-fading, Ricean, and Rayleigh fading) combined with either hard or soft decision Viterbi decoding are examined. The performance of BPSK in an AWGN plus noise-like pulse interference environment is evaluated in Chapter III. The same coded signals as in Chapter II, transmitted over non-fading and Rayleigh fading channels are examined. For hard decision decoding, the effects of pulse-noise interference with fixed pulse-noise interference as well as worst case are explored. For soft decision decoding, both the linear combining and noise-normalized receivers are evaluated. In Chapters IV and V, instead of BPSK demodulation, NCBFSK for the same conditions as Chapters II and III are investigated. Finally, in Chapter VI the results are summarized with some recommendations for further research.

II. PERFORMANCE OF BPSK IN AN AWGN ENVIRONMENT

A. INTRODUCTION

The performance of a BPSK modulated signal in an AWGN environment transmitted over different types of channels is examined in this chapter. First, the case of no fading is examined and next, the effect of Ricean and Rayleigh fading channels. In all cases, the signals are coded prior to transmission with a convolutional code. In this thesis, we examine convolutional codes with different code rates and different constraint lengths. Prior to the analysis of different communication schemes, some important concepts related to forward error correction coding and multipath fading channels are introduced.

B. FORWARD ERROR CORRECTION CODING

Reliability is a primary concern in digital communications. It is measured in terms of probability of bit error (P_b). Usually for data communications, the P_b is required to be approximately 10^{-5} . This is the target P_b throughout this thesis. In many cases, due to high levels of AWGN, jamming or multipath fading, the P_b can be large. As a result, FEC is necessary to obtain a reliable communication link. With FEC, redundancy is added to the transmitted signal by inserting extra bits. By exploiting this redundancy at the receiver, it is then possible to detect and correct errors. The specific codes analyzed in this thesis are convolutional codes. For these codes, the encoding process involves the convolution of the data bits with the impulse response of the encoder. As a result of this process, n bits are transmitted from the encoder for every k data bits, where $n > k$. The code rate is defined as $r = k/n$. Convolutional codes are further characterized by the constraint length ν , which for practical reasons, can vary from three to nine depending on the structure of the encoder. As a general rule, increasing the constraint length decreases the P_b , but the tradeoff is that the complexity of the decoder increases exponentially as ν increases. Convolutional codes are designed to correct random errors. In an environment where the errors are bursty such as multipath fading environments, an interleaver must be used as shown in Figure 1. The interleaver is a device that mixes up the channel symbols so that sequential channel symbols are separated during transmission.

The Viterbi algorithm is the most popular decoding technique for convolutional codes. The decoding algorithm works by computing the various path metrics through the convolutional code trellis and choosing the sequence corresponding to the path with the best metric. There are two types of decoding, hard and soft decision decoding. Hard decision decoding implies that the demodulator makes a decision regarding what coded bit was received on a bit-by-bit basis prior to the decoding operation. Soft decision decoding implies that the decoder utilizes the analog outputs of the demodulator matched filters. Generally, soft decision decoding is more effective than hard decision decoding. True soft decision decoding requires no quantization (i.e., infinite quantization) of the matched filter outputs, but realistically the quantization is finite. This results in a slight degradation in performance. Nevertheless, it has been found that an 8-level quantization matched filter output is almost as good as when the matched filter output is un-quantized. For the purposes of this thesis, soft decision decoding with infinite quantization is considered. [5]

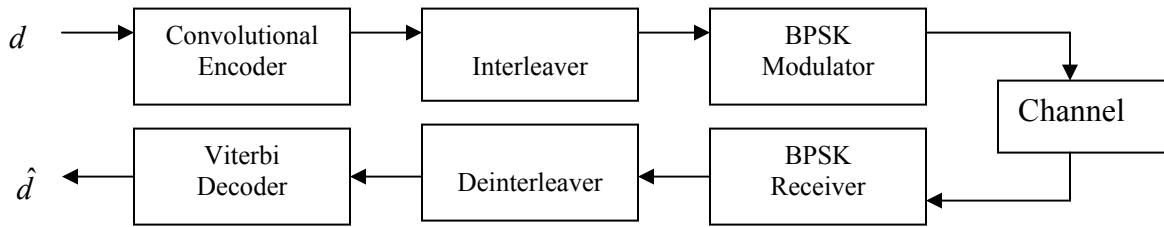


Figure 1. A simple communication system model.

C. BPSK IN AWGN WITHOUT FADING

1. Without Forward Error Correction Coding

The performance of a BPSK modulated signal transmitted over a channel with AWGN and no fading is examined first. When FEC coding is not used, the probability of bit error is given by [6]

$$P_b = Q\left(\sqrt{\frac{2E_b}{N_o}}\right) \quad (2.1)$$

where $Q(\bullet)$ is the Q-function, defined as

$$Q(z) = \frac{1}{2\pi} \int_z^\infty \exp\left(\frac{-\lambda^2}{2}\right) d\lambda \quad (2.2)$$

E_b is the average energy per bit, N_o is the one-sided noise power spectral density, and E_b/N_o is the signal-to-noise ratio. The performance of BPSK in an AWGN environment without fading or FEC coding is illustrated in Figure 2.

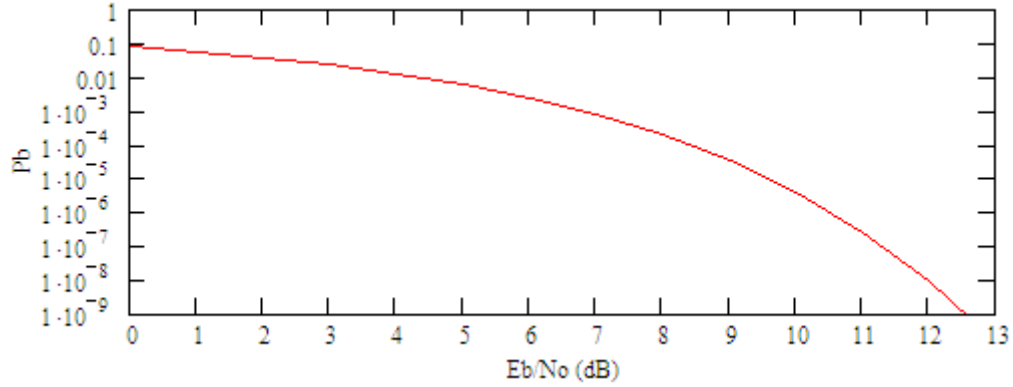


Figure 2. BPSK without FEC coding.

2. With FEC – Using Convolutional Codes

In order to determine performance when the signal is encoded with a convolutional code, it is necessary to specify the code rate, the constraint length of the code, and if the decoder uses hard or soft decision decoding.

With convolutional coding, the probability of bit error is upper-bounded by

$$P_b < \frac{1}{k} \sum_{d=d_{free}}^{\infty} B_d P_d \quad (2.3)$$

where d_{free} is the free distance of the code, the weight of the minimum-weight code sequence of any length produced by a nonzero information sequence, B_d is the total information weight of all code sequences of weight d and represents all possible bit errors that can occur when all-zero sequence is transmitted, and P_d is the probability of selecting a code sequence that differs from the correct sequence in d bits. [5]

a. Hard Decision Decoding

First, consider hard decision decoding (HDD). For hard decision decoding, the probability of selecting a code sequence that differs from the correct sequence in d bits is given by

$$P_d = \sum_{i=\frac{d+1}{2}}^d \binom{d}{i} p_e^i (1-p_e)^{d-i} \quad \text{when } d \text{ is odd}$$

$$P_d = \sum_{i=\frac{d}{2}+1}^d \binom{d}{i} p_e^i (1-p_e)^{d-i} + \frac{1}{2} \binom{d}{\frac{d}{2}} p_e^{\frac{d}{2}} (1-p_e)^{\frac{d}{2}} \quad \text{when } d \text{ is even}$$
(2.4)

where p_e is the probability of coded bit error, which is given by the P_b appropriate to the modulation type with the substitution $E_b/N_o \rightarrow r E_b/N_o$. For BPSK,

$$p_e = Q\left(\sqrt{\frac{2rE_b}{N_o}}\right).$$
(2.5)

Table 1 lists the information weight structure (B_d) for the best (maximum free distance) rate $r=1/3$ and $r=1/2$ convolutional codes.

Table 1. Information weight structures for $r=1/3$ and $r=1/2$. [11]

Rate	Constraint Length	d_{free}	$B_{d_{free}}$	$B_{d_{free}+1}$	$B_{d_{free}+2}$	$B_{d_{free}+3}$	$B_{d_{free}+4}$	$B_{d_{free}+5}$	$B_{d_{free}+6}$	$B_{d_{free}+7}$
$\frac{1}{3}$	$\nu=3$	8	3	0	15	0	58	0	201	0
	$\nu=5$	12	12	0	12	0	56	0	320	0
	$\nu=7$	15	7	8	22	44	22	0	0	0
$\frac{1}{2}$	$\nu=3$	5	1	4	12	32	80	192	448	1024
	$\nu=5$	7	4	12	20	72	225	500	1324	3680
	$\nu=7$	10	36	0	211	0	1404	0	11633	0
	$\nu=9$	12	33	0	281	0	2179	0	15035	0

Table 2 lists the information weight structure for the best rate $r = 2/3$ and $r = 3/4$ convolutional codes.

Table 2. Information weight structures for $r = 2/3$ and $r = 3/4$. [11]

Rate	Constraint Length	d_{free}	$B_{d_{free}}$	$B_{d_{free}+1}$	$B_{d_{free}+2}$	$B_{d_{free}+3}$	$B_{d_{free}+4}$
$\frac{2}{3}$	$K = 2$	3	1	10	54	226	853
	$K = 4$	5	25	112	357	1858	8406
	$K = 6$	6	1	81	402	1487	6793
	$K = 8$	8	97	0	2863	0	56633
$\frac{3}{4}$	$K = 2$	3	15	104	540	2520	11048
	$K = 4$	4	22	0	1687	0	66964
	$K = 6$	6	919	0	31137	0	1142571
	$K = 8$	6	12	342	1996	12296	78145

For rate $1/n$ codes (i.e., when $k = 1$) implemented with K memory elements, the constraint length of the code is $\nu = K + 1$.

The probabilities of bit error of BPSK for different convolutional encoders in an AWGN environment without interference or fading are illustrated in Figures 3, 4, 5, and 6.

The performance obtained by a convolutional encoder with a code rate of $1/3$ and for $K = 2$, $K = 4$, and $K = 6$ memory elements is illustrated in Figure 3. From this figure, we conclude that in order to get the target performance of 10^{-5} , the required E_b/N_o for the three different cases ($\nu = 3, \nu = 5$, and $\nu = 7$) are 8.3, 7, and 5.9 dB, respectively. Without FEC coding, the required $E_b/N_o = 9.6$ dB, and the resulting coding gains for the three cases are 1.3, 2.6, and 3.7 dB, respectively.

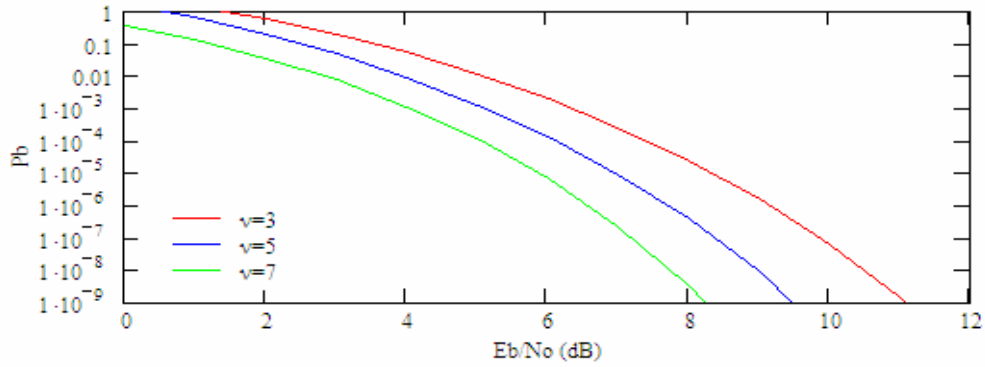


Figure 3. BPSK HDD with $r = 1/3$ and different values of constraint length.

The performance obtained by a convolutional encoder with a code rate of $1/2$ and for $K = 2$, $K = 4$, $K = 6$, and $K = 8$ memory elements is illustrated in Figure 4. From this figure, the required E_b / N_o for the four different cases ($\nu = 3, \nu = 5, \nu = 7$, and $\nu = 9$) are 8.1, 7.2, 6.5, and 5.8 dB, respectively, and the resulting coding gains for the four cases are 1.5, 2.4, 3.1, and 3.8 dB, respectively.

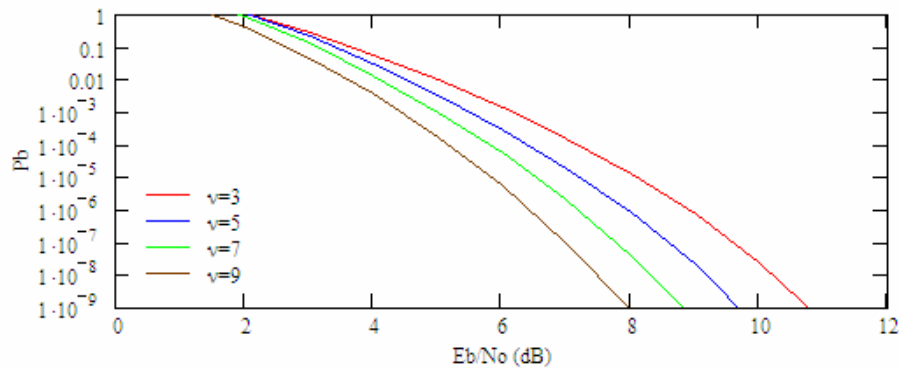


Figure 4. BPSK HDD with $r = 1/2$ and different values of constraint length.

The performance obtained by a convolutional encoder with a code rate of $2/3$ and for $K = 2$, $K = 4$, $K = 6$, and $K = 8$ memory elements is illustrated in Figure 5. Here, the required E_b / N_o for the four different cases are 8.8, 7.8, 6.9, and 6.5 dB, respectively, and the resulting coding gains for the four cases are 0.8, 1.8, 2.7, and 3.1 dB, respectively.

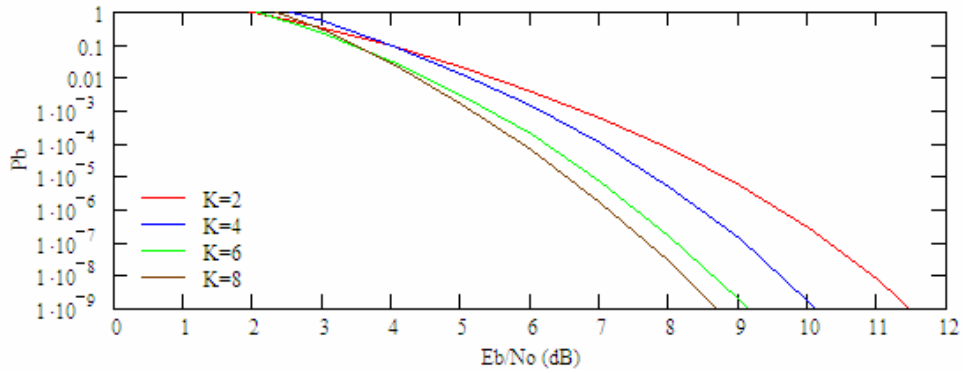


Figure 5. BPSK HDD with $r = 2/3$ and different values of constraint length.

The performance obtained by a convolutional encoder with a code rate of $3/4$ and for $K = 2$, $K = 4$, $K = 6$, and $K = 8$ memory elements is illustrated in Figure 6. Here, the required E_b/N_o for the four different cases are 9, 8.4, 7.7, and 6.8 dB, respectively, and the resulting coding gains for the four cases are 0.6, 1.2, 2.2, and 2.8 dB, respectively.

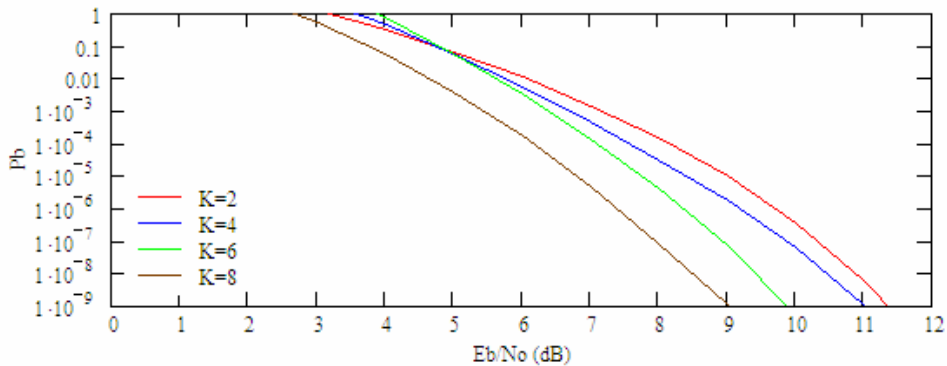


Figure 6. BPSK HDD with $r = 3/4$ and different values of constraint length.

The coding gains for BPSK with convolutional coding and HDD for several different combinations of code rates and number of memory elements are summarized in Table 3.

Table 3. Summary of coding gains for BPSK HDD.

	$K = 2$	$K = 4$	$K = 6$	$K = 8$
$r = 1/3$	1.3 dB	2.6 dB	3.7 dB	N/A
$r = 1/2$	1.5 dB	2.4 dB	3.1 dB	3.8 dB
$r = 2/3$	0.8 dB	1.8 dB	2.7 dB	3.1 dB
$r = 3/4$	0.6 dB	1.2 dB	2.2 dB	2.8 dB

From Table 3, we conclude that for a fixed code rate, the coding gain increases as the number of memory elements in the encoder increases. For a fixed number of memory elements, the coding gain increases as the code rate decreases expect for the case of $K = 2$.

b. Soft Decision Decoding

For soft decision decoding (SDD), P_d is given by

$$P_d = Q\left(\sqrt{2rd \frac{E_b}{N_o}}\right). \quad (2.6)$$

The probabilities of bit error of BPSK for different convolutional encoders in an AWGN environment without interference or fading are illustrated in Figures 7, 8, 9, and 10.

The performance obtained with a convolutional encoder with a code rate of $1/3$ and for $K = 2$, $K = 4$, and $K = 6$ memory elements is illustrated in Figure 7. From this figure, the required E_b/N_o for the three different cases ($\nu = 3$, $\nu = 5$, and $\nu = 7$) are 6, 4.6, and 3.8 dB, respectively, and the resulting coding gains for the three cases are 3.6, 5, and 5.8 dB, respectively.

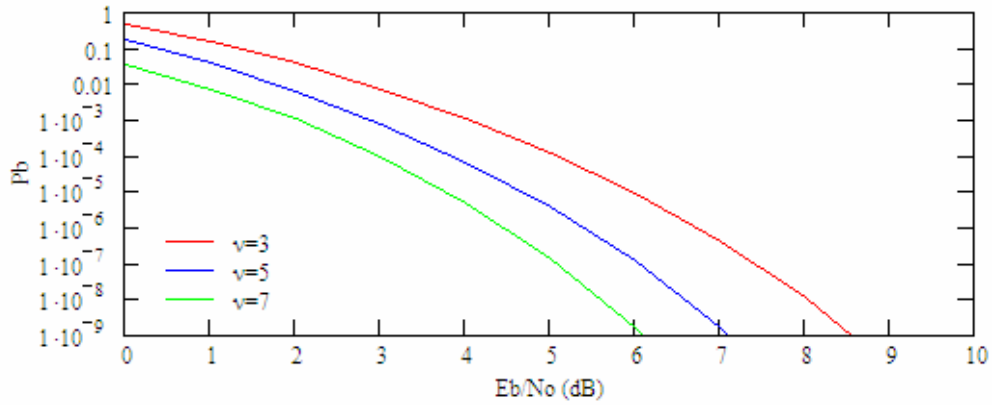


Figure 7. BPSK SDD with $r = 1/3$ and different values of constraint length.

The performance obtained with a convolutional encoder with a code rate of $1/2$ and for $K = 2$, $K = 4$, $K = 6$, and $K = 8$ memory elements is illustrated in Figure 8. Here, the required E_b / N_o for the four different cases ($\nu = 3, \nu = 5, \nu = 7$, and $\nu = 9$) are 5.9, 5, 4.2, and 3.5 dB, respectively, and the resulting coding gains are 3.7, 4.6, 5.4, and 6.1 dB, respectively.

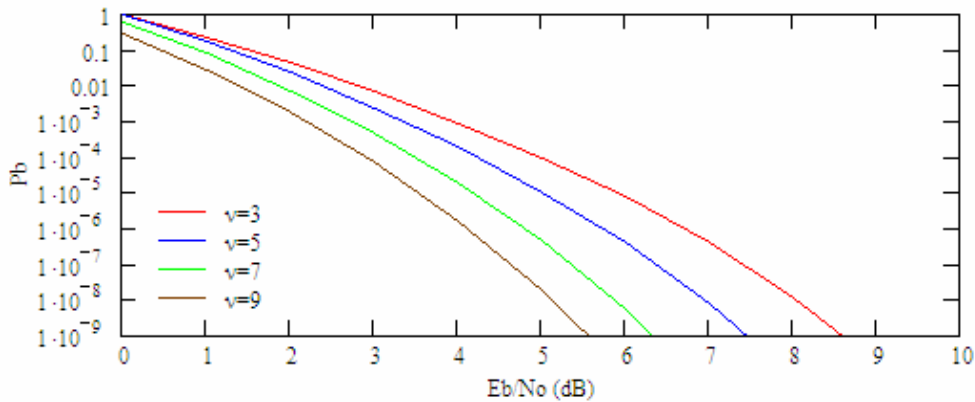


Figure 8. BPSK SDD with $r = 1/2$ and different values of constraint length.

The performance obtained with a convolutional encoder with a code rate of $2/3$ and for $K = 2$, $K = 4$, $K = 6$, and $K = 8$ memory elements is illustrated in Figure 9. Here, the required E_b / N_o for the four different cases are 6.4, 5.5, 4.6, and 4.1 dB, respectively, and the resulting coding gains are 3.2, 4.1, 5, and 5.5 dB, respectively.

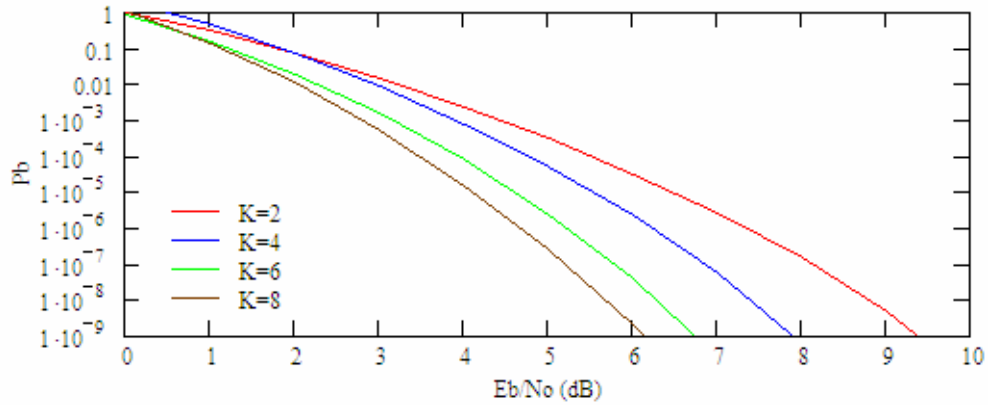


Figure 9. BPSK SDD with $r = 2/3$ and different values of constraint length.

The performance obtained with a convolutional encoder with a code rate of $3/4$ and for $K = 2$, $K = 4$, $K = 6$, and $K = 8$ memory elements is illustrated in Figure 10. Here, the required E_b/N_o for the four different cases are 6.8, 5.7, 5.2, and 4.4 dB, respectively, and the resulting coding gains are 2.8, 3.9, 4.4, and 5.2 dB, respectively.

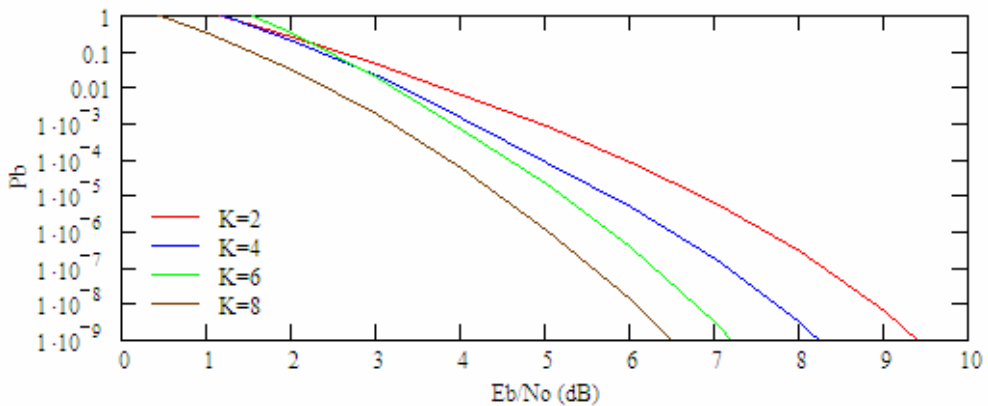


Figure 10. BPSK SDD with $r = 3/4$ and different values of constraint length.

The coding gains for BPSK with convolutional coding and SDD for several different combinations of code rates and number of memory elements are summarized in Table 4.

Table 4. Summary of coding gains for BPSK SDD.

	$K = 2$	$K = 4$	$K = 6$	$K = 8$
$r = 1/3$	3.6 dB	5 dB	5.8 dB	N/A
$r = 1/2$	3.7 dB	4.6 dB	5.4 dB	6.1 dB
$r = 2/3$	3.2 dB	4.1 dB	5 dB	5.5 dB
$r = 3/4$	2.8 dB	3.9 dB	4.4 dB	5.2 dB

From Table 4, we see that for BPSK, the coding gain obtained with SDD has the same general trend as that obtained with HDD: for a fixed code rate, the coding gain increases as the number of memory elements in the encoder increases; for a fixed number of memory elements, the coding gain increases as the code rate decreases.

A comparison of Tables 3 and 4 finds that the coding gain is 2.1 to 2.3 dB less if HDD is used instead of SDD.

D. DESCRIPTION OF MULTIPATH FADING CHANNELS

In wireless communications, the signal is carried by electromagnetic waves. In many cases, the electromagnetic waves reach the receiver through different paths. Destructive interference as a result of multipath propagation can create severe fading in the channel. Fading is caused by the interference of two or more components of the transmitted signal arriving at the receiver at different times and through different paths. The resultant received signal can vary widely in amplitude and phase. The number of paths and the attenuation and propagation delay associated with each of these paths differ from one multipath channel to another in an unpredictable manner, so the multipath fading channel is modeled as a random process.

An important characteristic of the fading channel is that its frequency response is not flat over the bandwidth of the signal. Another characteristic is the time variation of the channel transfer function due to the possible motion of either the receiver or the transmitter. Consequently, a multipath channel is a time-varying channel. As a result, a signal transmitted over a fading channel is distorted both in the time and frequency

domains. Thus, a fading channel is characterized by two parameters, one for its time variations and the other for its frequency variations. [7]

A multipath fading channel can be characterized by comparing the parameters of the channel to characteristics of the communication signal, specifically, the signal's bandwidth and symbol duration.

Channel frequency variations are characterized by the coherent bandwidth $(\Delta f)_c$ of the channel. These variations cause the transmitted signal to experience either flat or frequency selective fading. If the channel has a constant gain and linear phase response over a bandwidth (BW) , which is greater than the bandwidth of the transmitted signal (i.e., $(\Delta f)_c > BW$), the channel is said to be frequency-nonselective or flat fading. On the other hand, if $(\Delta f)_c < BW$, significant distortion of the signal occurs, and the channel is said to be frequency-selective. [7]

Channel time variations are characterized by the coherence time $(\Delta t)_c$. Depending on how rapidly the transmitted signal changes as compared to the rate of change of the channel, a channel may be classified either as a fast fading or slow fading channel. If the symbol duration (T_s) is smaller than the coherence time (i.e., $(\Delta t)_c > T_s$), then the received amplitude and phase are effectively constant for the duration of at least one symbol, and the channel is said to be slowly fading. On the other hand, if $(\Delta t)_c < T_s$, the channel is said to be fast fading. [7]

The Ricean and Rayleigh fading channels are the two widely used models of fading channels.

1. The Ricean Fading Channel

The Ricean model is used to describe a multipath fading channel in which there is a line-of-sight (LOS) between transmitter and receiver, and some part of the received signal power is also due to multipath. A general representation of a passband signal is

$$s(t) = \sqrt{2}a_c \cos[2\pi f_i(t)t + \theta(t)]. \quad (2.7)$$

For Ricean fading, the amplitude $\sqrt{2}a_c$ is modeled as a Ricean random variable with probability density function (pdf)

$$f_{A_c}(a_c) = \frac{a_c}{\sigma^2} \exp\left[\frac{-(a_c^2 + \alpha^2)}{2\sigma^2}\right] I_0\left(\frac{\alpha a_c}{\sigma^2}\right) u(a_c) \quad (2.8)$$

where α^2 is the power of the LOS signal, $2\sigma^2$ is the power of the multipath components, $\alpha^2 + 2\sigma^2 = \overline{a_c^2} = E(a_c^2)$ is the average received signal power, $I_0(\bullet)$ is the modified Bessel function of the first kind of order zero, and $u(a_c)$ is the unit step function.

An important parameter for fading channels is the ratio of direct-to-diffuse signal power:

$$\zeta = \frac{\alpha^2}{2\sigma^2}. \quad (2.9)$$

This parameter characterizes the strength of the multipath.

2. The Rayleigh Fading Channel

The Rayleigh model is used to describe a multipath fading channel in which there is no LOS direct path between transmitter and receiver, so all the received signal power is due to multipath. This type of channel is a special case of the Ricean fading channel where $\zeta = 0$.

The stronger the multipath, the smaller ζ , and $\zeta \rightarrow 0$ (no LOS) corresponds to Rayleigh fading. When $\zeta \rightarrow \infty$ (only LOS), there is no fading.

For Rayleigh fading, there is no LOS, so $\alpha = 0$ and

$$f_{A_c}(a_c) = \frac{a_c}{\sigma^2} \exp\left[\frac{-a_c^2}{2\sigma^2}\right] u(a_c). \quad (2.10)$$

Communication performance is better for Ricean fading than for Rayleigh.

3. Average Probability of Bit Error

In the case of multipath fading environments, the average probability of bit error is the focal point, which is obtained by recognizing that $P_b(a_c)$ is a function of the

random variable a_c , and the average probability of bit error is the expected value of $P_b(a_c)$:

$$P_b = \int_0^{\infty} P_b(a_c) f_{A_c}(a_c) da_c. \quad (2.11)$$

E. BPSK IN AWGN IN A FADING ENVIRONMENT

1. Without Forward Error Correction Coding

Using equation (2.11) for a Ricean fading channel and BPSK modulation, it can be shown that the average probability of bit error is given by [8]

$$P_b \approx \frac{1}{2\sqrt{\pi c}} \left[\frac{\zeta + 1}{\frac{E_b}{N_o} + \zeta + 1} \right] \exp \left[\frac{-\zeta \frac{E_b}{N_o}}{\frac{E_b}{N_o} + \zeta + 1} \right] \quad (2.12)$$

where $c = 1 + 0.1\zeta$ for $\zeta \leq 10$ and $c = 2$ for $\zeta > 10$.

For Rayleigh fading channel, the average probability of bit error is given by [7]

$$P_b = \frac{1}{2} \left(1 - \sqrt{\frac{\frac{E_b}{N_o}}{1 + \frac{E_b}{N_o}}} \right). \quad (2.13)$$

Figure 11 is obtained by using (2.12) and (2.13), which shows the probability of bit error for BPSK in an AWGN without FEC coding and for different fading environments (i.e., for different values of ζ). From Figure 11, we conclude that the effect of fading on performance is very severe as ζ gets smaller. The results of the analysis show that in a non-fading environment, the required E_b/N_o is 9.6 dB, while for Ricean channels with $\zeta = 20$ and 10, the required E_b/N_o are 12.6 and 17 dB, respectively. As for Rayleigh fading, the required E_b/N_o jumps to the 44.5 dB! The need for FEC coding in a fading environment is evident.

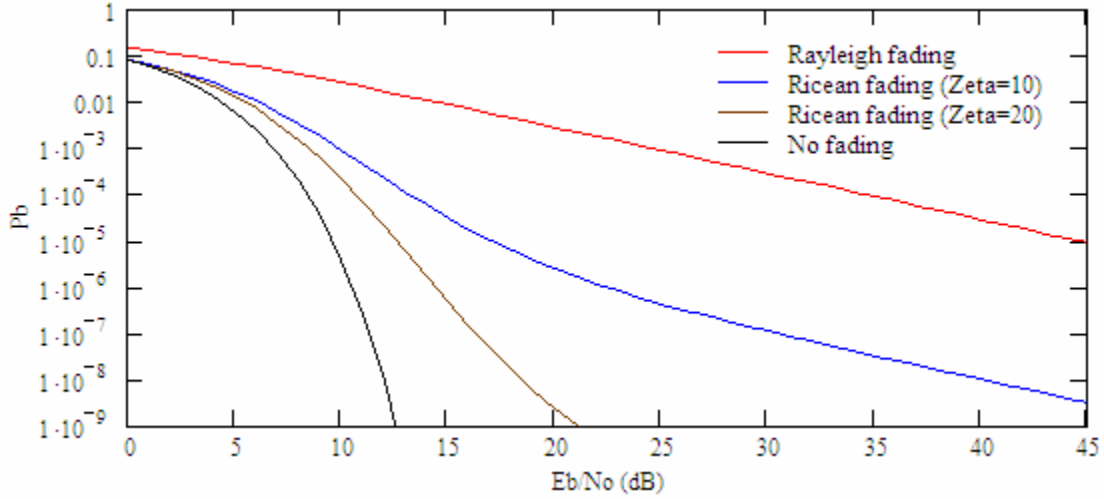


Figure 11. BPSK without FEC.

2. With FEC Coding and HDD

The performance of BPSK when using convolutional coding and implementing HDD is determined in this section. The probability of bit error is upper-bounded by (2.3), where P_d is given by (2.4), and p_e is the probability of coded bit error obtained by replacing $E_b/N_o \rightarrow r E_b/N_o$ in (2.12) and (2.13).

The probabilities of bit error of BPSK for different convolutional encoders in an AWGN environment with Rayleigh and Ricean fading are illustrated in Figures 12, 13, 14, and 15.

The performance obtained with a convolutional encoder for a code rate of 1/3 and constraint lengths $\nu=3$, $\nu=5$, and $\nu=7$ is illustrated in Figure 12. Three different fading environment cases are examined in this chapter: Rayleigh fading ($\zeta = 0$) and Ricean fading with $\zeta = 10$ and $\zeta = 20$.

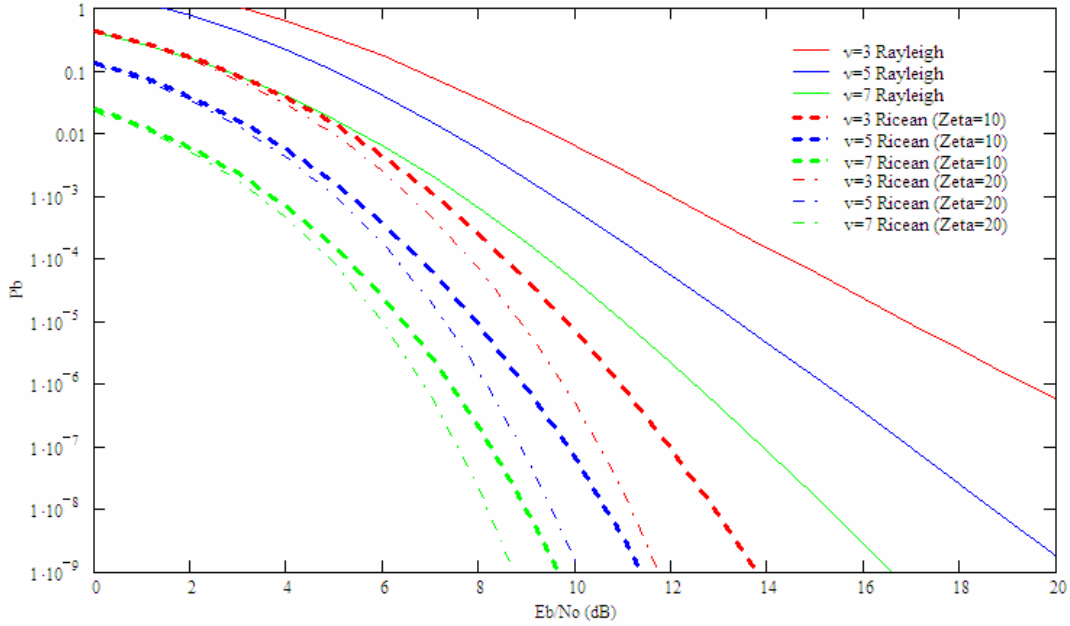


Figure 12. BPSK with FEC and HDD when $r = 1/3$.

From Figure 12, we can determine the E_b / N_o required to achieve the target P_b of 10^{-5} . For the three different cases ($\nu = 3, \nu = 5$, and $\nu = 7$) and Rayleigh fading, the required E_b / N_o is 16.9, 13.4, and 11 dB, respectively; for Ricean fading with $\zeta = 10$, the required E_b / N_o is 9.8, 7.9, and 6.4 dB, respectively; for Ricean fading with $\zeta = 20$, the required E_b / N_o is 8.8, 7.3, and 6 dB, respectively. The resulting coding gains are shown in Table 5.

Table 5. Summary of coding gains for BPSK HDD with $r = 1/3$ in fading environment.

	$K = 2$	$K = 4$	$K = 6$
Rayleigh fading	27.6 dB	31.1 dB	33.5 dB
Ricean fading $\zeta = 10$	7.2 dB	9.1 dB	10.6 dB
Ricean fading $\zeta = 20$	3.8 dB	5.3 dB	6.6 dB

The performance obtained with a convolutional encoder for a code rate of 1/2 and constraint lengths $\nu = 3$, $\nu = 5$, $\nu = 7$, and $\nu = 9$ is illustrated in Figure 13.

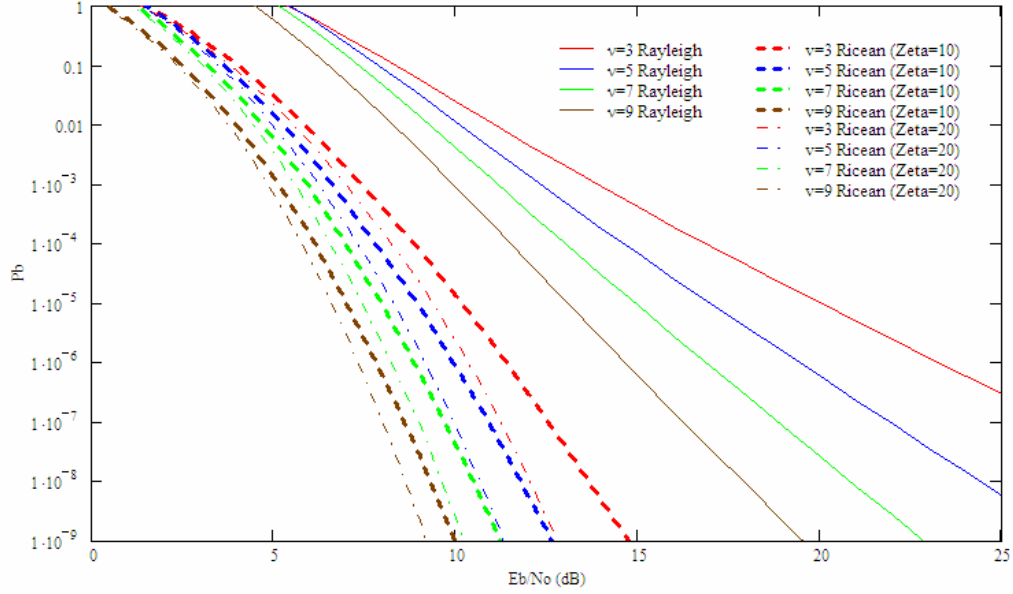


Figure 13. BPSK with FEC and HDD when $r = 1/2$.

Here, the required E_b/N_o for the four different cases ($\nu = 3, \nu = 5, \nu = 7$, and $\nu = 9$) and Rayleigh fading is 20.2, 17, 14.9, and 13.1 dB, respectively; for Ricean fading with $\zeta = 10$, the required E_b/N_o is 10.2, 8.9, 7.9, and 7 dB, respectively; for Ricean fading with $\zeta = 20$, the required E_b/N_o is 9.4, 8.2, 7.4, and 6.6 dB, respectively. The resulting coding gains are shown in Table 6.

Table 6. Summary of coding gains for BPSK HDD with $r = 1/2$ in fading environment.

	$K = 2$	$K = 4$	$K = 6$	$K = 8$
Rayleigh fading	24.3 dB	27.5 dB	29.6 dB	31.4 dB
Ricean fading $\zeta = 10$	6.8 dB	8.1 dB	9.1 dB	10 dB
Ricean fading $\zeta = 20$	3.2 dB	4.4 dB	5.2 dB	6 dB

The performance obtained with a convolutional encoder for a code rate of $2/3$ and memory elements $K = 2$, $K = 4$, $K = 6$, and $K = 8$ is illustrated in Figure 14.

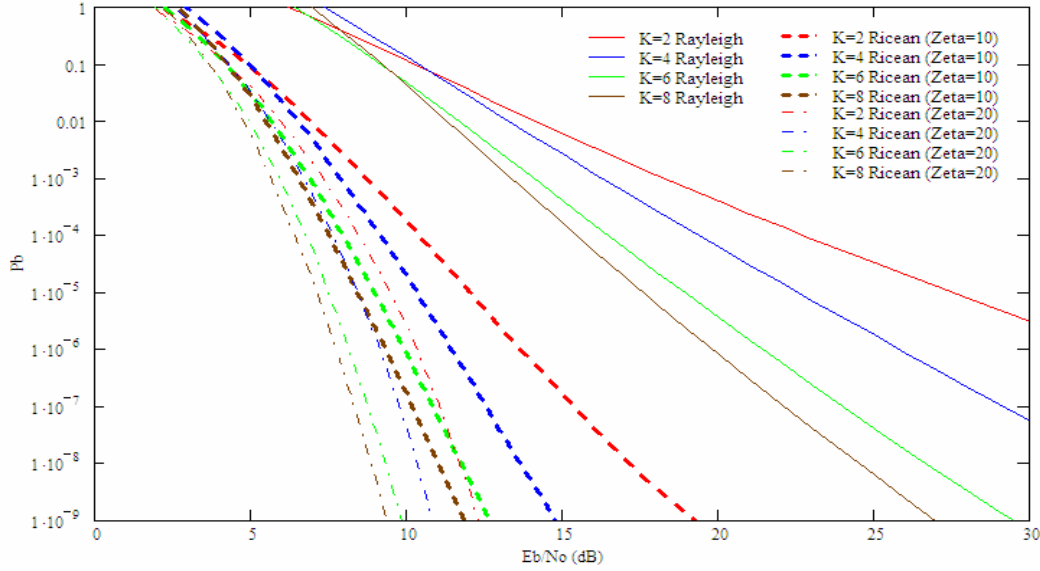


Figure 14. BPSK with FEC and HDD when $r = 2/3$.

Here, the required E_b / N_o for the four different cases ($K = 2$, $K = 4$, $K = 6$, and $K = 8$) and Rayleigh fading is 27.4, 22.5, 18.9, and 17.6 dB, respectively; for Ricean fading with $\zeta = 10$, the required E_b / N_o is 12, 10.3, 8.9, and 8.4 dB, respectively; for Ricean fading with $\zeta = 20$, the required E_b / N_o is 9.4, 8.4, 7.5, and 7.1 dB, respectively. The resulting coding gains are shown in Table 7.

Table 7. Summary of coding gains for BPSK HDD with $r = 2/3$ in fading environment.

	$K = 2$	$K = 4$	$K = 6$	$K = 8$
Rayleigh fading	17.1 dB	22 dB	25.6 dB	26.9 dB
Ricean fading $\zeta = 10$	5 dB	6.7 dB	8.1 dB	8.6 dB
Ricean fading $\zeta = 20$	3.2 dB	4.2 dB	5.1 dB	5.5 dB

The performance obtained with a convolutional encoder for a code rate of $3/4$ and memory elements $K = 2$, $K = 4$, $K = 6$, and $K = 8$ is illustrated in Figure 15.

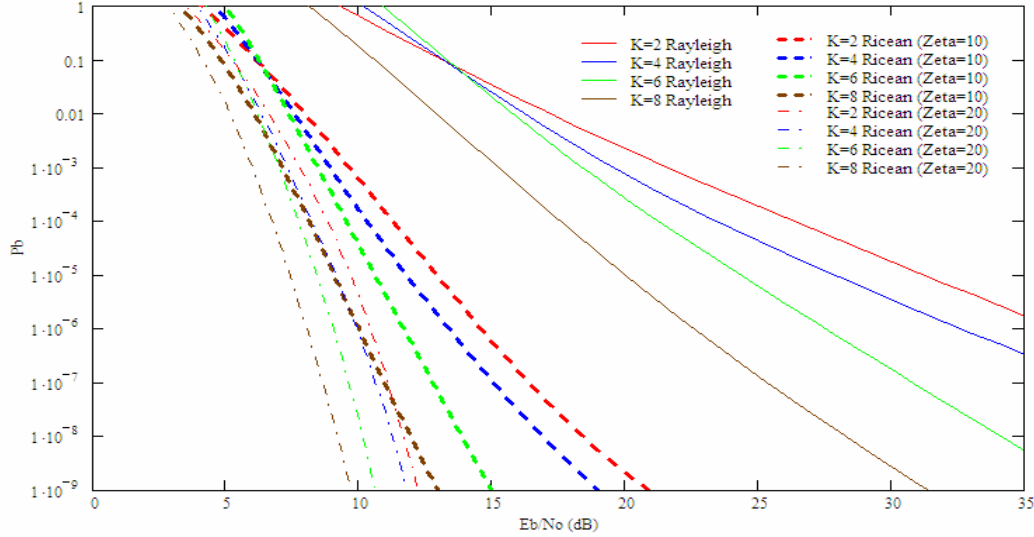


Figure 15. BPSK with FEC and HDD when $r = 3/4$.

Here, the required E_b / N_o for the four different cases ($K = 2$, $K = 4$, $K = 6$, and $K = 8$) and Rayleigh fading is 31.2, 27.9, 24.2, and 20 dB, respectively; for Ricean fading with $\zeta = 10$, the required E_b / N_o is 12.9, 11.7, 10.6, and 9.1 dB, respectively; for Ricean fading with $\zeta = 20$, the required E_b / N_o is 9.7, 9.1, 8.4, and 7.4 dB, respectively. The resulting coding gains are shown in Table 8.

Table 8. Summary of coding gains for BPSK HDD with $r = 3/4$ in fading environment.

	$K = 2$	$K = 4$	$K = 6$	$K = 8$
Rayleigh fading	13.3 dB	16.6 dB	20.3 dB	24.5 dB
Ricean fading $\zeta = 10$	4.1 dB	5.3 dB	6.4 dB	7.9 dB
Ricean fading $\zeta = 20$	2.9 dB	3.5 dB	4.2 dB	5.2 dB

The coding gains obtained with BPSK and HDD for different code rates and for the three different fading cases being examined are shown in Tables 9, 10, and 11.

Table 9. Summary of coding gains for BPSK HDD in Rayleigh fading.

	$K = 2$	$K = 4$	$K = 6$	$K = 8$
$r = 1/3$	27.6 dB	31.1 dB	33.5 dB	N/A
$r = 1/2$	24.3 dB	27.5 dB	29.6 dB	31.4 dB
$r = 2/3$	17.1 dB	22 dB	25.6 dB	26.9 dB
$r = 3/4$	13.3 dB	16.6 dB	20.3 dB	24.5 dB

Table 10. Summary of coding gains for BPSK HDD in Ricean fading with $\zeta = 10$.

	$K = 2$	$K = 4$	$K = 6$	$K = 8$
$r = 1/3$	7.2 dB	9.1 dB	10.6 dB	N/A
$r = 1/2$	6.8 dB	8.1 dB	9.1 dB	10 dB
$r = 2/3$	5 dB	6.7 dB	8.1 dB	8.6 dB
$r = 3/4$	4.1 dB	5.3 dB	6.4 dB	7.9 dB

Table 11. Summary of coding gains for BPSK HDD in Ricean fading with $\zeta = 20$.

	$K = 2$	$K = 4$	$K = 6$	$K = 8$
$r = 1/3$	3.8 dB	5.3 dB	6.6 dB	N/A
$r = 1/2$	3.2 dB	4.4 dB	5.2 dB	6 dB
$r = 2/3$	3.2 dB	4.2 dB	5.1 dB	5.5 dB
$r = 3/4$	2.9 dB	3.5 dB	4.2 dB	5.2 dB

From Tables 9, 10, and 11, it is then possible to conclude that for BPSK with HDD in fading channels, the coding gain increases as the number of memory element

increases or as the code rate decreases. The more severe the fading, the greater the coding gain achieved for a given code rate and number of memory elements.

3. With FEC Coding and SDD

The performance of BPSK with convolutional coding and SDD is determined in this section. The probability of bit error is upper-bounded by (2.3), where P_d is given by [8]

$$P_d \approx \frac{1}{2\sqrt{\pi rc}} \left[\frac{2(1+\zeta)}{2(1+\zeta)+r\frac{E_b}{N_o}} \right]^d \exp \left[\frac{-\zeta dr \frac{E_b}{N_o}}{2(1+\zeta)+r\frac{E_b}{N_o}} \right] \quad (2.14)$$

where $c = 1 + 0.1\zeta$ for $\zeta \leq 10$ and $c = 2$ for $\zeta > 10$.

The probabilities of bit error of BPSK for different convolutional encoders in an AWGN environment with Rayleigh and Rician fading are illustrated in Figures 16, 17, 18, and 19.

The performance obtained with a convolutional encoder for a code rate of 1/3 and constraint lengths $\nu = 3$, $\nu = 5$, and $\nu = 7$ is illustrated in Figure 16.

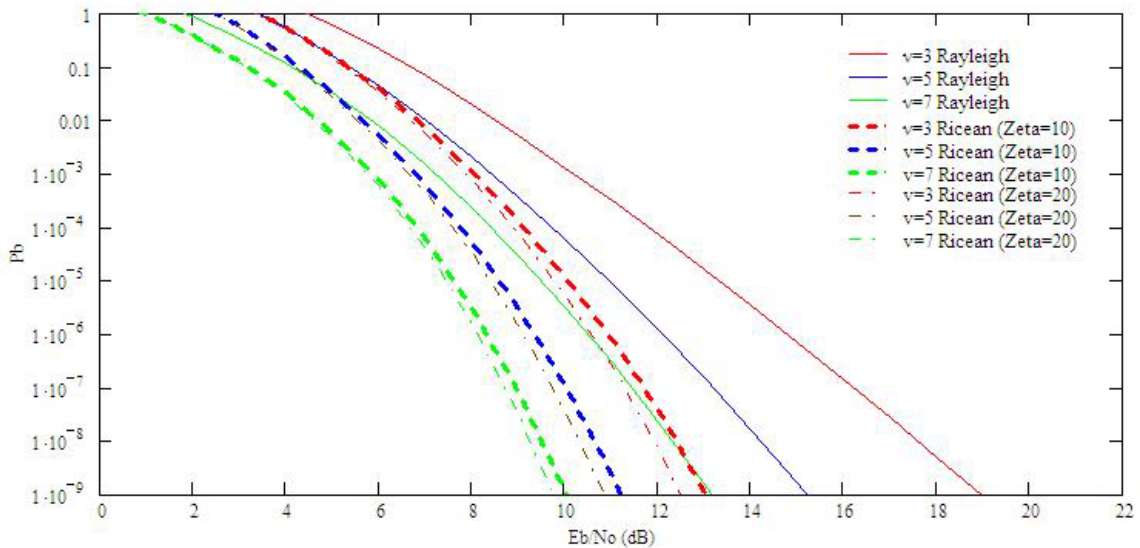


Figure 16. BPSK with FEC and SDD when $r = 1/3$.

From Figure 16, we can determine the E_b / N_o required to achieve the target P_b of 10^{-5} . For the three different cases ($\nu = 3, \nu = 5$, and $\nu = 7$) and Rayleigh fading, the required E_b / N_o is 13.3, 10.9, and 9.5 dB, respectively; for Ricean fading with $\zeta = 10$, the required E_b / N_o is 10.1, 8.6, and 7.6 dB, respectively; for Ricean fading with $\zeta = 20$, the required E_b / N_o is 9.8, 8.4, and 7.4 dB, respectively. The resulting coding gains are shown in Table 12.

Table 12. Summary of coding gains for BPSK SDD with $r = 1/3$ in fading environment.

	$K = 2$	$K = 4$	$K = 6$
Rayleigh fading	32.2 dB	33.6 dB	35 dB
Ricean fading $\zeta = 10$	6.9 dB	8.4 dB	9.4 dB
Ricean fading $\zeta = 20$	2.8 dB	4.2 dB	5.2 dB

The performance obtained with a convolutional encoder for a code rate of $1/2$ and constraint lengths $\nu = 3, \nu = 5, \nu = 7$, and $\nu = 9$ is illustrated in Figure 17.

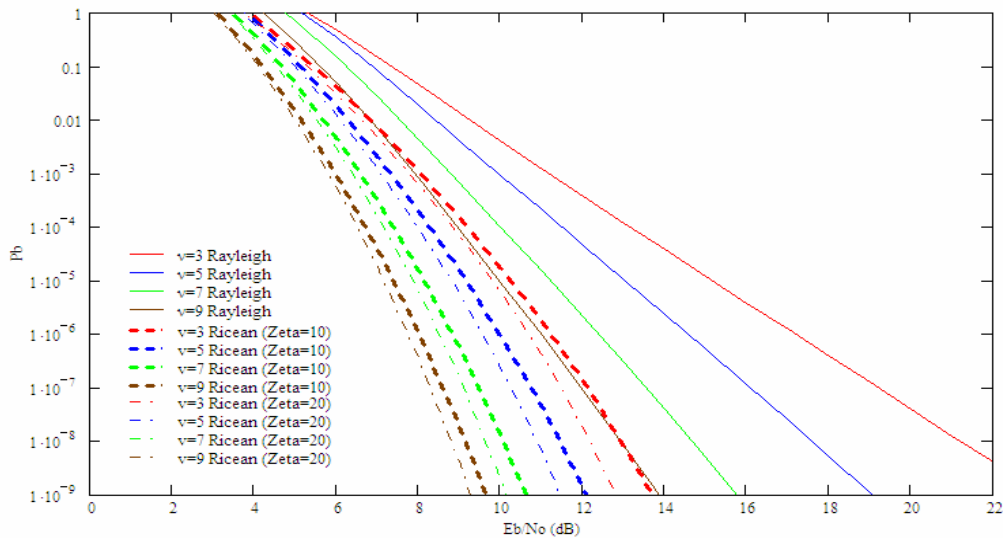


Figure 17. BPSK with FEC and SDD when $r = 1/2$.

Here, the required E_b/N_o for the four different cases ($\nu = 3, \nu = 5, \nu = 7,$ and $\nu = 9$) and Rayleigh fading is 15.1, 13, 11.2, and 10 dB, respectively; for Ricean fading with $\zeta = 10$, the required E_b/N_o is 10.2, 9.2, 8.1, and 7.4 dB, respectively; for Ricean fading with $\zeta = 20$, the required E_b/N_o is 9.8, 8.8, 7.8, and 7.1 dB, respectively. The resulting coding gains are shown in Table 13.

Table 13. Summary of coding gains for BPSK SDD with $r = 1/2$ in fading environment.

	$K = 2$	$K = 4$	$K = 6$	$K = 8$
Rayleigh fading	29.4 dB	31.5 dB	33.3 dB	34.5 dB
Ricean fading $\zeta = 10$	6.8 dB	7.8 dB	8.9 dB	9.6 dB
Ricean fading $\zeta = 20$	2.8 dB	3.8 dB	4.8 dB	5.5 dB

The performance obtained with a convolutional encoder for a code rate of $2/3$ and memory elements $K = 2, K = 4, K = 6,$ and $K = 8$ is illustrated in Figure 18.

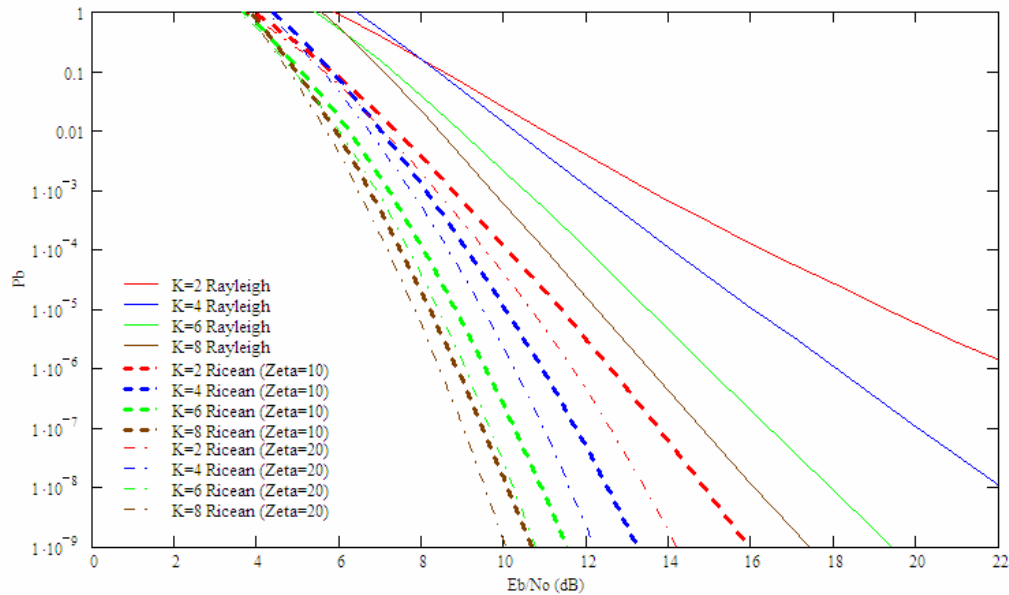


Figure 18. BPSK with FEC and SDD when $r = 2/3$.

Here, the required E_b/N_o for the four different cases ($K = 2$, $K = 4$, $K = 6$, and $K = 8$) and Rayleigh fading is 19.3, 16, 13.5, and 12.2 dB, respectively; for Ricean fading with $\zeta = 10$, the required E_b/N_o is 11.3, 10, 8.8, and 8.2 dB, respectively; for Ricean fading with $\zeta = 20$, the required E_b/N_o is 10.6, 9.5, 8.4, and 7.8 dB, respectively. The resulting coding gains are shown in Table 14.

Table 14. Summary of coding gains for BPSK SDD with $r = 2/3$ in fading environment.

	$K = 2$	$K = 4$	$K = 6$	$K = 8$
Rayleigh fading	25.2 dB	28.5 dB	31 dB	32.3 dB
Ricean fading $\zeta = 10$	5.7 dB	7 dB	8.2 dB	8.8 dB
Ricean fading $\zeta = 20$	2 dB	3.1 dB	4.2 dB	4.8 dB

The performance obtained with a convolutional encoder for a code rate of $3/4$ and memory elements $K = 2$, $K = 4$, $K = 6$, and $K = 8$ is illustrated in Figure 19.

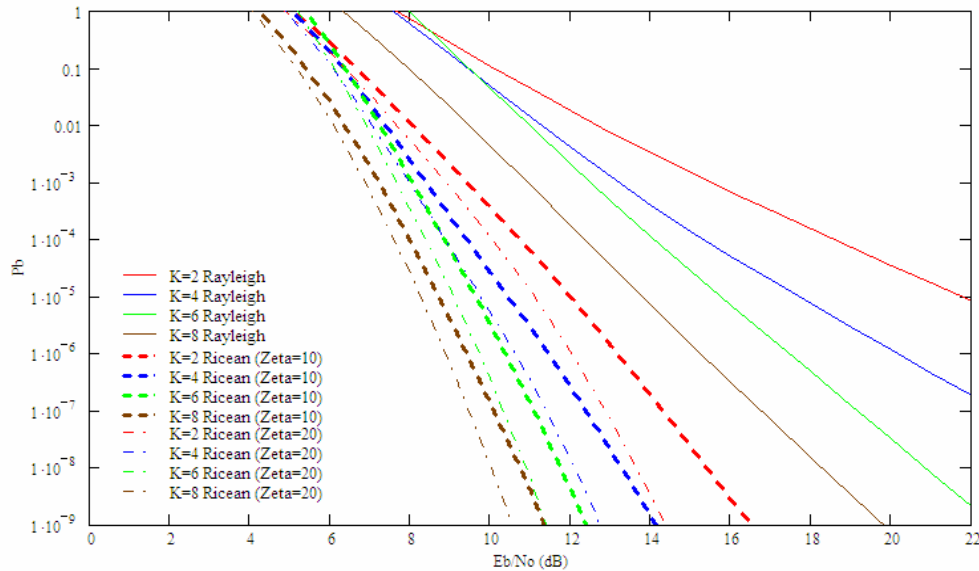


Figure 19. BPSK with FEC and SDD when $r = 3/4$.

Here, the required E_b/N_o for the four different cases ($K = 2$, $K = 4$, $K = 6$, and $K = 8$) and Rayleigh fading is 21.7, 17.6, 15.7, and 13.8 dB, respectively; for Ricean fading with $\zeta = 10$, the required E_b/N_o is 12, 10.5, 9.6, and 8.7 dB, respectively; for Ricean fading with $\zeta = 20$, the required E_b/N_o is 11.1, 9.8, 9.1, and 8.2 dB, respectively. The resulting coding gains are shown in Table 15.

Table 15. Summary of coding gains for BPSK SDD with $r = 3/4$ in fading environment.

	$K = 2$	$K = 4$	$K = 6$	$K = 8$
Rayleigh fading	22.8 dB	26.9 dB	28.8 dB	30.7 dB
Ricean fading $\zeta = 10$	5 dB	6.5 dB	7.4 dB	8.3 dB
Ricean fading $\zeta = 20$	1.5 dB	2.8 dB	3.5 dB	4.4 dB

The coding gains obtained with BPSK and SDD for different code rates and for the three different fading cases being examined are shown in Tables 16, 17, and 18.

Table 16. Summary of coding gains for BPSK SDD in Rayleigh fading.

	$K = 2$	$K = 4$	$K = 6$	$K = 8$
$r = 1/3$	32.2 dB	33.6 dB	35 dB	N/A
$r = 1/2$	29.4 dB	31.5 dB	33.3 dB	34.5 dB
$r = 2/3$	25.2 dB	28.5 dB	31 dB	32.3 dB
$r = 3/4$	22.8 dB	26.9 dB	28.8 dB	30.7 dB

Table 17. Summary of coding gains for BPSK SDD in Ricean fading with $\zeta = 10$.

	$K = 2$	$K = 4$	$K = 6$	$K = 8$
$r = 1/3$	6.9 dB	8.4 dB	9.4 dB	N/A
$r = 1/2$	6.8 dB	7.8 dB	8.9 dB	9.6 dB
$r = 2/3$	5.7 dB	7 dB	8.2 dB	8.8 dB
$r = 3/4$	5 dB	6.5 dB	7.4 dB	8.3 dB

Table 18. Summary of coding gains for BPSK SDD in Ricean fading with $\zeta = 20$.

	$K = 2$	$K = 4$	$K = 6$	$K = 8$
$r = 1/3$	2.8 dB	4.2 dB	5.2 dB	N/A
$r = 1/2$	2.8 dB	3.8 dB	4.8 dB	5.5 dB
$r = 2/3$	2 dB	3.1 dB	4.2 dB	4.8 dB
$r = 3/4$	1.5 dB	2.8 dB	3.5 dB	4.4 dB

From Tables 16, 17, and 18, we conclude that for BPSK transmitted over a fading channel with SDD, the coding gain increases as the number of memory elements increases or as the code rate decreases.

Generally, the expectation is that decoding with SDD yields better performance than with HDD. However, compare Tables 9, 10, and 11 with Tables 16, 17, and 18, respectively, and note that only for Rayleigh fading does SDD outperforms HDD for all code rates. For Ricean fading with $\zeta = 10$, SDD outperforms HDD when $r = 2/3$ and $r = 3/4$, but not for $r = 1/3$ and $r = 1/2$. For Ricean fading with $\zeta = 20$, SDD underperforms HDD for all code rates. This discrepancy is attributed to equation (2.14), which is an approximation and not exact. Small errors generated by equation (2.14) are magnified when the results of equation (2.14) are used to compute P_b for systems with FEC coding.

F. CHAPTER SUMMARY

The performance of the BPSK modulation in AWGN, both with and without FEC convolutional coding and for different fading environments were analyzed in this chapter. A non-fading channel, a Rayleigh fading channel and two different types of Ricean fading channels were examined. Next, the same modulation scheme for different fading environments is studied but now with the addition of pulse-noise interference.

THIS PAGE INTENTIONALLY LEFT BLANK

III. PERFORMANCE OF BPSK IN AN PULSE-NOISE INTERFERENCE ENVIRONMENT

A. INTRODUCTION

The performance of a BPSK modulated signal in an AWGN plus pulse-noise interference environment transmitted over different types of fading channels is analyzed in this chapter. First, BPSK with FEC and HDD transmitted over a non-fading channel with fixed pulse-noise interference as well as a worst case scenario is examined, and the effect of a Rayleigh fading channel in a continuous jamming environment is researched. Next, BPSK with FEC and SDD using a linear combing receiver transmitted over both a non-fading channel and over a Rayleigh fading channel in a continuous jamming environment is studied. Lastly, the effect of the noise-normalized receiver with FEC and SDD for a non-fading channel is explored.

B. PULSE-NOISE INTERFERENCE

The AWGN and pulse-noise interference are both modeled as Gaussian independent random processes. Thus, for continuous interference, the total PSD (N_t) is the sum of the PSD of AWGN (N_o) and the PSD of the interference (N_I). In short, $N_t = N_o + N_I$.

For pulsed interference, assume that the average interference power is constant, so the PSD of pulsed interference is inversely proportional to the duty cycle ρ ($0 < \rho \leq 1$), that is the fraction of the time the jammer is on. This means N_I is replaced by N_I/ρ , so when pulsed interference is present with AWGN, the average energy per symbol-to-noise PSD ratio can be expressed as

$$SNIR = \frac{E_b}{N_o + \frac{N_I}{\rho}}. \quad (3.1)$$

C. WITH CONVOLUTIONAL CODING AND HDD

1. Without Fading

The probability that a particular channel symbol is affected by the pulsed interference is ρ , and the probability that a particular symbol is affected by AWGN only is $(1 - \rho)$. As a result, the probability of channel bit error is given by

$$p_e = \rho P_b(\text{interference and AWGN}) + (1 - \rho) P_b(\text{AWGN only}). \quad (3.2)$$

For BPSK with FEC and HDD in an AWGN plus jamming environment combined with a non-fading channel, the probability of bit error is upper-bounded by (2.3), where P_d is given by (2.4), and p_e is the probability of coded bit error obtained from (3.2) and is expressed as [7]

$$p_e = \rho Q \left(\sqrt{\frac{2rE_b}{N_o + \frac{N_I}{\rho}}} \right) + (1 - \rho) Q \left(\sqrt{\frac{2rE_b}{N_o}} \right). \quad (3.3)$$

In this section, the duty cycles $\rho = 1$ (continuous jamming), $\rho = 0.3$, $\rho = 0.1$, $\rho = 0.01$, and the worst case ρ_{wc} are examined.

For the worst case, assuming $E_b/N_o \gg 1$ and $N_I/\rho \gg N_o$, the duty cycle factor for the worst case $\rho_{wc} \approx 0.72(E_b/N_I)^{-1}$ is obtained. Substituting ρ_{wc} into (3.3), results in [9]

$$(p_e)_{wc} \approx 0.72 \left(\frac{E_b}{N_o} \right)^{-1} Q(1.2\sqrt{r}). \quad (3.4)$$

The SIR vs. E_b/N_o for BPSK when the jammer uses different duty cycles, and when convolutional coding is used with HDD with different code rates and different numbers of memory elements at the target P_b of 10^{-5} are illustrated in Figures 20, 21, 22, and 23. Those plots show the areas of successful communications in the link ($P_b < 10^{-5}$),

which happen in the upper right areas of the curves. In the opposite areas, the P_b is greater than 10^{-5} .

The SIR vs. E_b/N_o obtained with a convolutional encoder for a code rate of 1/3 and various numbers of memory elements in a non-fading channel but a jammed environment with different duty cycles is illustrated in Figure 20

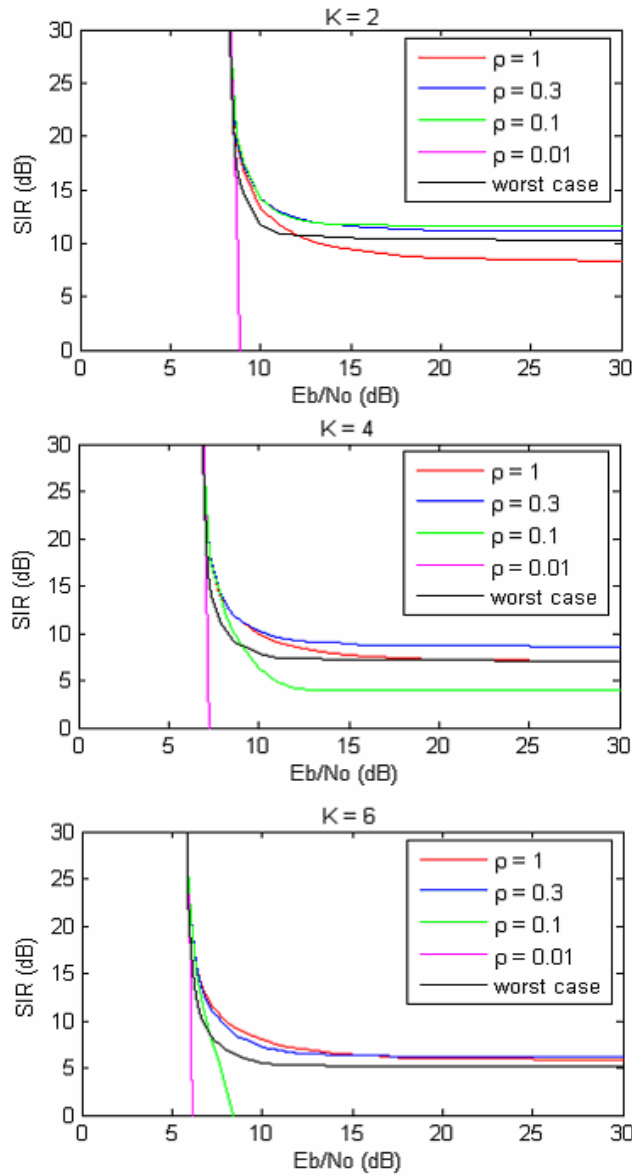


Figure 20. BPSK with FEC and HDD when $r = 1/3$ in a jammed channel.

As expected, the greater the number of memory elements, the better the performance of the system. By examining Figure 20, we see that there are two limiting cases. First, if the interference power is low, the performance is limited by E_b/N_o . On the other hand, if the AWGN power is low, the performance is limited by the interference power and the duty cycle factor. As K increases, the worst case value of ρ approaches one. For $K = 2$, the duty cycle for the worst performance is $\rho = 0.1$, while for $K = 6$, the duty cycle for the worst performance is $\rho = 1$. In all cases, interference with $\rho = 0.01$ is not efficient. The curve associated with the ρ_{wc} does not always result in the worst performance as it is an approximation.

The SIR vs. E_b/N_o obtained with a convolutional encoder for a code rate of $1/2$ and various numbers of memory elements in a non-fading channel but a jammed environment with different duty cycles is illustrated in Figure 21.

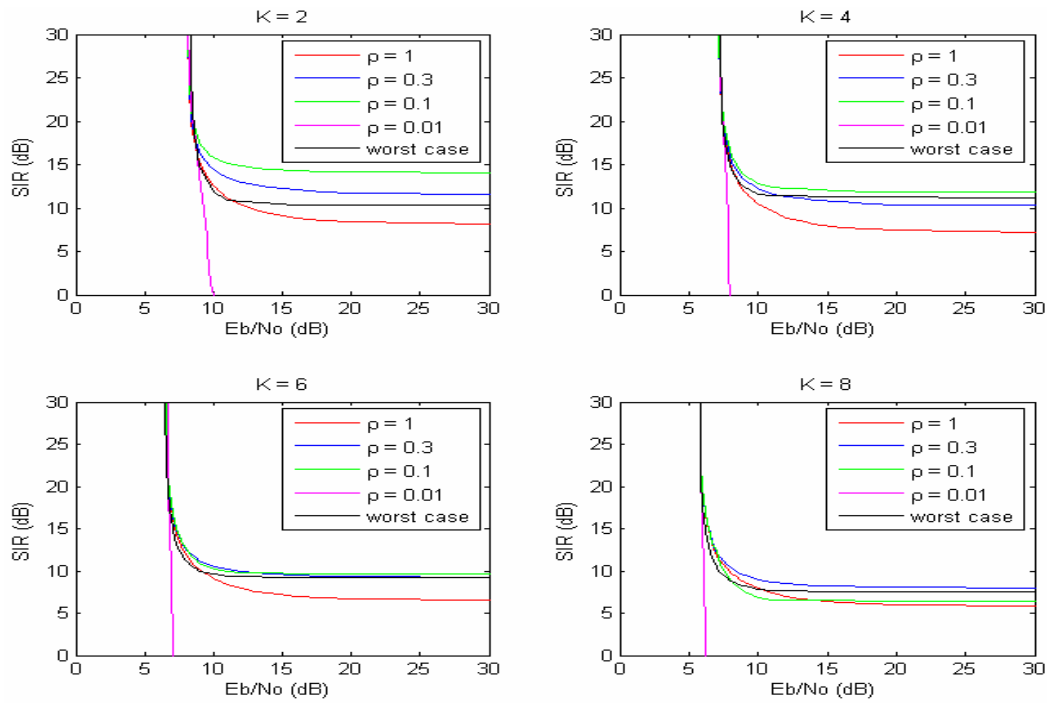


Figure 21. BPSK with FEC and HDD when $r = 1/2$ in a jammed channel.

The results for $r = 1/2$ are similar to those for $r = 1/3$. The $\rho = 0.01$ does not result in efficient jamming. For $K = 2$ and $K = 4$, the duty cycle for the worst performance is $\rho = 0.1$, while for $K = 8$, the duty cycle for the worst performance is $\rho = 0.3$. As K increases, the difference between worst case performance and performance with $\rho = 1$ decreases.

The SIR vs. E_b/N_o obtained with a convolutional encoder for a code rate of $2/3$ and various numbers of memory elements in a non-fading channel but a jammed environment with different duty cycles is illustrated in Figure 22.

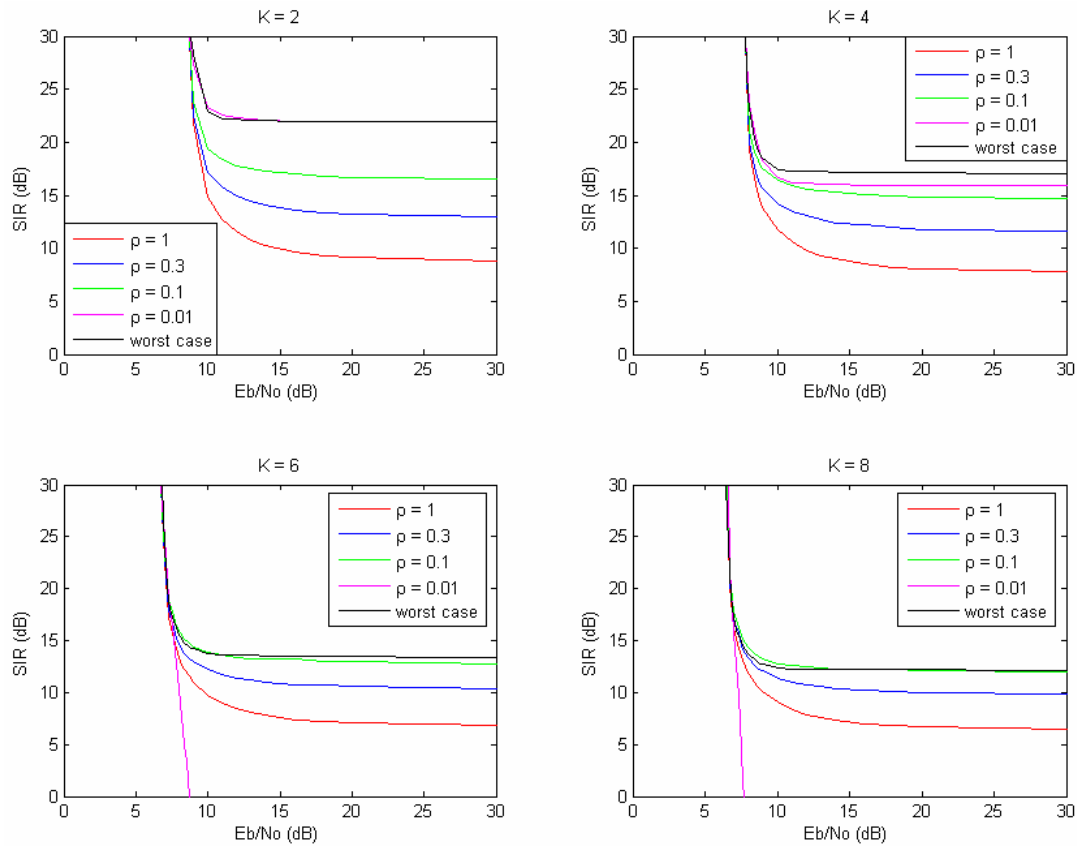


Figure 22. BPSK with FEC and HDD when $r = 2/3$ in a jammed channel.

In this case, the duty cycle $\rho = 0.01$ results in the worst performance when the number of memory elements are $K = 2$ and $K = 4$ but gives poor interference when the number of memory elements are $K = 6$ and $K = 8$, when the duty cycle $\rho = 0.1$ results in the worst performance. Also, the approximate worst case duty cycle is accurate in this case. As with the lower code rates examined, as K increases, the value of ρ leading to worst case performance increases.

The SIR vs. E_b/N_o obtained with a convolutional encoder for a code rate of $3/4$ and various numbers of memory elements in a non-fading channel but a jammed environment with different duty cycles is illustrated in Figure 23.

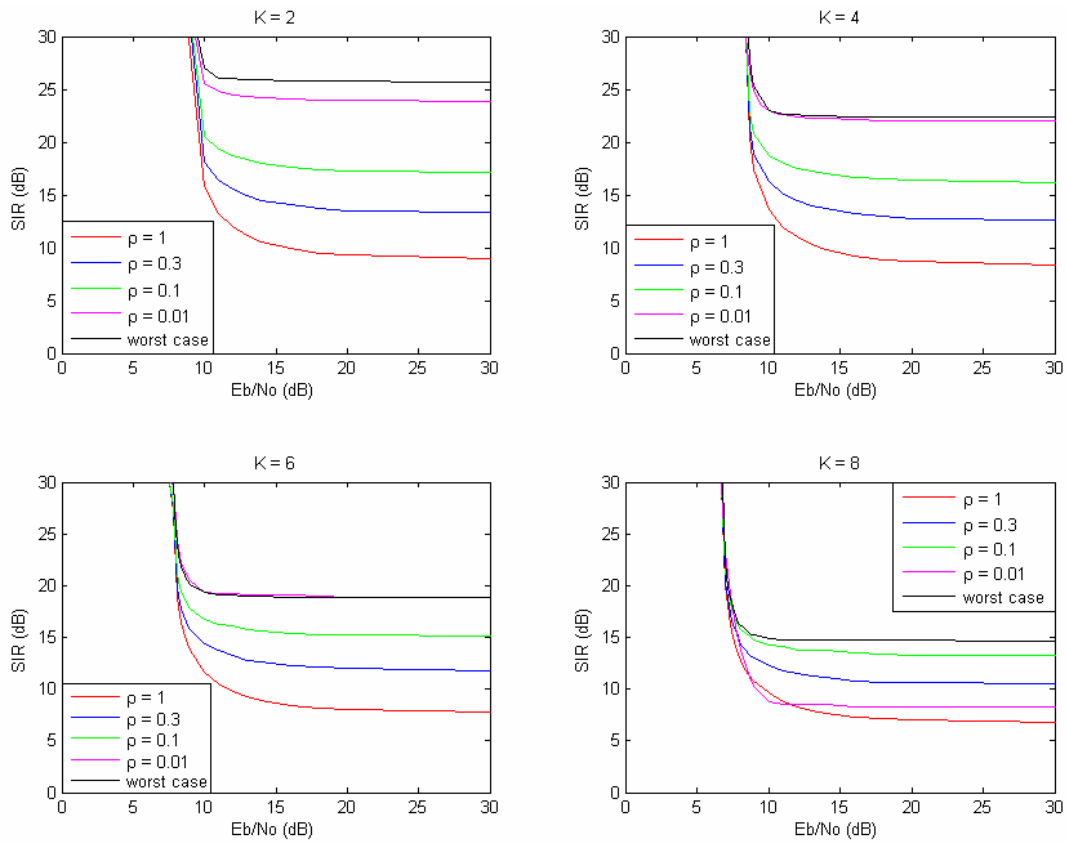


Figure 23. BPSK with FEC and HDD when $r = 3/4$ in a jammed channel.

In this case, the duty cycle $\rho = 0.01$ results in the worst performance for the number of memory elements $K = 2$, $K = 4$, and $K = 6$, while for $K = 8$, the duty cycle $\rho = 0.1$ results in the worst performance. Also, the approximate worst case duty cycle is accurate in this case, and increasing K results in increasing ρ for a worst case performance.

Comparing Figures 20, 21, 22, and 23, we conclude that increasing the number of memory elements and/or decreasing the code rate not only makes the low-duty cycle pulse-noise interference less efficient but also reduces the difference between the worst case performance and the interference with $\rho = 1$.

2. With Rayleigh Fading and Continuous Jamming

The performance of BPSK transmitted over a Rayleigh fading channel with FEC and HDD in an AWGN plus continuous jamming environment is determined in this section. The probability of bit error is upper-bounded by (2.3), where P_d is given by (2.4), and p_e is the probability of coded bit error obtained by replacing $E_b/N_o \rightarrow r E_b/(N_o + N_I)$ in (2.13).

The SIR vs. E_b/N_o obtained with a convolutional encoder for different code rates and various numbers of memory elements in a Rayleigh fading channel and a continuous jammed environment is illustrated in Figure 24.

From Figure 24, we conclude that for BPSK transmitted over a Rayleigh fading channel with FEC, HDD, and continuous jamming, the performance improves as the number of memory elements increases and/or as the code rate decreases. Also, it is evident that the target P_b of 10^{-5} is much more difficult to achieve in this case due to the nature of the multipath fading channel.

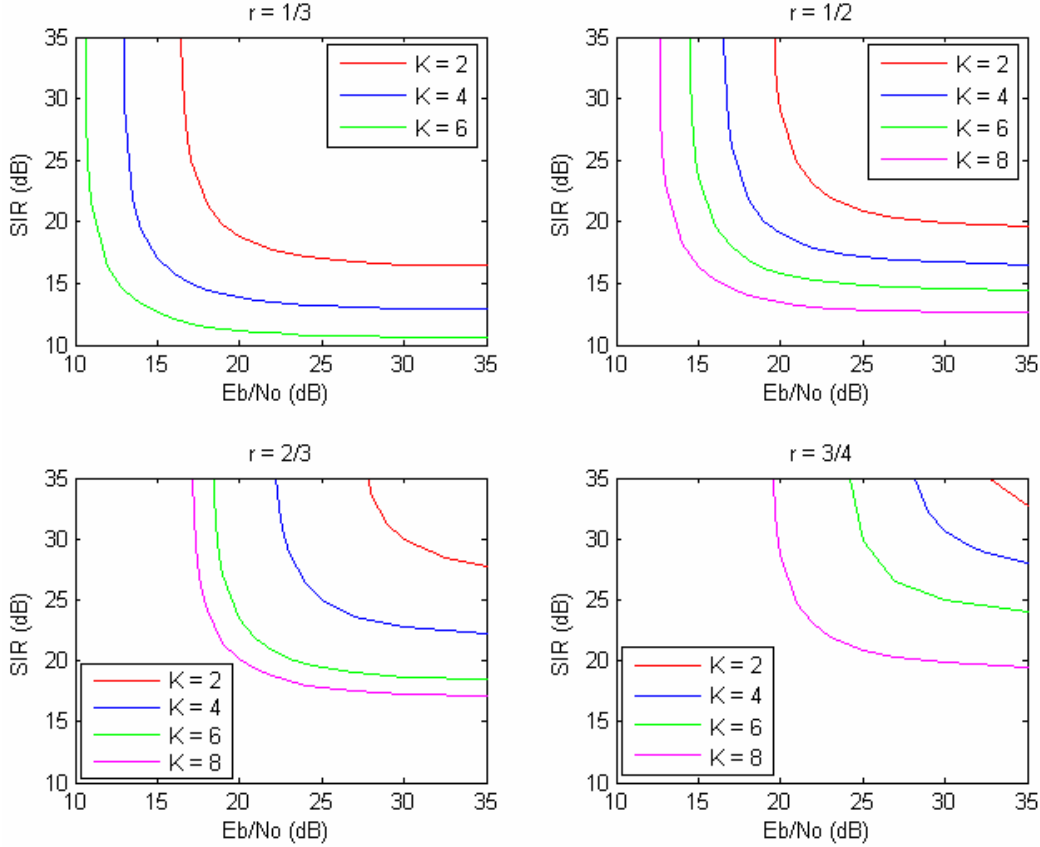


Figure 24. BPSK with FEC and HDD in a jammed channel with Rayleigh fading.

D. WITH CONVOLUTIONAL CODING AND SDD

1. Using a Linear Combining Receiver in a Non-Fading Channel

The performance of BPSK transmitted over a non-fading channel when using convolutional coding with SDD and different code rates in a jammed environment with different duty cycles is determined in this section.

First, the case of a linear combining receiver is examined. Assume that only i bits are jammed of the d independent received bits. Thus, $(d - i)$ bits are affected only by AWGN. As a result, the probability of bit error is upper-bounded by (2.3), where P_d , the probability of selecting a path that is a Hamming distance d from the correct path when i of the d bits are jammed, is expressed by [7]

$$P_d = \sum_{i=0}^d \binom{d}{i} \rho^i (1 - \rho)^{d-i} P_d(i) \quad (3.5)$$

where

$$P_d(i) = Q \left[\sqrt{1 + \frac{i}{d} \left(\frac{\frac{E_b}{N_o}}{\rho \frac{E_b}{N_I}} \right)} \right] \cdot \sqrt{\frac{2dr \frac{E_b}{N_o}}{\left(\frac{E_b}{N_o} \right)^{-1} + \left(\frac{E_b}{N_I} \right)^{-1}}} \quad (3.6)$$

In the case of continuous jamming ($\rho = 1$ and $i = d$), (3.5) becomes

$$P_d = Q \left(\sqrt{2dr \left[\left(\frac{E_b}{N_o} \right)^{-1} + \left(\frac{E_b}{N_I} \right)^{-1} \right]^{-1}} \right) \quad (3.7)$$

The SIR vs. E_b/N_o for BPSK obtained when using a linear combining receiver and when the jammer uses different duty cycles for convolutional coding with SDD with different code rates and different numbers of memory elements at the target P_b of 10^{-5} are illustrated in Figures 25, 26, 27, and 28.

The SIR vs. E_b/N_o obtained with a convolutional encoder for a code rate of 1/3 and various numbers of memory elements in a non-fading channel but a jammed environment with different duty cycles is illustrated in Figure 25.

From Figure 25, we conclude that for BPSK transmitted over a non-fading channel with FEC and SDD when using a linear combining receiver, the performance improves as the number of memory elements increases and/or as the duty cycle increases. Also, the interference with $\rho = 0.01$ is the most efficient regardless of the number of memory elements. This is in direct contrast to the results obtained with HDD.

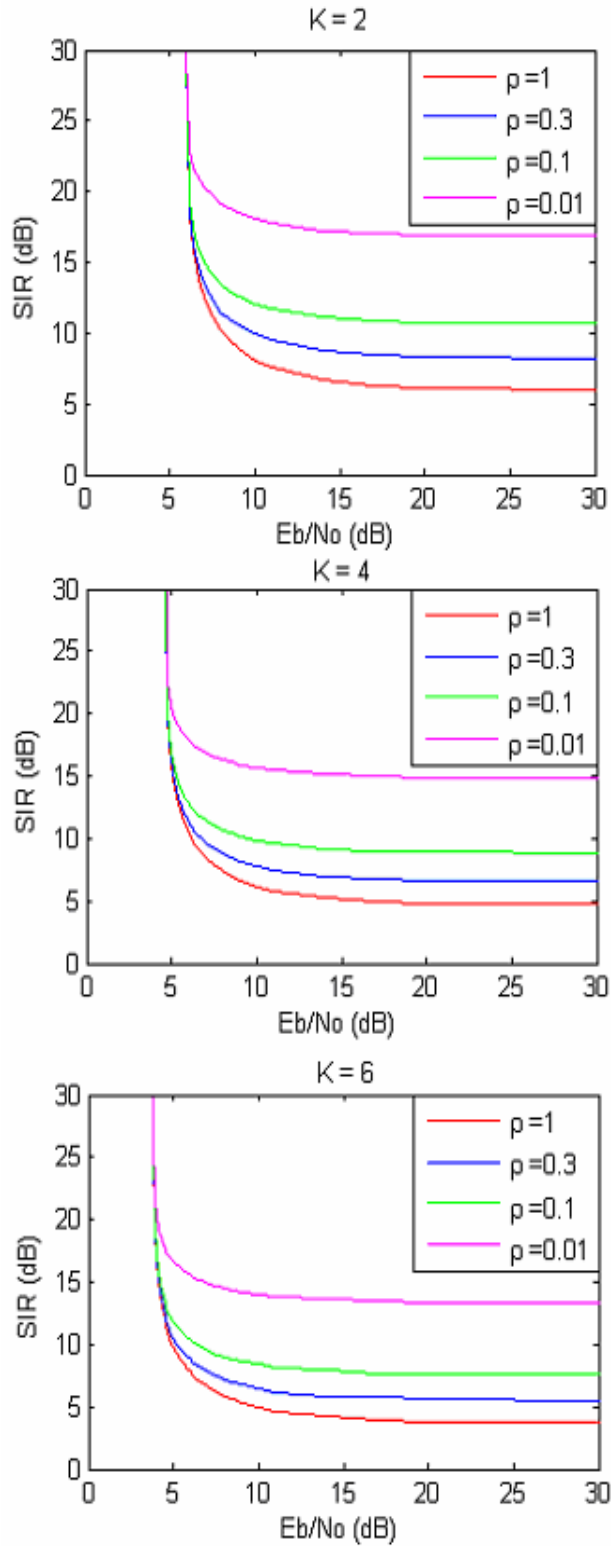


Figure 25. BPSK with FEC and SDD using a linear combining receiver when $r = 1/3$.

The SIR vs. E_b/N_o obtained with a convolutional encoder for a code rate of 1/2 and various number of memory elements in a non-fading channel but a jammed environment with different duty cycles is illustrated in Figure 26.

From Figure 26, we conclude that the performance improves as the number of memory elements increases and/or as the duty cycle increases. As a result, the interference with $\rho = 0.01$ is the most efficient regardless of the number of memory elements. Again, this is in direct contrast to the results obtained with HDD.

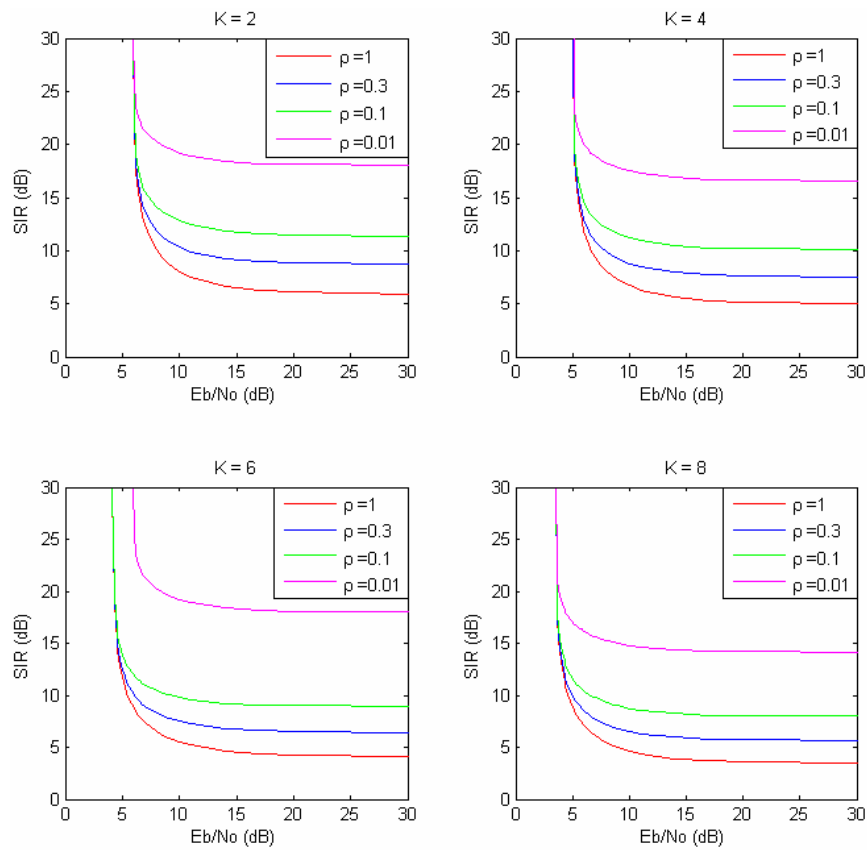


Figure 26. BPSK with FEC and SDD using a linear combining receiver when $r = 1/2$.

The SIR vs. E_b/N_o obtained with a convolutional encoder for a code rate of 2/3 and various number of memory elements in a non-fading channel but a jammed environment with different duty cycles is illustrated in Figure 27.

From Figure 27, we reach the same conclusion as for the lower code rates. The performance improves as the number of memory elements increases and/or as the duty cycle increases. For $K = 2$ and $K = 4$, the result obtained with SDD has the same general trend as that obtained with HDD, but SDD has better performance than HDD. For $K = 6$ and $K = 8$, the interference with $\rho = 0.01$ is the most efficient, and this is in direct contrast to the results obtained with HDD.

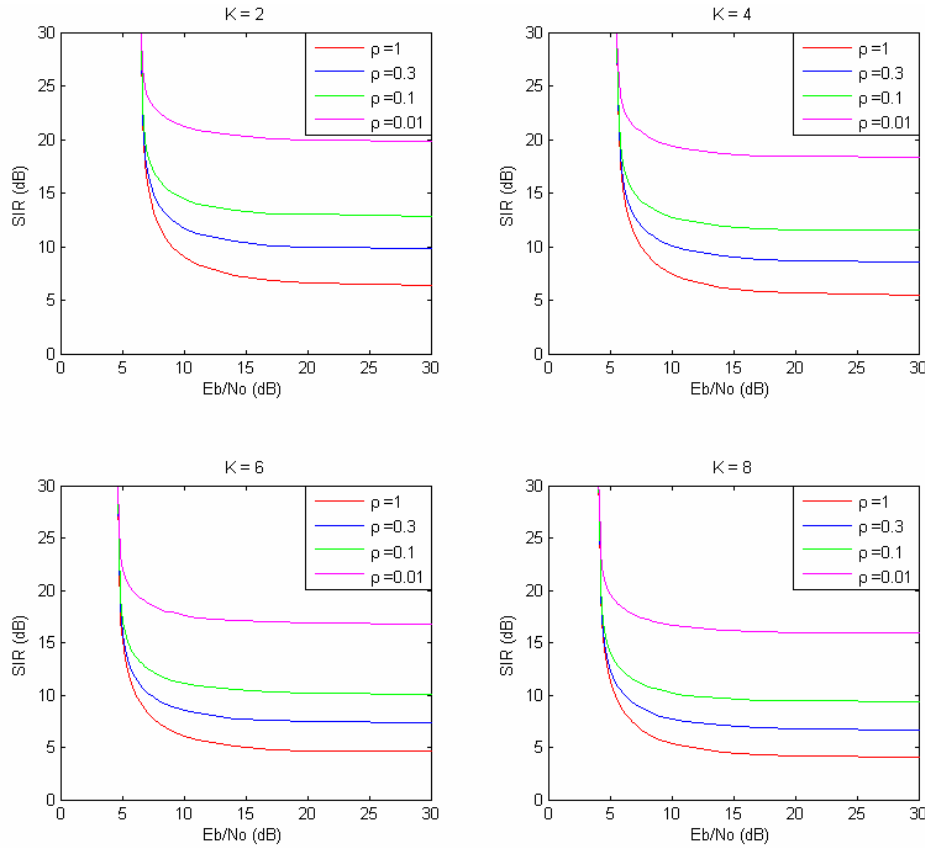


Figure 27. BPSK with FEC and SDD using a linear combining receiver when $r = 2/3$.

The SIR vs. E_b/N_o obtained with a convolutional encoder for a code rate of $3/4$ and various number of memory elements in a non-fading channel but a jammed environment with different duty cycles is illustrated in Figure 28.

From Figure 28, we reach the same conclusion as for the lower code rates. The performance improves as the number of memory elements increases and/or as the duty cycle increases. For $K = 2$, $K = 4$, and $K = 6$, the result obtained with SDD has the same general trend as that obtained with HDD, but SDD has better performance than HDD. For $K = 8$, the most efficient interference is $\rho = 0.01$ for SDD; while for HDD, the most efficient interference is $\rho = 0.1$.

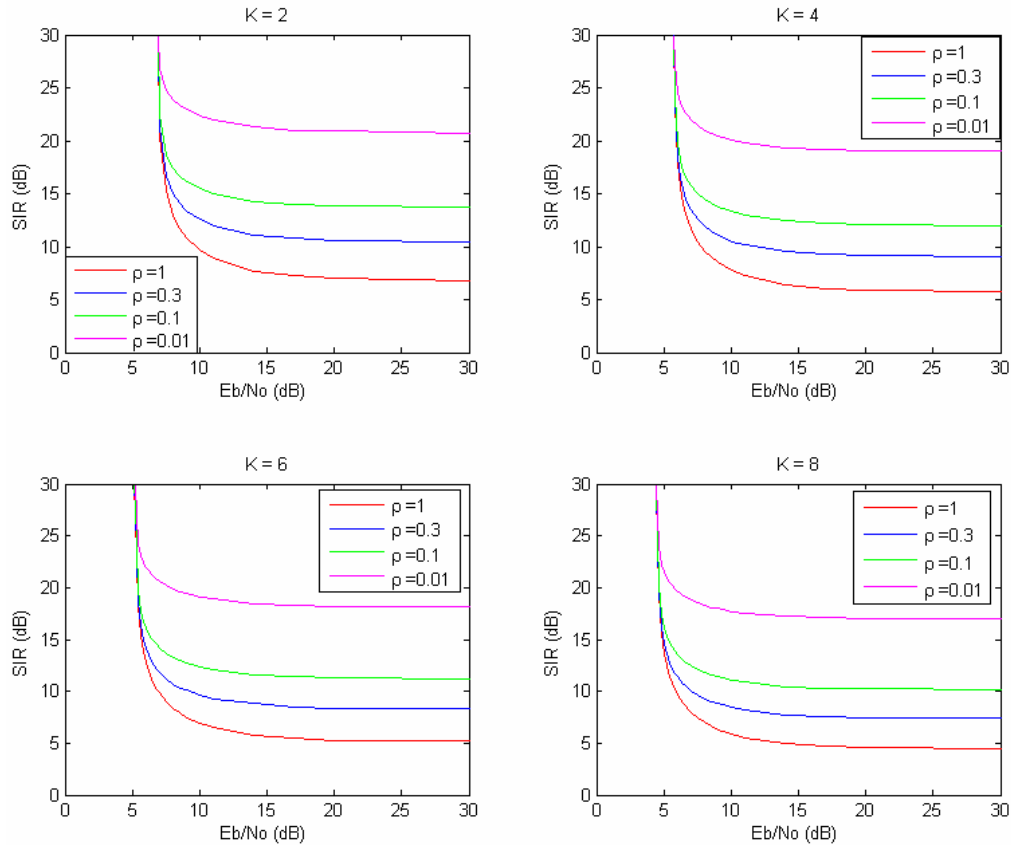


Figure 28. BPSK with FEC and SDD using a linear combining receiver when $r = 3/4$.

From Figures 25, 26, 27, and 28, we conclude that for BPSK with linear combining, FEC, and SDD in a jammed environment but without fading, the performance worsens as ρ decreases and the interference with $\rho = 0.01$ is the most efficient. Also, increasing the number of memory elements and/or decreasing the code rate slightly reduces the difference between the worst and the best performance.

Comparing Figures 20, 21, 22, and 23 with Figures 25, 26, 27, and 28, respectively, we conclude that:

- For code rates $r = 1/2$ and $r = 1/3$, when the jamming power is low, the coding gain obtained with SDD is higher than that obtained with HDD by approximately 1.5 to 3 dB, but as the jamming power increases and the duty cycle decreases, the difference between the coding gains decreases. When the jamming power is high and $\rho = 0.01$, the performance obtained with SDD is poorer than that obtained with HDD.
- For code rates $r = 2/3$ and $r = 3/4$, when the jamming power is low, the coding gain obtained with SDD is higher than that obtained with HDD by approximately 2 to 3 dB; while, when the jamming power is high, the coding gain obtained with SDD is higher than that obtained with HDD by approximately 1 to 4 dB, except for the cases when $\rho = 0.01$ for $r = 2/3$ with $K = 4$, $K = 6$, and $K = 8$, and for $r = 3/4$ with $K = 8$, where the performance obtained with SDD is poorer than that obtained with HDD.
- From above, we can conclude that HDD outperforms SDD when jamming power is high.

2. Using a Linear Combining Receiver in a Rayleigh Fading

The performance of BPSK transmitted over Rayleigh fading channel with FEC and SDD in an AWGN plus continuous jamming environment when using a linear combining receiver is determined in this section. The probability of bit error is upper-bounded by (2.3), where P_d is obtained by replacing $N_o \rightarrow N_o + N_I$ in (2.14) and with $\zeta = 0$.

The SIR vs. E_b/N_o obtained with a convolutional encoder for different code rates and various numbers of memory elements in a Rayleigh fading channel and a continuous jammed environment is illustrated in Figure 29.

From Figure 29, we conclude that for BPSK transmitted over a Rayleigh fading channel with FEC, SDD, and continuous jamming, there is better performance as the number of memory elements increases and/or as the code rate decreases. Also, it is clear that the nature of the fading channel makes communications more difficult since a much stronger signal is necessary to achieve the desired performance.

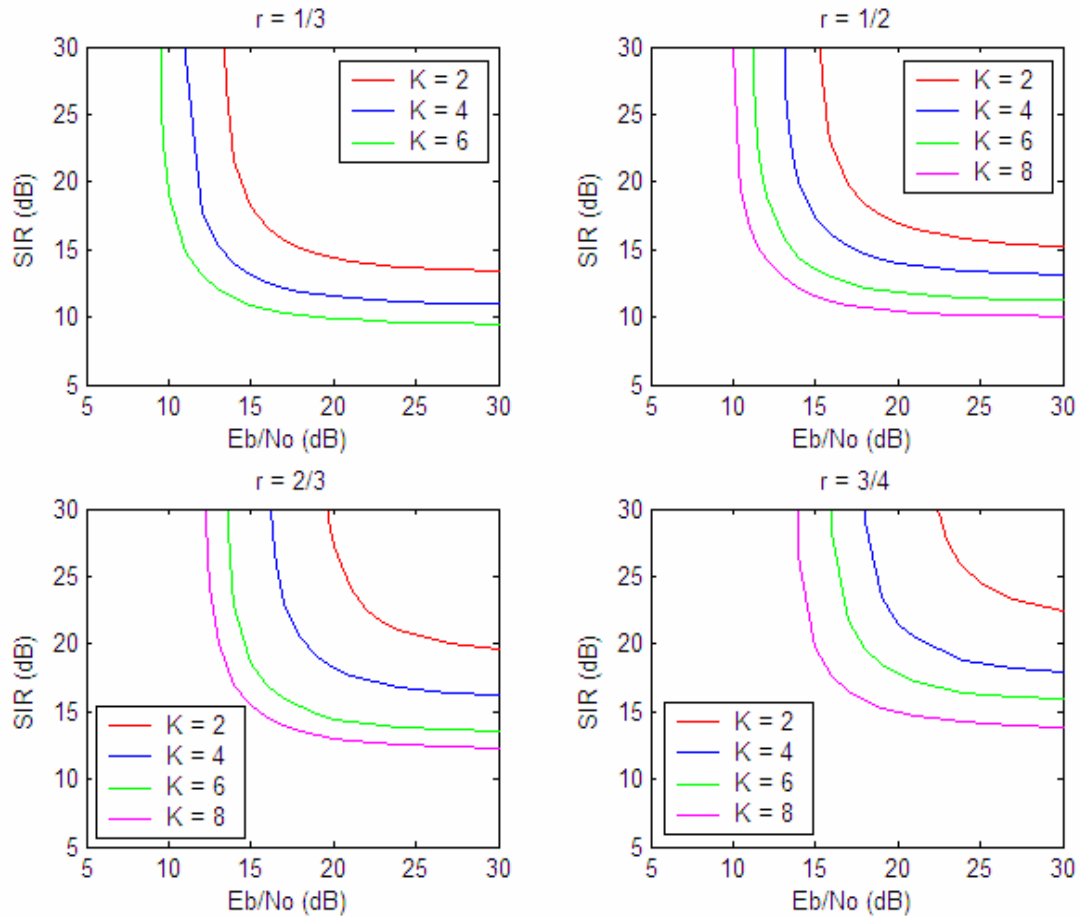


Figure 29. BPSK with FEC and SDD using a linear combining receiver in Rayleigh fading.

3. Using a Noise-Normalized Receiver in a Non-Fading Channel

The performance of BPSK transmitted over a non-fading channel with convolutional coding and SDD with different code rates in a jammed environment with different duty cycles when using a noise-normalized receiver is examined in this section.

In this case, the probability of bit error is upper-bounded by (2.3), where P_d is given by (3.5), and $P_d(i)$ is expressed as [7]

$$P_d(i) = Q \left[\frac{2rE_b}{dN_o} \left(d - i + \frac{i}{1 + \left(\frac{E_b}{N_o} \right)^{1/2} \left(\rho \frac{E_b}{N_I} \right)} \right)^2 \right] \quad (3.8)$$

The SIR vs. E_b/N_o for BPSK obtained when using a noise-normalized receiver, when the jammer uses different duty cycles, and when convolutional coding is used with SDD with different code rates and different numbers of memory elements at the target P_b of 10^{-5} are illustrated in Figures 30, 31, 32, and 33.

The SIR vs. E_b/N_o obtained with a convolutional encoder for a code rate of 1/3 and various number of memory elements in a non-fading channel but a jammed environment with different duty cycles is illustrated in Figure 30.

From Figure 30, we conclude that for BPSK transmitted over a non-fading channel with FEC, SDD and a code rate of 1/3 when using a noise-normalized receiver, the performance improves as the number of memory elements increases and/or as the duty cycle decreases. As a result, the interference with $\rho = 0.01$ is not efficient regardless of the number of memory elements. This is analogous to the results obtained with HDD but in direct contrast to those obtained with SDD when using a linear combining receiver for the same conditions. Comparing Figures 25 and 30, we conclude that the use of noise-normalized receiver negates the effect of the pulse-noise interference. Also, the worst performance obtained when using a noise-normalized receiver is as good or better than the best performance obtained when using a linear combining receiver for the same conditions. Comparing Figures 20 and 30, we conclude that the results obtained with SDD when using a noise-normalized receiver are better than those obtained with HDD for the same conditions.

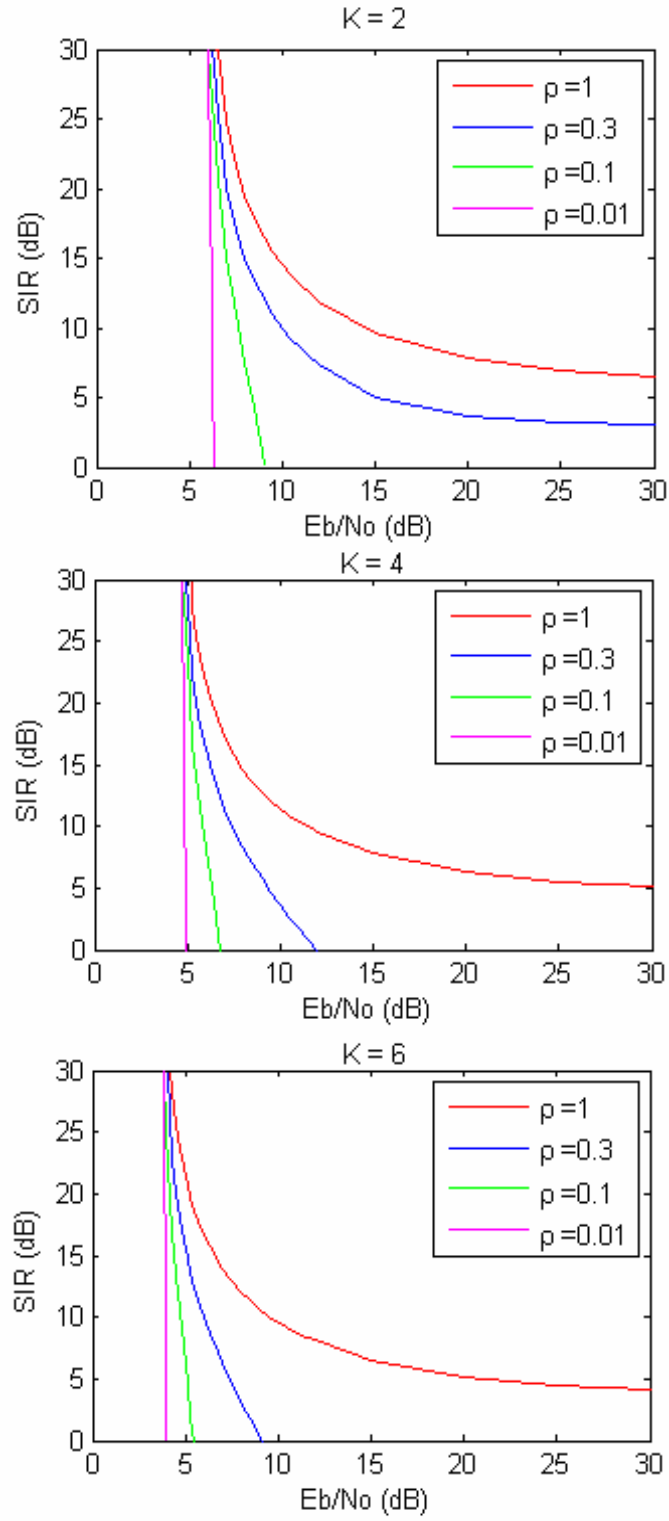


Figure 30. BPSK with FEC and SDD using a noise-normalized receiver when $r = 1/3$.

The SIR vs. E_b/N_o obtained with a convolutional encoder for a code rate of 1/2 and various number of memory elements in a non-fading channel but a jammed environment with different duty cycles is illustrated in Figure 31.

From Figure 31, we reach the same conclusion as for the lower code rates. Generally, the performance improves as the number of memory elements increases and/or as the duty cycle decreases. Also, the result obtained with SDD when using a noise-normalized receiver is better than that obtained with HDD for the same conditions.

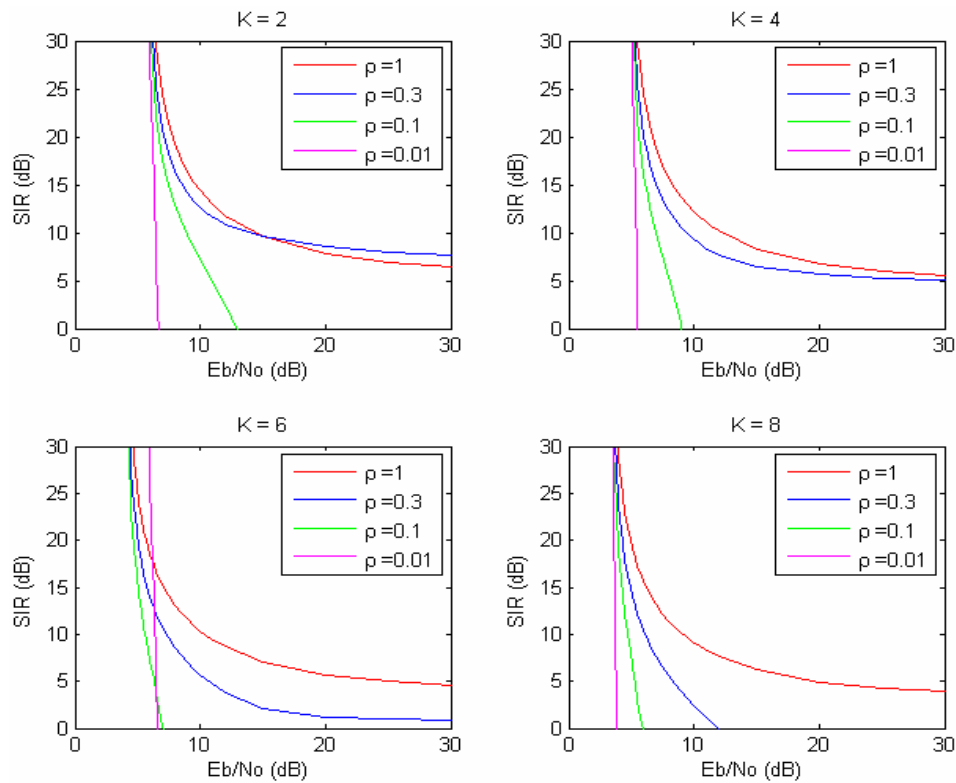


Figure 31. BPSK with FEC and SDD using a noise-normalized receiver when $r = 1/2$.

The SIR vs. E_b/N_o obtained with a convolutional encoder for a code rate of 2/3 and various number of memory elements in a non-fading channel but a jammed environment with different duty cycles is illustrated in Figure 32.

From Figure 32, we conclude that for BPSK transmitted over a non-fading channel with FEC and SDD for a code rate of 2/3 when using a noise-normalized

receiver, the interference with $\rho = 0.01$ is not efficient regardless of the number of memory elements, and that $\rho = 0.1$ is not efficient when $K = 6$ or $K = 8$. Also, the worst case value of ρ approaches one as K increases. The result obtained with SDD when using a noise-normalized receiver is better than that obtained with HDD for the same conditions.

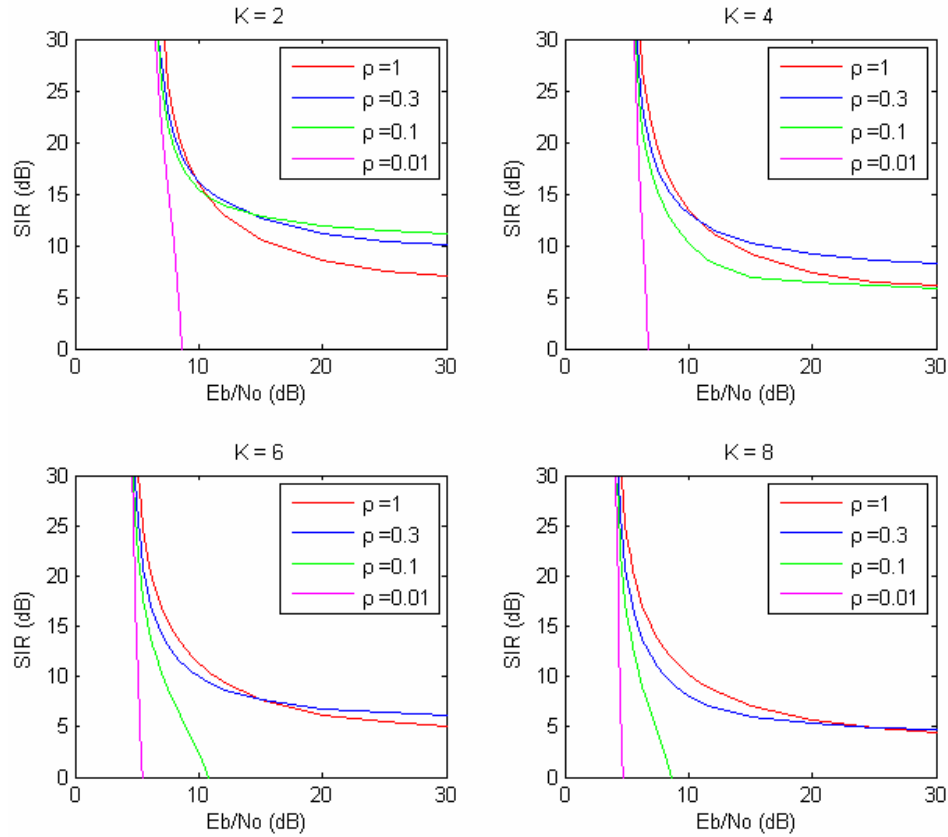


Figure 32. BPSK with FEC and SDD using a noise-normalized receiver when $r = 2/3$.

The SIR vs. E_b/N_o obtained with a convolutional encoder for a code rate of $3/4$ and various number of memory elements in a non-fading channel but a jammed environment with different duty cycles is illustrated in Figure 33.

From Figure 33, we conclude that for BPSK transmitted over a non-fading channel with FEC and SDD for a code rate of $3/4$ when using a noise-normalized

receiver, the interference with $\rho = 0.01$ is not efficient regardless of the number of memory elements, and $\rho = 0.1$ is not efficient for $K = 8$. Also, the worst case value of ρ increases as K increases. The result obtained with SDD when using a noise-normalized receiver is better than that obtained with HDD for the same conditions

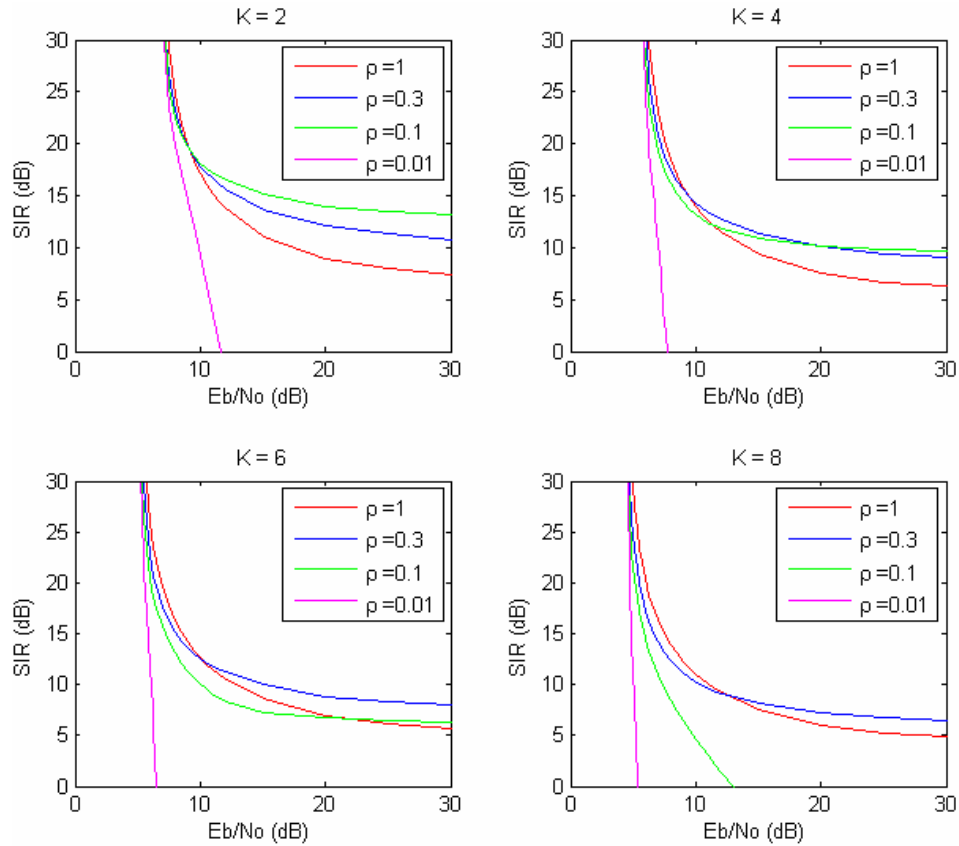


Figure 33. BPSK with FEC and SDD using a noise-normalized receiver when $r = 3/4$.

Comparing Figures 25, 26, 27, and 28 to Figures 30, 31, 32, and 33, respectively, we conclude that when the jamming power is low, the coding gain obtained with SDD when a noise-normalized receiver is used is approximately equal to that obtained with SDD when a linear combining receiver is used, but as the jamming power increases, the coding gain obtained with the noise-normalized receiver is significantly better than that obtained with the linear combining receiver. Also, the performance obtained with SDD when the noise-normalized receiver is used is always better than that obtained with HDD,

with the difference in coding gain about 2 to 5 dB. As a result, we realize a great advantage when using the noise-normalized receiver.

E. CHAPTER CONCLUSION

In this chapter, the performance of a BPSK modulated signal in an AWGN plus pulse-noise interference environment transmitted over different types of fading channels was analyzed. First, BPSK with FEC and HDD transmitted over a non-fading channel, with different duty cycles as well as for the worst case was examined, and the effect of a Rayleigh fading channel in a continuous jamming environment was examined. Next, BPSK with FEC and SDD transmitted over a non-fading channel as well as a Rayleigh fading channel in a continuous jamming environment with a linear combing receiver was examined. Lastly, the effect of the noise-normalized receiver with FEC and SDD for a non-fading channel was examined. Next, we examine NCBFSK in an AWGN environment transmitted over different types of channels.

THIS PAGE INTENTIONALLY LEFT BLANK

IV. PERFORMANCE OF NCBFSK IN AN AWGN ENVIRONMENT

A. INTRODUCTION

The performance of a noncoherently detected binary frequency-shift keying (NCBFSK) modulated signal in an AWGN environment transmitted over different types of channels is analyzed in this chapter. The case of no fading as well as the effect of both Ricean and Rayleigh fading channels is examined. The signals are coded prior to transmission with a convolutional code with different code rates and different constraint lengths.

B. NCBFSK IN AWGN WITHOUT FADING

1. Without Forward Error Correction Coding

The performance of a NCBFSK modulated signal transmitted over a channel with AWGN and no fading is first examined. When FEC coding is not used, the probability of bit error is given by [6]

$$P_b = \frac{1}{2} \exp\left(-\frac{E_b}{2N_o}\right). \quad (4.1)$$

The performance of NCBFSK in an AWGN environment without fading or FEC coding is illustrated in Figure 34.

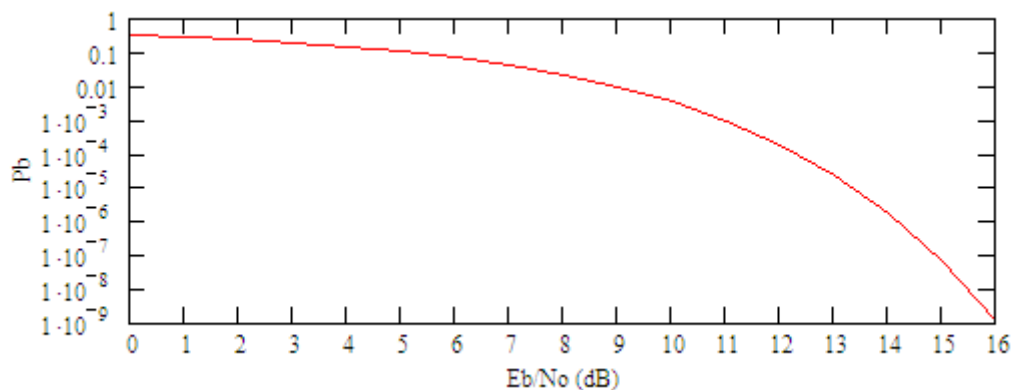


Figure 34. NCBFSK without FEC coding

2. With FEC – Using Convolutional Codes

a. Hard Decision Decoding

First, the performance of NCBFSK is determined when using convolutional coding and implementing HDD. The probability of bit error is upper-bounded by (2.3), where P_d is given by (2.4), and p_e is the probability of coded bit error obtained by replacing $E_b/N_o \rightarrow r E_b/N_o$ in (4.1).

The probabilities of bit error of NCBFSK for different convolutional encoders in an AWGN environment without interference or fading are illustrated in Figures 35, 36, 37, and 38.

The performance obtained by a convolutional encoder with a code rate of 1/3 and for $K = 2$, $K = 4$, and $K = 6$ memory elements is illustrated in Figure 35. From this figure, we conclude that in order to obtain the target P_b of 10^{-5} , the required E_b/N_o for the three different cases ($\nu = 3$, $\nu = 5$, and $\nu = 7$) are 13.1, 12, and 11.2 dB, respectively. Without FEC coding, the required $E_b/N_o = 13.3$ dB, and the resulting coding gains for the three cases are 0.2, 1.3, and 2.1 dB, respectively.

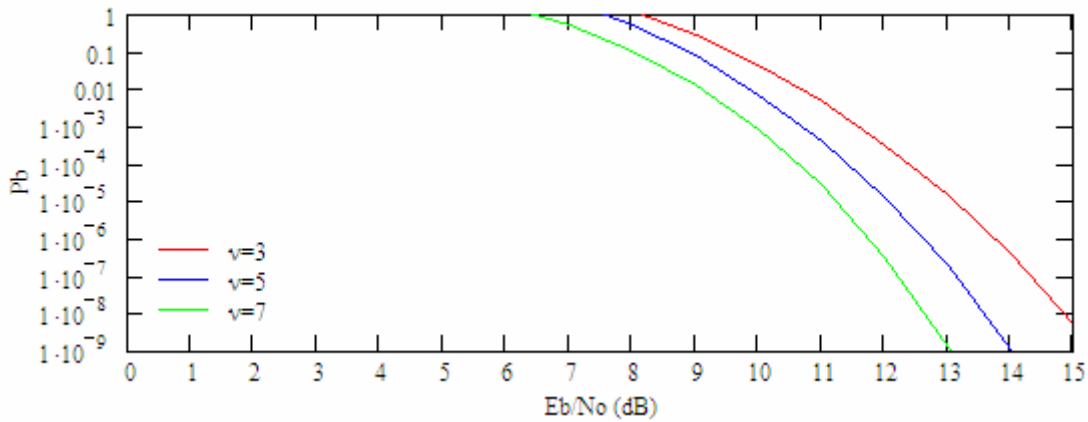


Figure 35. NCBFSK HDD with $r = 1/3$ and different values of constraint length.

The performance obtained by a convolutional encoder with a code rate of 1/2 and for $K = 2$, $K = 4$, $K = 6$, and $K = 8$ memory elements is illustrated in Figure

36. From this figure, the required E_b/N_o for the four different cases ($\nu = 3, \nu = 5, \nu = 7,$ and $\nu = 9$) are 12.5, 11.8, 11.3, and 10.7 dB, respectively, and the resulting coding gains for the four cases are 0.8, 1.5, 2, 2.6 dB, respectively.

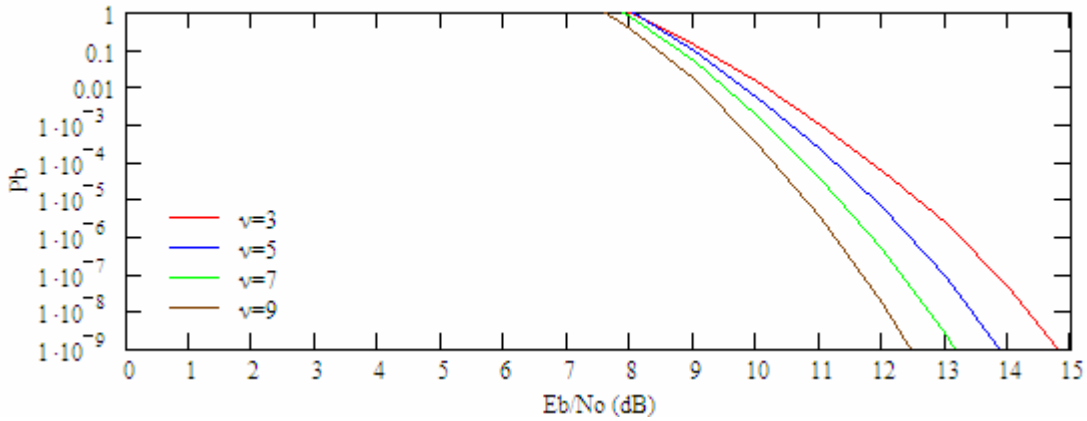


Figure 36. NCBFSK HDD with $r = 1/2$ and different values of constraint length.

The performance obtained by a convolutional encoder with a code rate of $2/3$ and for $K = 2, K = 4, K = 6,$ and $K = 8$ memory elements is illustrated in Figure 37. Here, the required E_b/N_o for the four different cases are 12.9, 12.1, 11.3, 11 dB, respectively, and the resulting coding gains for the four cases are 0.4, 1.2, 2, 2.3 dB, respectively.

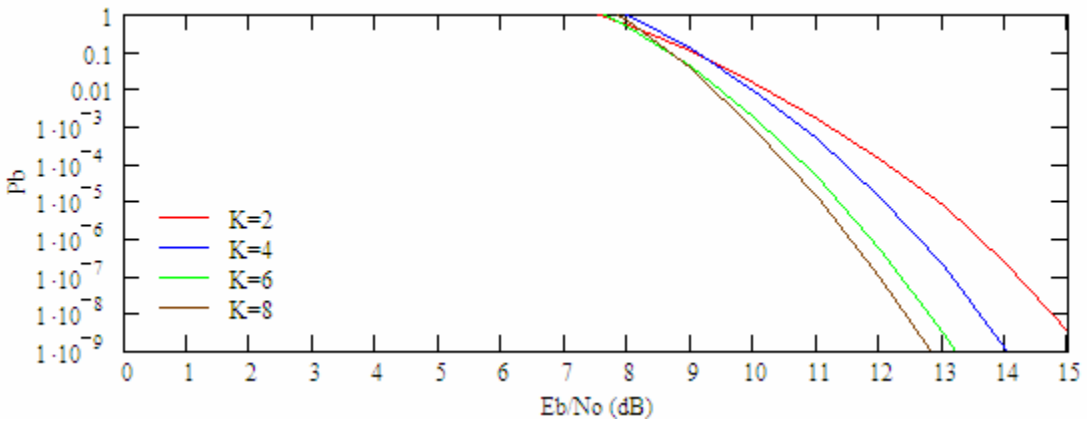


Figure 37. NCBFSK HDD with $r = 2/3$ and different values of constraint length.

The performance obtained by a convolutional encoder with a code rate of $3/4$ and for $K = 2$, $K = 4$, $K = 6$, and $K = 8$ memory elements is illustrated in Figure 38. Here, the required E_b/N_o for the four different cases are 13, 12.5, 12, 11.1 dB, respectively, and the resulting coding gains for the four cases are 0.3, 0.8, 1.3, 2.2 dB, respectively.

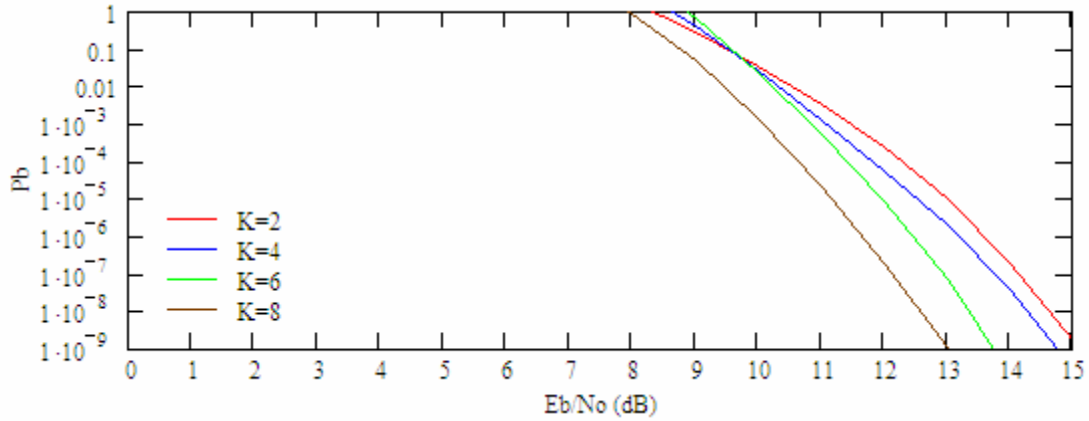


Figure 38. NCBFSK HDD with $r = 3/4$ and different values of constraint length.

The coding gains for NCBFSK with convolutional coding and HDD for several different combinations of code rates and number of memory elements are summarized in Table 19.

Table 19. Summary of coding gains for NCBFSK HDD.

	$K = 2$	$K = 4$	$K = 6$	$K = 8$
$r = 1/3$	0.2 dB	1.3 dB	2.1 dB	N/A
$r = 1/2$	0.8 dB	1.5 dB	2 dB	2.6 dB
$r = 2/3$	0.4 dB	1.2 dB	2 dB	2.3 dB
$r = 3/4$	0.3 dB	0.8 dB	1.3 dB	2.2 dB

From Table 19, we conclude that for NCBFSK with HDD, the optimum code rate is $r = 1/2$. Also, for a fixed code rate, the coding gain increases as the number of memory elements increases.

Comparing Tables 3 and 19, we see that the coding gain obtained with NCBFSK is about 0.3 to 1.3 dB less than obtained with BPSK for the same conditions.

b. Soft Decision Decoding

The performance of NCBFSK is determined when using convolutional coding and implementing SDD. The probability of bit error is upper-bounded by (2.3), where P_d is given by [7]

$$P_d = \frac{1}{2^{2^{d-1}}} \exp\left(\frac{-drE_b}{2N_o}\right) \sum_{n=0}^{d-1} c_n \left(\frac{drE_b}{2N_o}\right)^n \quad (4.2)$$

where

$$c_n = \frac{1}{n!} \sum_{m=0}^{d-1-n} \binom{2d-1}{m}. \quad (4.3)$$

The probabilities of bit error for NCBFSK for different convolutional encoders in an AWGN environment without interference or fading are illustrated in Figures 39, 40, 41, and 42.

The performance obtained with a convolutional encoder with a code rate of $1/3$ and for $K = 2$, $K = 4$, and $K = 6$ memory elements is illustrated in Figure 39. From this figure, the required E_b / N_o for the three different cases ($\nu = 3$, $\nu = 5$, and $\nu = 7$) are 11.4, 10.5, and 9.8 dB, respectively, and the resulting coding gains for the three cases are 1.9, 2.8, and 3.5 dB, respectively.

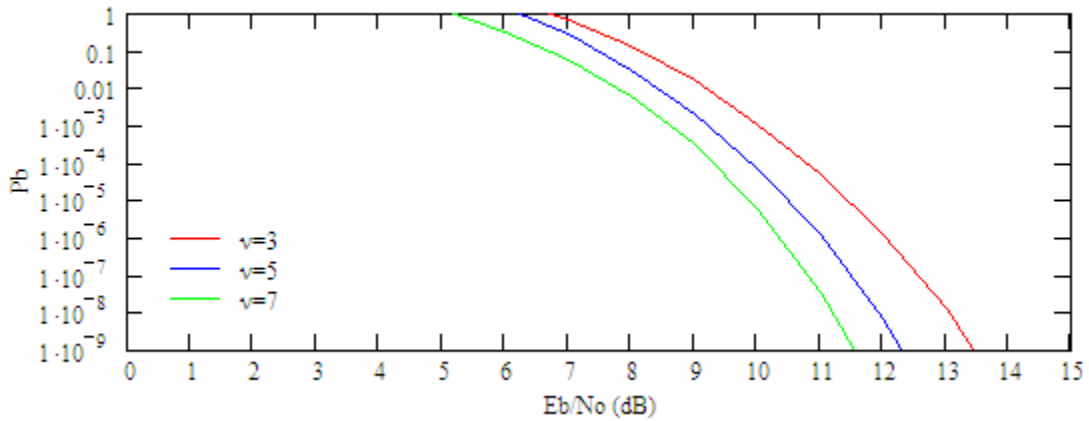


Figure 39. NCBFSK SDD with $r = 1/3$ and different values of constraint length.

The performance obtained with a convolutional encoder with a code rate of $1/2$ and for $K = 2$, $K = 4$, $K = 6$, and $K = 8$ memory elements is illustrated in Figure 40. Here, the required E_b / N_o for the four different cases ($\nu = 3, \nu = 5, \nu = 7$, and $\nu = 9$) are 11, 10.3, 9.6, 9.2 dB, respectively, and the resulting coding gains are 2.3, 3, 3.7, and 4.1 dB, respectively.

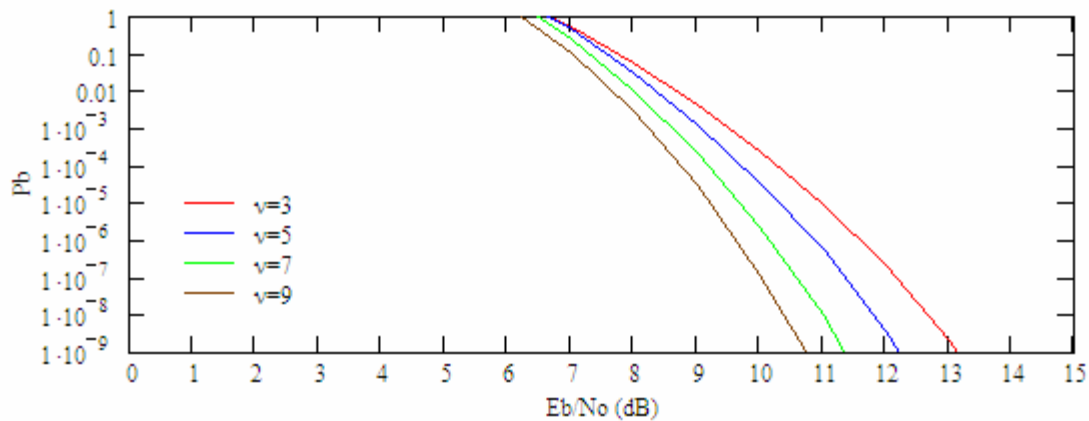


Figure 40. NCBFSK SDD with $r = 1/2$ and different values of constraint length.

The performance obtained with a convolutional encoder with a code rate of $2/3$ and for $K = 2$, $K = 4$, $K = 6$, and $K = 8$ memory elements is illustrated in Figure

41. Here, the required E_b / N_o for the four different cases are 11.1, 10.4, 9.7, 9.3 dB, respectively, and the resulting coding gains are 2.2, 2.9, 3.6, and 4 dB, respectively.

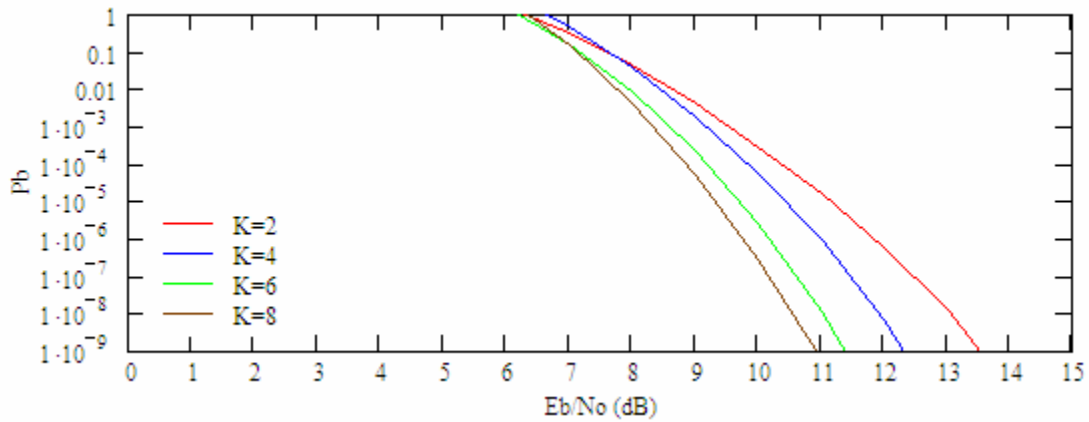


Figure 41. NCBFSK SDD with $r = 2/3$ and different values of constraint length.

The performance obtained with a convolutional encoder with a code rate of $3/4$ and for $K = 2$, $K = 4$, $K = 6$, and $K = 8$ memory elements is illustrated in Figure 42. Here, the required E_b / N_o for the four different cases are 11.3, 10.5, 10, 9.5 dB, respectively, and the resulting coding gains are 2, 2.8, 3.3, 3.8 dB, respectively.

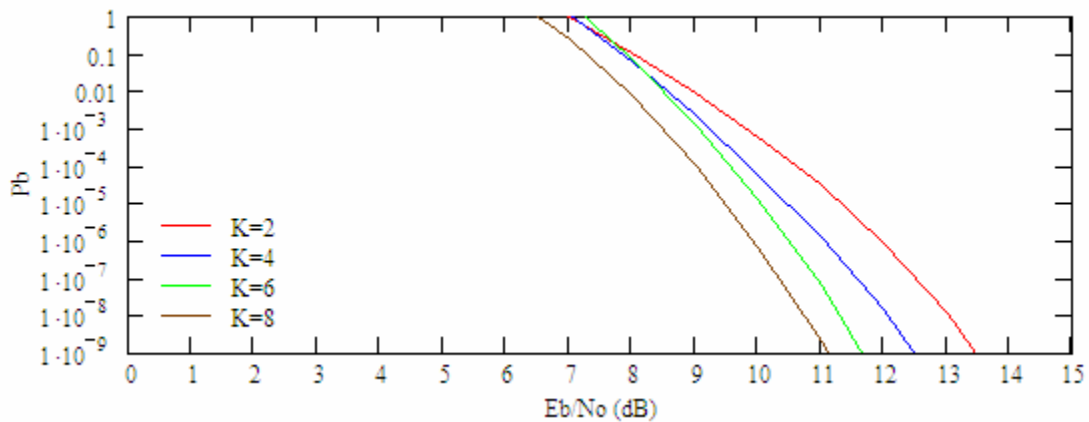


Figure 42. NCBFSK SDD with $r = 3/4$ and different values of constraint length.

The coding gains for NCBFSK with convolutional coding and SDD for several different combinations of code rates and number of memory elements are summarized in Table 20.

Table 20. Summary of coding gains for NCBFSK SDD.

	$K = 2$	$K = 4$	$K = 6$	$K = 8$
$r = 1/3$	1.9 dB	2.8 dB	3.5 dB	N/A
$r = 1/2$	2.3 dB	3 dB	3.7 dB	4.1 dB
$r = 2/3$	2.2 dB	2.9 dB	3.6 dB	4 dB
$r = 3/4$	2 dB	2.8 dB	3.3 dB	3.8 dB

From Table 20, we conclude that for NCBFSK with SDD, the optimum code rate is still $r = 1/2$. Also, for a fixed code rate, the coding gain increases as the number of memory elements increases.

Comparing Tables 19 and 20, we see that for NCBFSK, the coding gain is 1.4 to 2 dB less if HDD is used instead of SDD. Comparing Tables 4 and 20 finds that the coding gain obtained with NCBFSK is about 0.8 to 2.2 dB less than that obtained with BPSK for the same conditions.

C. NCBFSK IN AWGN IN A FADING ENVIRONMENT

1. Without FEC Coding

Using equation (2.11) for a Ricean fading channel and NCBFSK modulation, it can be shown that the average probability of bit error is given by [8]

$$P_b = \frac{1 + \zeta}{2(1 + \zeta) + \frac{E_b}{N_o}} \exp \left(\frac{-\zeta \frac{E_b}{N_o}}{2(1 + \zeta) + \frac{E_b}{N_o}} \right). \quad (4.4)$$

For a Rayleigh fading channel, the average probability of bit error is given by [7]

$$P_b = \frac{1}{2 + \frac{E_b}{N_o}}. \quad (4.5)$$

Using (4.4) and (4.5), Figure 43 is obtained, which shows the probability of bit error for NCBFSK in an AWGN without FEC coding and for different fading environments. From Figure 29, we conclude that the effect of fading on performance is very severe as ζ gets smaller. The results of the analysis show that in a non-fading environment, the required E_b/N_o is 13.3 dB, while for Ricean channels with $\zeta = 20$ and 10, the required E_b/N_o are 16.3 and 21.9 dB, respectively. As for Rayleigh fading, the required E_b/N_o jumps to the 50 dB! As for BPSK, the need for FEC coding in a fading environment is evident for NCBFSK.

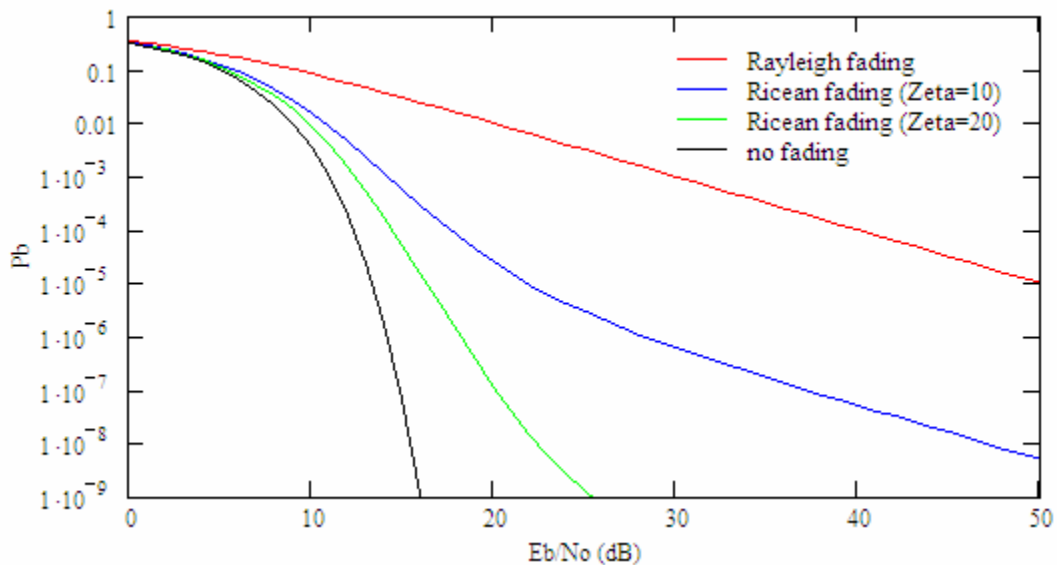


Figure 43. NCBFSK without FEC.

2. With FEC Coding and HDD

The performance of NCBFSK when using convolutional coding and implement HDD is determined in this section. The probability of bit error is upper-bounded by (2.3), where P_d is given by (2.4), and p_e is the probability of coded bit error obtained by replacing $E_b/N_o \rightarrow r E_b/N_o$ in either (4.4) or (4.5).

The probabilities of bit error of NCBFSK for different convolutional encoders in an AWGN environment with Rayleigh and Ricean fading are illustrated in Figures 44, 45, 46, and 47.

The performance obtained with a convolutional encoder for a code rate of $1/3$ and constraint lengths $\nu = 3$, $\nu = 5$, and $\nu = 7$ is illustrated in Figure 44. Three different fading environment cases are examined as in Chapter II: Rayleigh fading ($\zeta = 0$) and Ricean fading with $\zeta = 10$ and $\zeta = 20$.

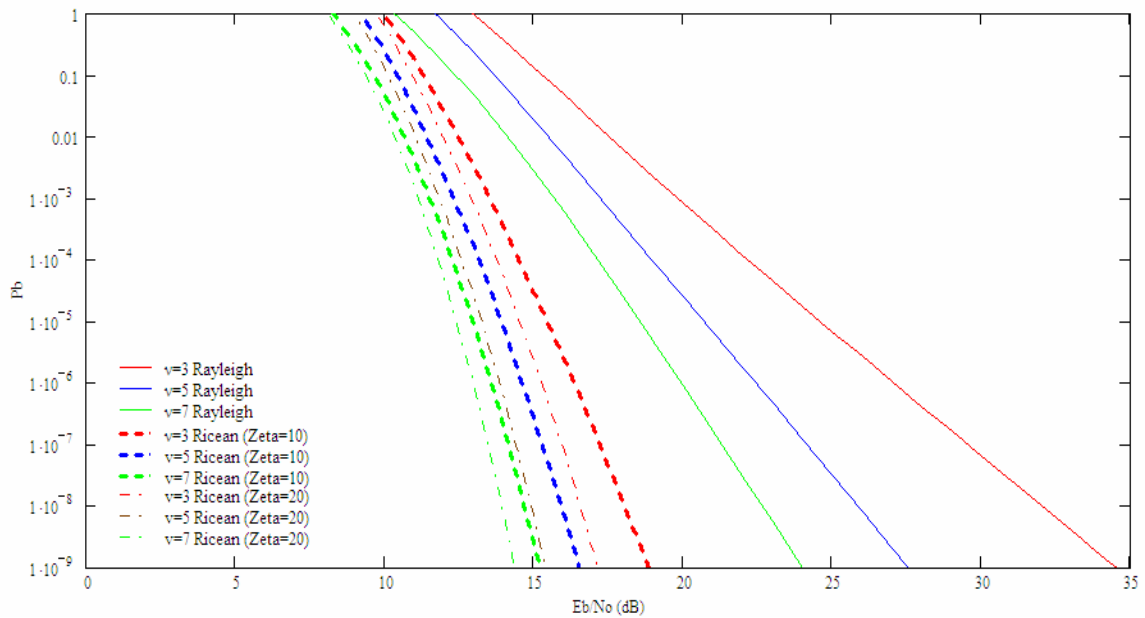


Figure 44. NCBFSK with FEC and HDD when $r = 1/3$.

From Figure 44, we can determine the E_b / N_o required to achieve the target P_b of 10^{-5} . For the three different cases ($\nu = 3, \nu = 5$, and $\nu = 7$) and Rayleigh fading, the required E_b / N_o is 24.6, 20.7, and 18.5 dB, respectively; for Ricean fading with $\zeta = 10$, the required E_b / N_o is 15.4, 13.9, and 12.9 dB, respectively; for Ricean fading with $\zeta = 20$, the required E_b / N_o is 14.5, 13.2, and 12.4 dB, respectively. The resulting coding gains are shown in Table 21.

Table 21. Summary of coding gains for NCBFSK HDD with $r = 1/3$ in fading environment.

	$K = 2$	$K = 4$	$K = 6$
Rayleigh fading	25.4 dB	29.3 dB	31.5 dB
Ricean fading $\zeta = 10$	6.5 dB	8 dB	9 dB
Ricean fading $\zeta = 20$	1.8 dB	3.1 dB	3.9 dB

The performance obtained with a convolutional encoder for a code rate of $1/2$ and constraint lengths $\nu = 3, \nu = 5, \nu = 7,$ and $\nu = 9$ is illustrated in Figure 45.

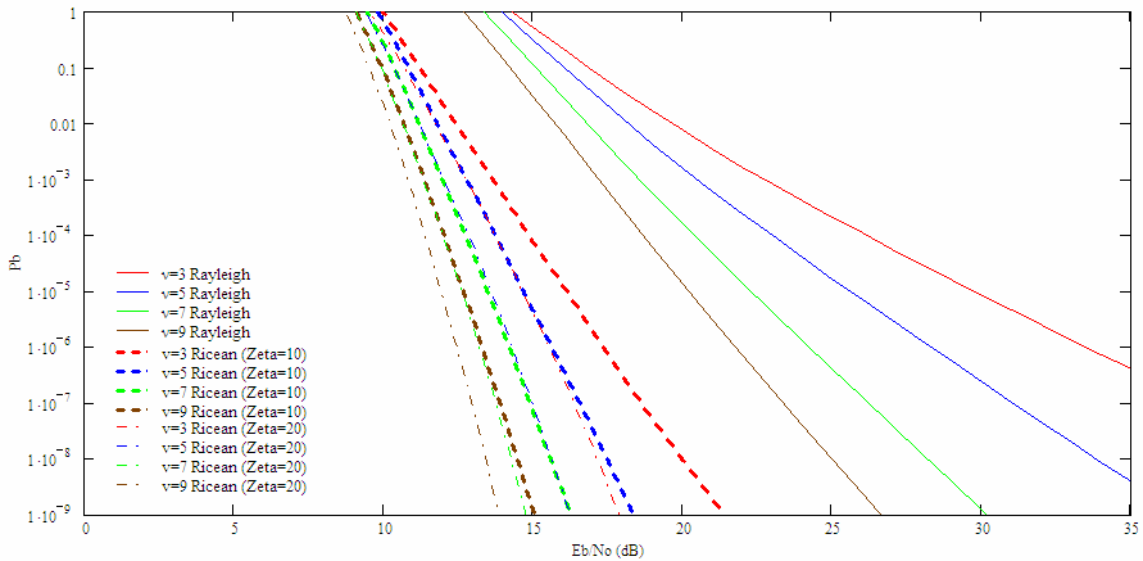


Figure 45. NCBFSK with FEC and HDD when $r = 1/2$.

Here, the required E_b / N_o for the four different cases ($\nu = 3, \nu = 5, \nu = 7,$ and $\nu = 9$) and Rayleigh fading is 29.7, 25.6, 22.3, and 20.2 dB, respectively; for Ricean fading with $\zeta = 10$, the required E_b / N_o is 16.1, 14.7, 13.5, and 12.7 dB, respectively; for Ricean fading with $\zeta = 20$, the required E_b / N_o is 14.7, 13.5, 12.6, and 11.9 dB, respectively. The resulting coding gains are shown in Table 22.

Table 22. Summary of coding gains for NCBFSK HDD with $r = 1/2$ in fading environment.

	$K = 2$	$K = 4$	$K = 6$	$K = 8$
Rayleigh fading	20.3 dB	24.4 dB	27.7 dB	29.8 dB
Ricean fading $\zeta = 10$	5.8 dB	7.2 dB	8.4 dB	9.2 dB
Ricean fading $\zeta = 20$	1.6 dB	2.8 dB	3.7 dB	4.4 dB

The performance obtained with a convolutional encoder for a code rate of $2/3$ and memory elements $K = 2$, $K = 4$, $K = 6$, and $K = 8$ is illustrated in Figure 46.

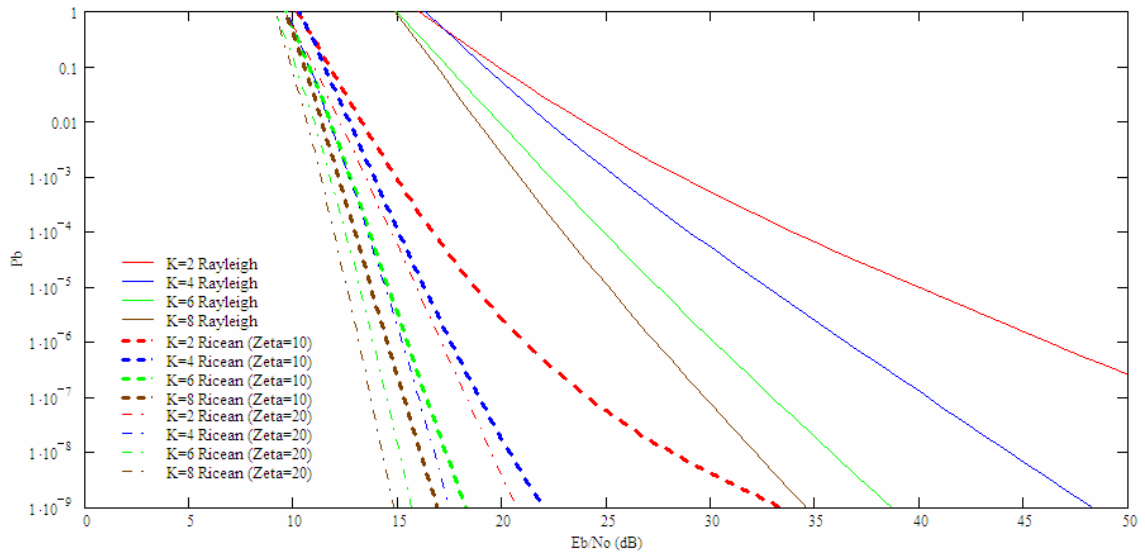


Figure 46. NCBFSK with FEC and HDD when $r = 2/3$.

Here, the required E_b / N_o for the four different cases ($K = 2$, $K = 4$, $K = 6$, and $K = 8$) and Rayleigh fading is 39.8, 32.6, 27.4, and 25 dB, respectively; for Ricean fading with $\zeta = 10$, the required E_b / N_o is 18.7, 16.2, 14.5, and 13.7 dB, respectively; for Ricean fading with $\zeta = 20$, the required E_b / N_o is 15.9, 13.7, 13.1, and 12.5 dB, respectively. The resulting coding gains are shown in Table 23.

Table 23. Summary of coding gains for NCBFSK HDD with $r = 2/3$ in fading environment.

	$K = 2$	$K = 4$	$K = 6$	$K = 8$
Rayleigh fading	10.2 dB	17.4 dB	22.6 dB	25 dB
Ricean fading $\zeta = 10$	3.2 dB	5.7 dB	7.4 dB	8.2 dB
Ricean fading $\zeta = 20$	0.4 dB	2.6 dB	3.2 dB	3.8 dB

The performance obtained with a convolutional encoder for a code rate of $3/4$ and memory elements $K = 2$, $K = 4$, $K = 6$, and $K = 8$ is illustrated in Figure 47.

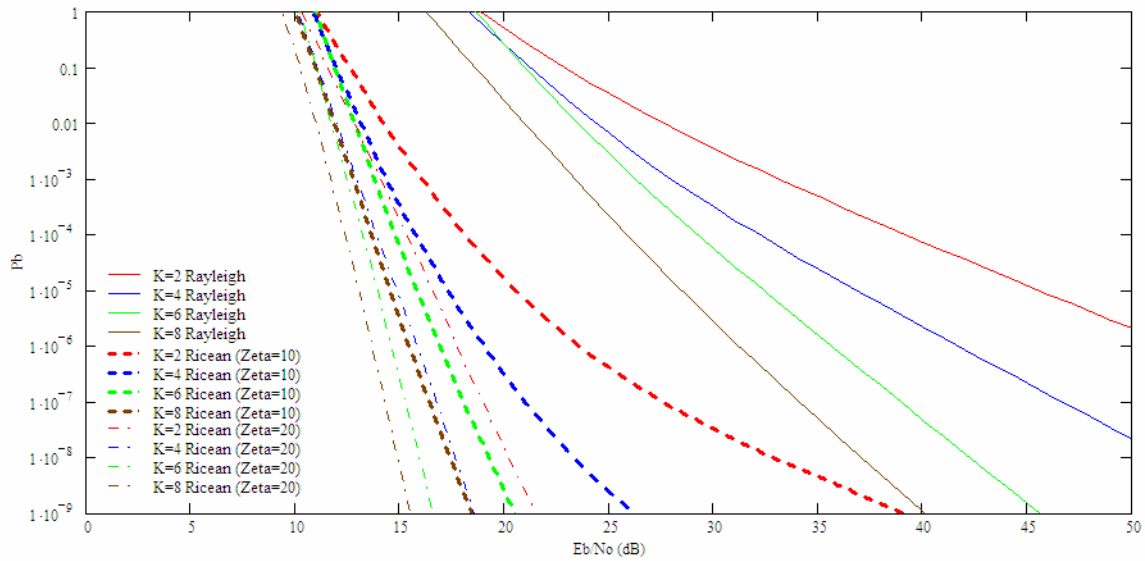


Figure 47. NCBFSK with FEC and HDD when $r = 3/4$.

Here, the required E_b / N_o for the four different cases ($K = 2$, $K = 4$, $K = 6$, and $K = 8$) and Rayleigh fading is 45.5, 36.7, 32.3, and 28.4 dB, respectively; for Ricean fading with $\zeta = 10$, the required E_b / N_o is 20.5, 17.3, 15.8, and 14.5 dB, respectively; for Ricean fading with $\zeta = 20$, the required E_b / N_o is 16.5, 14.8, 13.9, and 13 dB, respectively. The resulting coding gains are shown in Table 24.

Table 24. Summary of coding gains for NCBSK HDD with $r = 3/4$ in fading environment.

	$K = 2$	$K = 4$	$K = 6$	$K = 8$
Rayleigh fading	4.5 dB	13.3 dB	17.7 dB	21.6 dB
Ricean fading $\zeta = 10$	1.4 dB	4.6 dB	6.1 dB	7.4 dB
Ricean fading $\zeta = 20$	-0.2 dB	1.5 dB	2.4 dB	3.3 dB

The coding gains obtained with NCBFSK and HDD for different code rates and for the three different fading cases being examined are shown in Tables 25, 26, and 27.

Table 25. Summary of coding gains for NCBFSK HDD in Rayleigh fading.

	$K = 2$	$K = 4$	$K = 6$	$K = 8$
$r = 1/3$	25.4 dB	29.3 dB	31.5 dB	N/A
$r = 1/2$	20.3 dB	24.4 dB	27.7 dB	29.8 dB
$r = 2/3$	10.2 dB	17.4 dB	22.6 dB	25 dB
$r = 3/4$	4.5 dB	13.3 dB	17.7 dB	21.6 dB

Table 26. Summary of coding gains for NCBFSK HDD in Ricean fading with $\zeta = 10$.

	$K = 2$	$K = 4$	$K = 6$	$K = 8$
$r = 1/3$	6.5 dB	8 dB	9 dB	N/A
$r = 1/2$	5.8 dB	7.2 dB	8.4 dB	9.2 dB
$r = 2/3$	3.2 dB	5.7 dB	7.4 dB	8.2 dB
$r = 3/4$	1.4 dB	4.6 dB	6.1 dB	7.4 dB

Table 27. Summary of coding gains for NCBFSK HDD in Ricean fading with $\zeta = 20$.

	$K = 2$	$K = 4$	$K = 6$	$K = 8$
$r = 1/3$	1.8 dB	3.1 dB	3.9 dB	N/A
$r = 1/2$	1.6 dB	2.8 dB	3.7 dB	4.4 dB
$r = 2/3$	0.4 dB	2.6 dB	3.2 dB	3.8 dB
$r = 3/4$	-0.2 dB	1.5 dB	2.4 dB	3.3 dB

From Tables 25, 26, and 27, we conclude that for NCBFSK transmitted over fading channels with HDD, the coding gain increases as the number of memory elements increases and/or as the code rate decreases. This is contrary to what was found for the non-fading channel, when $r = 1/2$ is optimum. As might be expected, this phenomenon is most pronounced for Rayleigh fading and lessens as ζ increases.

3. With FEC Coding and SDD

The performance of NCBFSK with convolutional coding and SDD is determined in this section. The probability of bit error is upper-bounded by (2.3), where P_d is given by [7]

$$\begin{aligned}
 P_d = & \left[\frac{1+\zeta}{2(1+\zeta)+r\frac{E_b}{N_o}} \right]^d \exp \left[\frac{-\zeta dr \frac{E_b}{N_o}}{2(1+\zeta)+r\frac{E_b}{N_o}} \right] \\
 & \times \sum_{n=0}^{d-1} \left[\frac{1+\zeta+r\frac{E_b}{N_o}}{2(1+\zeta)+r\frac{E_b}{N_o}} \right]^n \sum_{p=0}^n \frac{1}{p!} \binom{d-1+n}{n-p} \left[\frac{\zeta(1+\zeta)dr\frac{E_b}{N_o}}{2(1+\zeta)^2+(2+\zeta)r\frac{E_b}{N_o}} \right]^p.
 \end{aligned} \tag{4.6}$$

The probabilities of bit error of NCBFSK for different convolutional encoders in an AWGN environment with Rayleigh and Ricean fading are illustrated in Figures 48, 49, 50, and 51.

The performance obtained with a convolutional encoder for a code rate of $1/3$ and constraint lengths $\nu = 3$, $\nu = 5$, and $\nu = 7$ is illustrated in Figure 48.

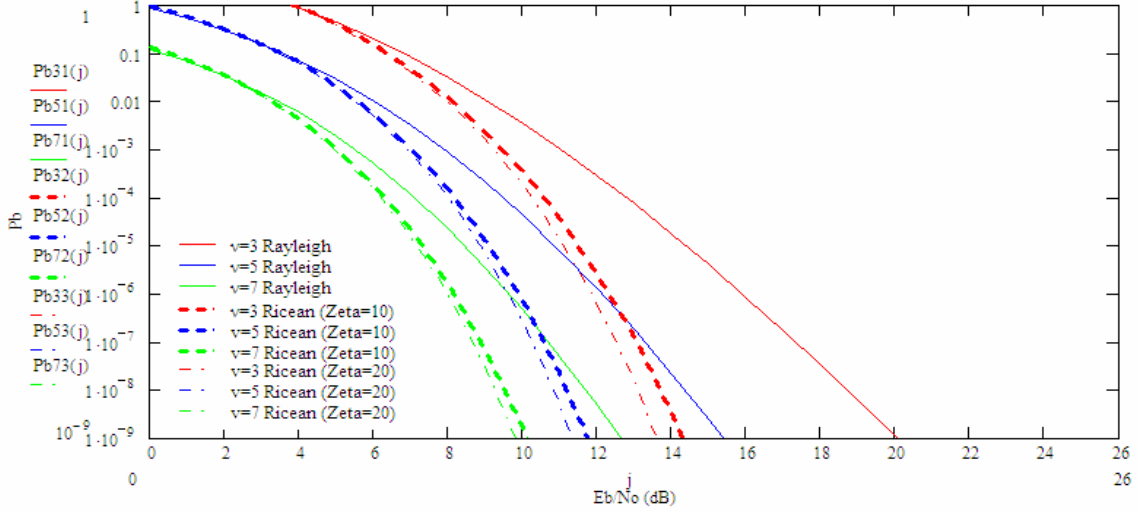


Figure 48. NCBFSK with FEC and SDD when $r = 1/3$.

From Figure 48, we can determine the E_b / N_o required to achieve the target P_b of 10^{-5} . For the three different cases ($\nu = 3, \nu = 5$, and $\nu = 7$) and Rayleigh fading, the required E_b / N_o is 14.4, 10.8, and 8.4 dB, respectively; for Ricean fading with $\zeta = 10$, the required E_b / N_o is 11.5, 9.1, AND 7.3 dB, respectively; for Ricean fading with $\zeta = 20$, the required E_b / N_o is 11.1, 8.9, and 7.1 dB, respectively. The resulting coding gains are shown in Table 28.

Table 28. Summary of coding gains for NCBFSK SDD with $r = 1/3$ in fading environment.

	$K = 2$	$K = 4$	$K = 6$
Rayleigh fading	35.6 dB	39.2 dB	41.6 dB
Ricean fading $\zeta = 10$	10.4 dB	12.8 dB	14.6 dB
Ricean fading $\zeta = 20$	5.2 dB	7.4 dB	9.2 dB

The performance obtained with a convolutional encoder for a code rate of 1/2 and constraint lengths $\nu = 3$, $\nu = 5$, $\nu = 7$, and $\nu = 9$ is illustrated in Figure 49.

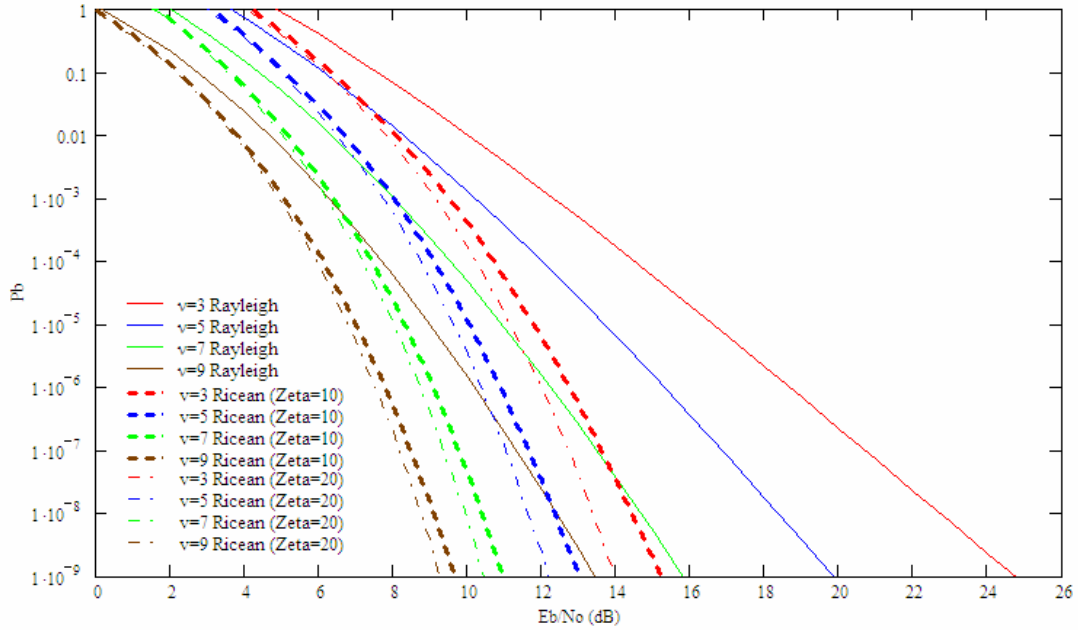


Figure 49. NCBFSK with FEC and SDD when $r = 1/2$.

Here, the required E_b/N_o for the four different cases ($\nu = 3, \nu = 5, \nu = 7$, and $\nu = 9$) and Rayleigh fading is 16.6, 13.6, 10.9, and 9 dB, respectively; for Ricean fading with $\zeta = 10$, the required E_b/N_o is 11.8, 10, 8.3, and 7 dB, respectively; for Ricean fading with $\zeta = 20$, the required E_b/N_o is 11.1, 9.6, 8, and 6.7 dB, respectively. The resulting coding gains are shown in Table 29.

Table 29. Summary of coding gains for NCBFSK SDD with $r = 1/2$ in fading environment.

	$K = 2$	$K = 4$	$K = 6$	$K = 8$
Rayleigh fading	33.4 dB	36.4 dB	39.1 dB	41 dB
Ricean fading $\zeta = 10$	10.1 dB	11.9 dB	13.6 dB	14.9dB
Ricean fading $\zeta = 20$	5.2 dB	6.7 dB	8.3 dB	9.6 dB

The performance obtained with a convolutional encoder for a code rate of $2/3$ and memory elements $K = 2$, $K = 4$, $K = 6$, and $K = 8$ is illustrated in Figure 50.

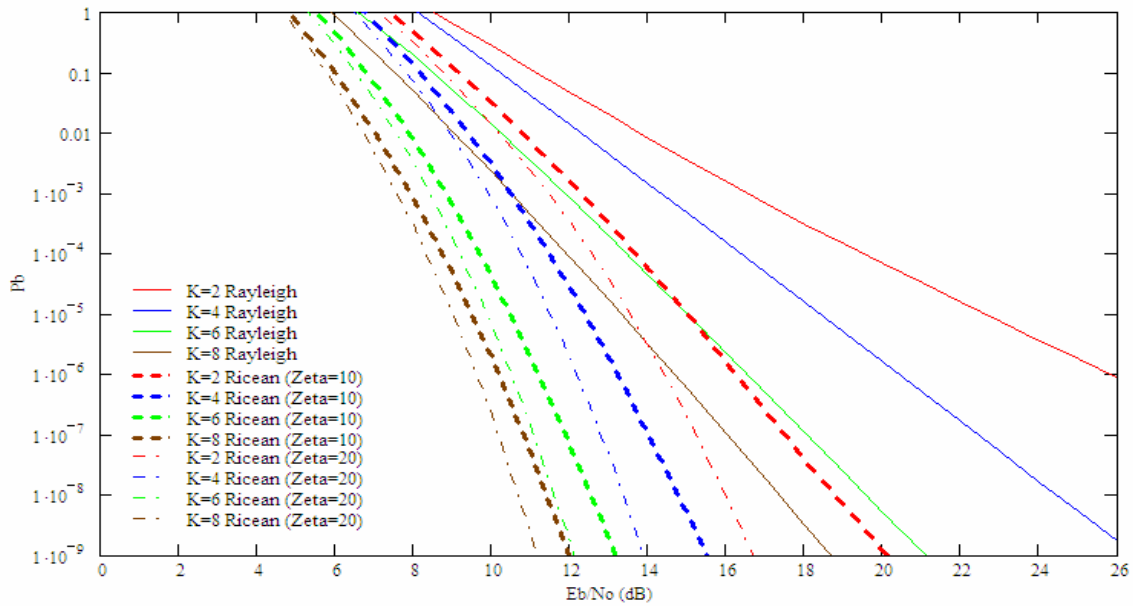


Figure 50. NCBFSK with FEC and SDD when $r = 2/3$.

Here, the required E_b / N_o for the four different cases ($K = 2$, $K = 4$, $K = 6$, and $K = 8$) and Rayleigh fading is 22.5, 18.4, 15, and 13.3 dB, respectively; for Ricean fading with $\zeta = 10$, the required E_b / N_o is 15, 12.8, 10.5, and 9.5 dB, respectively; for Ricean fading with $\zeta = 20$, the required E_b / N_o is 13.5, 11.5, 9.8, and 9 dB, respectively. The resulting coding gains are shown in Table 30.

Table 30. Summary of coding gains for NCBFSK SDD with $r = 2/3$ in fading environment.

	$K = 2$	$K = 4$	$K = 6$	$K = 8$
Rayleigh fading	27.5 dB	31.6 dB	35 dB	36.7 dB
Ricean fading $\zeta = 10$	6.9 dB	9.1 dB	11.4 dB	12.4 dB
Ricean fading $\zeta = 20$	2.8 dB	4.8 dB	6.5 dB	7.3 dB

The performance obtained with a convolutional encoder for a code rate of 3/4 and memory elements $K = 2$, $K = 4$, $K = 6$, and $K = 8$ is illustrated in Figure 51.

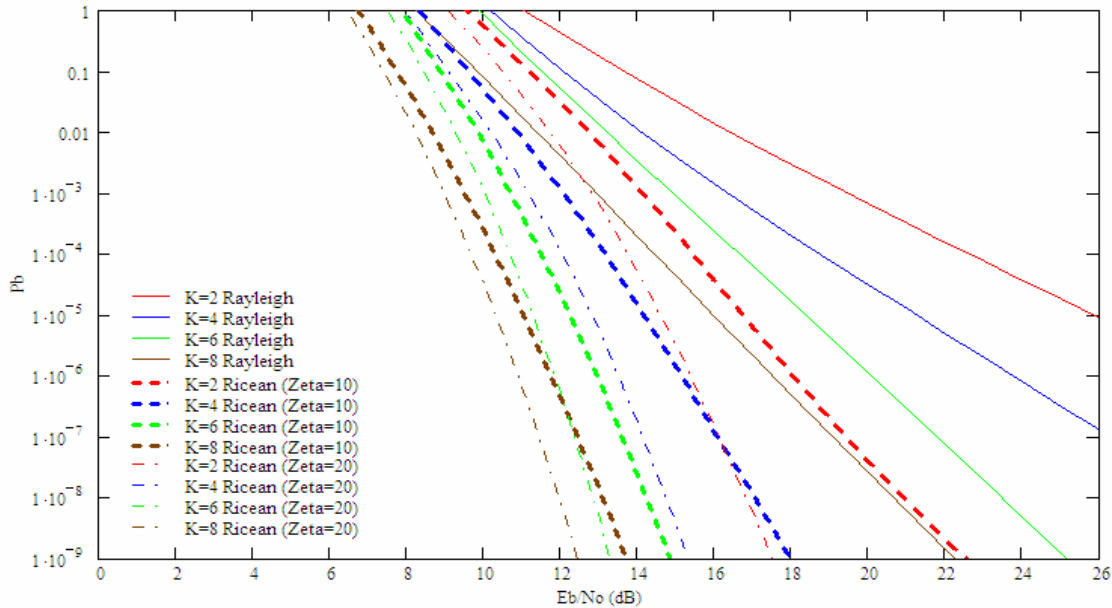


Figure 51. NCBFSK with FEC and SDD when $r = 3/4$.

Here, the required E_b / N_o for the four different cases ($K = 2$, $K = 4$, $K = 6$, and $K = 8$) and Rayleigh fading is 25.8, 21.2, 18.3, and 15.9 dB, respectively; for Ricean fading with $\zeta = 10$, the required E_b / N_o is 16.7, 14.1, 12.2, and 11 dB, respectively; for Ricean fading with $\zeta = 20$, the required E_b / N_o is 14.6, 12.8, 11.2, and 10.2 dB, respectively. The resulting coding gains are shown in Table 31.

Table 31. Summary of coding gains for NCBFSK SDD with $r = 3/4$ in fading environment.

	$K = 2$	$K = 4$	$K = 6$	$K = 8$
Rayleigh fading	24.2 dB	28.8 dB	31.7 dB	34.1 dB
Ricean fading $\zeta = 10$	5.2 dB	7.8 dB	9.7 dB	10.9 dB
Ricean fading $\zeta = 20$	1.7 dB	3.5 dB	5.1 dB	6.1 dB

The coding gains obtained with NCBFSK and SDD for different code rates and for the three different fading cases being examined are shown in Tables 32, 33, and 34.

Table 32. Summary of coding gains for NCBFSK SDD in Rayleigh fading.

	$K = 2$	$K = 4$	$K = 6$	$K = 8$
$r = 1/3$	35.6 dB	39.2 dB	41.6 dB	N/A
$r = 1/2$	33.4 dB	36.4 dB	39.1 dB	41 dB
$r = 2/3$	27.5 dB	31.6 dB	35 dB	36.7 dB
$r = 3/4$	24.2 dB	28.8 dB	31.7 dB	34.1 dB

Table 33. Summary of coding gains for NCBFSK SDD in Ricean fading with $\zeta = 10$.

	$K = 2$	$K = 4$	$K = 6$	$K = 8$
$r = 1/3$	10.4 dB	12.8 dB	14.6 dB	N/A
$r = 1/2$	10.1 dB	11.9 dB	13.6 dB	14.9dB
$r = 2/3$	6.9 dB	9.1 dB	11.4 dB	12.4 dB
$r = 3/4$	5.2 dB	7.8 dB	9.7 dB	10.9 dB

Table 34. Summary of coding gains for NCBFSK SDD in Ricean fading with $\zeta = 20$.

	$K = 2$	$K = 4$	$K = 6$	$K = 8$
$r = 1/3$	5.2 dB	7.4 dB	9.2 dB	N/A
$r = 1/2$	5.2 dB	6.7 dB	8.3 dB	9.6 dB
$r = 2/3$	2.8 dB	4.8 dB	6.5 dB	7.3 dB
$r = 3/4$	1.7 dB	3.5 dB	5.1 dB	6.1 dB

From Tables 32, 33, and 34, we summarize that for NCBFSK transmitted over fading channels with SDD, the coding gain increases as the number of memory elements increases or as the code rate decreases. We also note that as with HDD, $r = 1/2$ is no longer the optimum code rate when channel fading is present.

D. CHAPTER SUMMARY

The performance of NCBFSK modulation in AWGN, both with and without FEC convolutional coding and for different fading environments was analyzed in this chapter. A non-fading channel, a Rayleigh fading channel, and two different types of Ricean fading channels were examined. Next, NCBFSK in different fading environments is examined but now with the addition of pulse-noise interference.

THIS PAGE INTENTIONALLY LEFT BLANK

V. PERFORMANCE OF NCBFSK IN AN PULSE-NOISE INTERFERENCE ENVIRONMENT

A. INTRODUCTION

The performance of a NCBFSK modulated signal in an AWGN plus pulse-noise interference environment transmitted over different types of channels is analyzed in this chapter. First, the case with FEC and HDD in a non-fading channel with fixed pulse-noise interference as well as worst case is examined, and then the effect of a Rayleigh fading channel in a continuous jamming environment is examined. Next, the case with FEC and SDD using a linear combing receiver in a non-fading channel is analyzed, and the effect of a Rayleigh fading channel in a continuous jamming environment is studied. Lastly, the case with FEC and SDD using a noise-normalized receiver in a non-fading channel is investigated.

B. WITH CONVOLUTIONAL CODING AND HDD

1. Without Fading

For NCBFSK with FEC and HDD in an AWGN plus jamming environment combined with a non-fading channel, the probability of bit error is upper-bounded by (2.3), where P_d is given by (2.4), and p_e is the probability of coded bit error obtained from (3.2) and given by [7]

$$p_e = \frac{\rho}{2} \exp \left[\frac{-rE_b}{2 \left(N_o + \frac{N_I}{\rho} \right)} \right] + \frac{1-\rho}{2} \exp \left[\frac{-rE_b}{2N_o} \right]. \quad (5.1)$$

The cases with different duty cycles $\rho = 1$, $\rho = 0.3$, $\rho = 0.1$, $\rho = 0.01$, and worst case are examined in this section.

To obtain worst case, assume $E_b/N_o \gg 1$ and $N_I/\rho \gg N_o$, which results in the duty cycle factor for the worst case $\rho_{wc} \approx 2(rE_b/N_I)^{-1}$. Substituting ρ_{wc} into (5.1), we obtain [9]

$$(p_e)_{wc} \simeq \left(\frac{erE_b}{N_I} \right)^{-1}. \quad (5.2)$$

The SIR vs. E_b/N_o for NCBFSK when the jammer uses different duty cycles and when convolutional coding is used with HDD for different code rates and different numbers of memory elements at the target P_b of 10^{-5} are illustrated in Figures 52, 53, 54, and 55.

The SIR vs. E_b/N_o obtained with a convolutional encoder for a code rate of 1/3 and various numbers of memory elements in a non-fading channel but a jammed environment with different duty cycles is illustrated in Figure 52.

In general, the greater the number of memory elements, the better the performance of the system. From Figure 52, we conclude that no general rule exists for the value of duty cycle ρ that results in the most efficient jamming, but notice that increasing K reduces the difference between performance obtained with ρ_{wc} and that obtained with $\rho = 1$. Here, the performance obtained from the approximate ρ_{wc} is close to the worst performance for all cases with different duty cycles. Also, the interference with $\rho = 0.01$ is not efficient regardless of the number of memory elements; while for $K = 6$, the interference with $\rho = 0.1$ is not efficient either. In addition, there are two limiting cases in the curves. When the interference power is low (vertical part of the curves), the interference with the higher duty cycle is more efficient for all cases. When the AWGN power is low (horizontal part of the curves), the interference with $\rho = 0.1$ is the most efficient for $K = 2$; while for $K = 4$ and $K = 6$, the jammer with $\rho = 0.3$ is the most efficient.

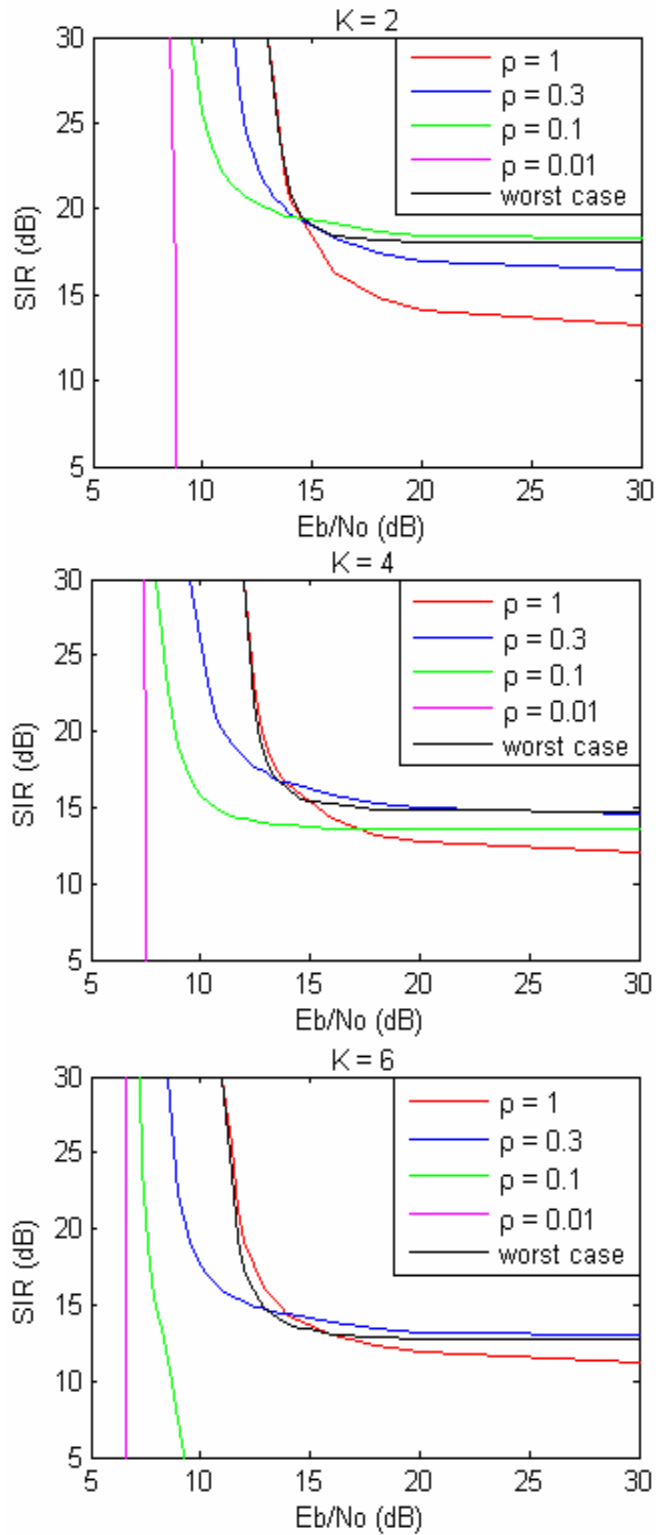


Figure 52. NCBFSK with FEC and HDD when $r=1/3$ in a jammed channel.

The SIR vs. E_b/N_o obtained with a convolutional encoder for a code rate of 1/2 and various numbers of memory elements in a non-fading channel but a jammed environment with different duty cycles is illustrated in Figure 53.

From Figure 53, we conclude that the interference with $\rho = 0.01$ is not efficient regardless of the number of memory elements. In addition, when the interference power is low, the interference with higher duty cycle is more efficient for all cases. When the AWGN power is low, the interference with $\rho = 0.1$ is the most efficient for all cases.

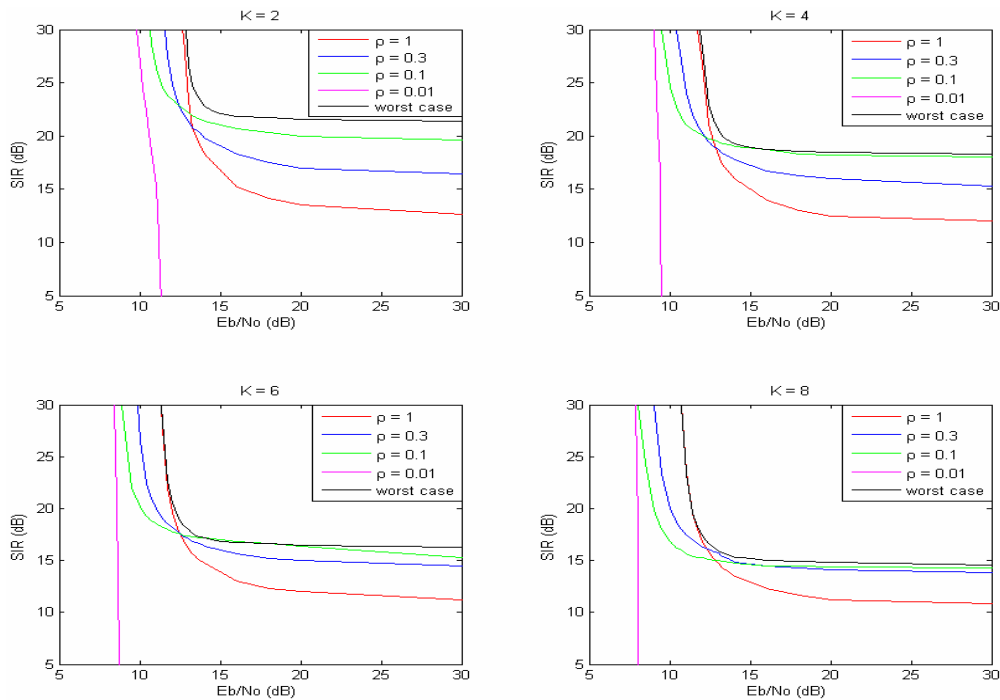


Figure 53. NCBFSK with FEC and HDD when $r=1/2$ in a jammed channel.

The SIR vs. E_b/N_o obtained with a convolutional encoder for a code rate of 2/3 and various numbers of memory elements in a non-fading channel but a jammed environment with different duty cycles is illustrated in Figure 54.

From Figure 54, we conclude that the interference with $\rho = 0.01$ is the most efficient for $K = 2$ and $K = 4$, whose performance are close to those obtained from the $(\rho)_{wc}$. For $K = 6$ and $K = 8$, the interference with $\rho = 0.01$ is not efficient, and when the

AWGN power is low (approximately $E_b/N_o > 15$ dB), the interference with $\rho = 0.1$ is the most efficient.

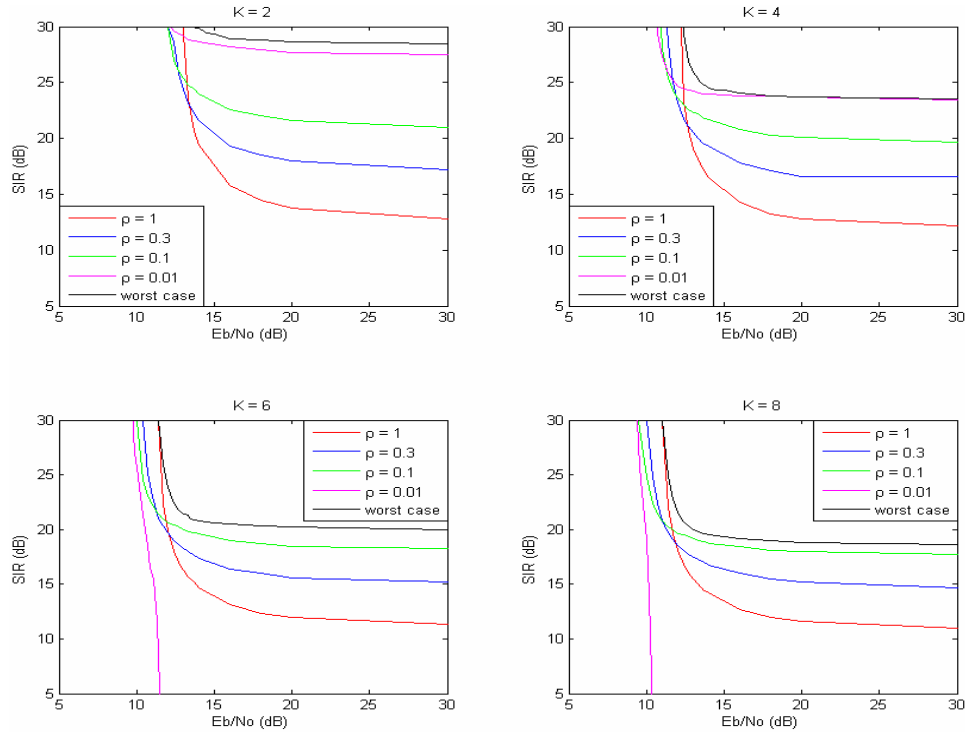


Figure 54. NCBFSK with FEC and HDD when $r=2/3$ in a jammed channel.

The SIR vs. E_b/N_o obtained with a convolutional encoder for a code rate of $3/4$ and various numbers of memory elements in a non-fading channel but a jammed environment with different duty cycles is illustrated in Figure 55.

From Figure 55, we conclude that the interference with $\rho = 0.01$ is the most efficient regardless of the number of memory elements, whose performance are close to those obtained from the $(\rho)_{wc}$. For $K = 2$, the SIR value obtained from $(\rho)_{wc}$ is above 30 dB regardless of E_b/N_o . For $K = 8$, the interference with $\rho = 0.1$ is efficient as well.

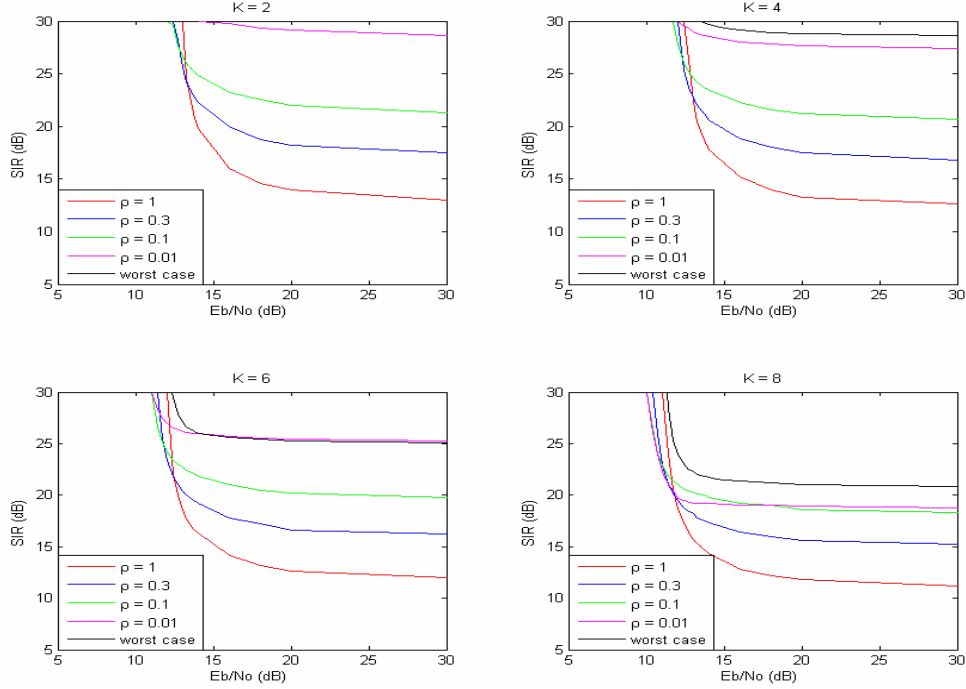


Figure 55. NCBFSK with FEC and HDD when $r=3/4$ in a jammed channel.

Comparing Figures 52, 53, 54, and 55, we conclude that increasing the number of memory elements and/or decreasing the code rate not only makes the low-duty cycle pulse-noise interference less efficient but also reduces the difference between the worst case performance and the interference with $\rho = 1$.

2. With Rayleigh Fading and Continuous Jamming ($\rho = 1$)

The performance of NCBFSK transmitted over the Rayleigh fading channel with FEC and HDD in an AWGN plus continuous jamming environment is discussed in this subsection. The probability of bit error is upper-bounded by (2.3), where P_d is given by (2.4), and p_e is the probability of coded bit error obtained by replacing $E_b/N_o \rightarrow r E_b/(N_o + N_I)$ in (4.5).

The SIR vs. E_b/N_o obtained with a convolutional encoder for different code rates and various numbers of memory elements in a Rayleigh fading channel and a continuous jammed environment is illustrated in Figure 56.

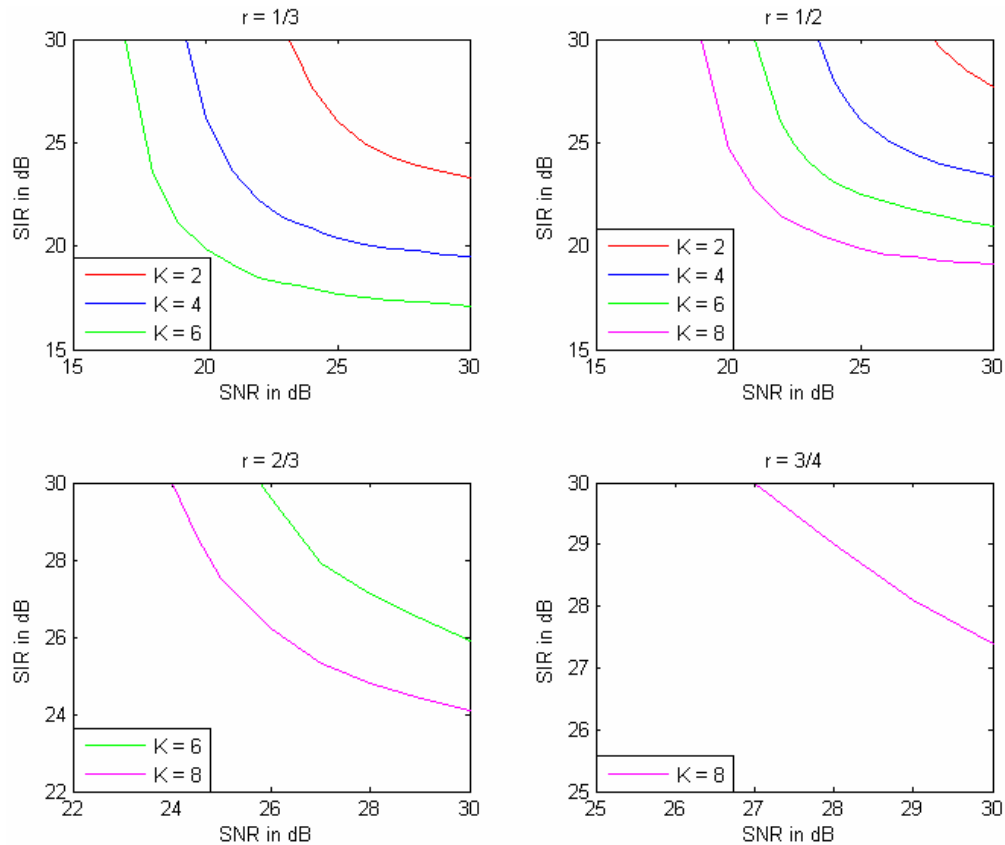


Figure 56. NCBFSK with FEC and HDD in a jammed channel with Rayleigh fading.

From Figure 56, we conclude that for NCBFSK transmitted over a Rayleigh fading channel with FEC, HDD, and continuous jamming, better performance occurs as the number of memory elements increases and/or as the code rate decreases. Also, it is evident that the target P_b of 10^{-5} is much more difficult to achieve in this case due to the nature of the multipath fading channel.

C. WITH CONVOLUTIONAL CODING AND SDD COMBINED WITH A LINEAR COMBINING RECEIVER

1. Using a Linear Combining Receiver in a Non-Fading Channel

The performance of NCBFSK transmitted over a non-fading channel when using convolutional coding with SDD and different code rates in a jammed environment with different duty cycles is examined in this section.

First, a linear combining receiver is examined. Assume that only i bits are jammed of the d independently received bits. The probability of bit error is upper-bounded by

(2.3), where P_d is given by (3.5). When there is no jamming, $P_d(i = 0)$ is given by (4.2). When there is continuous jamming, $P_d(i = d)$ is obtained by replacing $N_o \rightarrow N_o + N_i$ in (4.2). Analytically, it is difficult to estimate the value of $P_d(i)$ when $i \neq 0$ or $i \neq d$. Since $P_d(i = d) \geq P_d(i)$ for all i , an upper bound on P_d is given by

$$P_{d,u} \leq \binom{d}{0} \rho^0 (1-\rho)^d P_d(i=0) + \sum_{i=1}^d \binom{d}{i} \rho^i (1-\rho)^{d-i} P_d(i=d). \quad (5.3)$$

The equality holds when $\rho = 1$.

Only the upper bound is examined in this section since the analysis involves the worst case scenario for communications.

The SIR vs. E_b/N_o for NCBFSK obtained when using a linear combining receiver when the jammer uses different duty cycles and when convolutional coding is used with SDD with different code rates and different numbers of memory elements at the target P_b of 10^{-5} are illustrated in Figures 57, 58, 59, and 60.

The SIR vs. E_b/N_o obtained with a convolutional encoder for a code rate of 1/3 and various number of memory elements in a non-fading channel but a jammed environment with different duty cycles is illustrated in Figure 57.

From Figure 57, we conclude that for NCBFSK transmitted over a non-fading channel with FEC and SDD when using a linear combining receiver, the performance improves as the number of memory elements increases and/or as the duty cycle increases. In addition, the interference with $\rho = 0.01$ is the most efficient regardless of the number of memory elements.

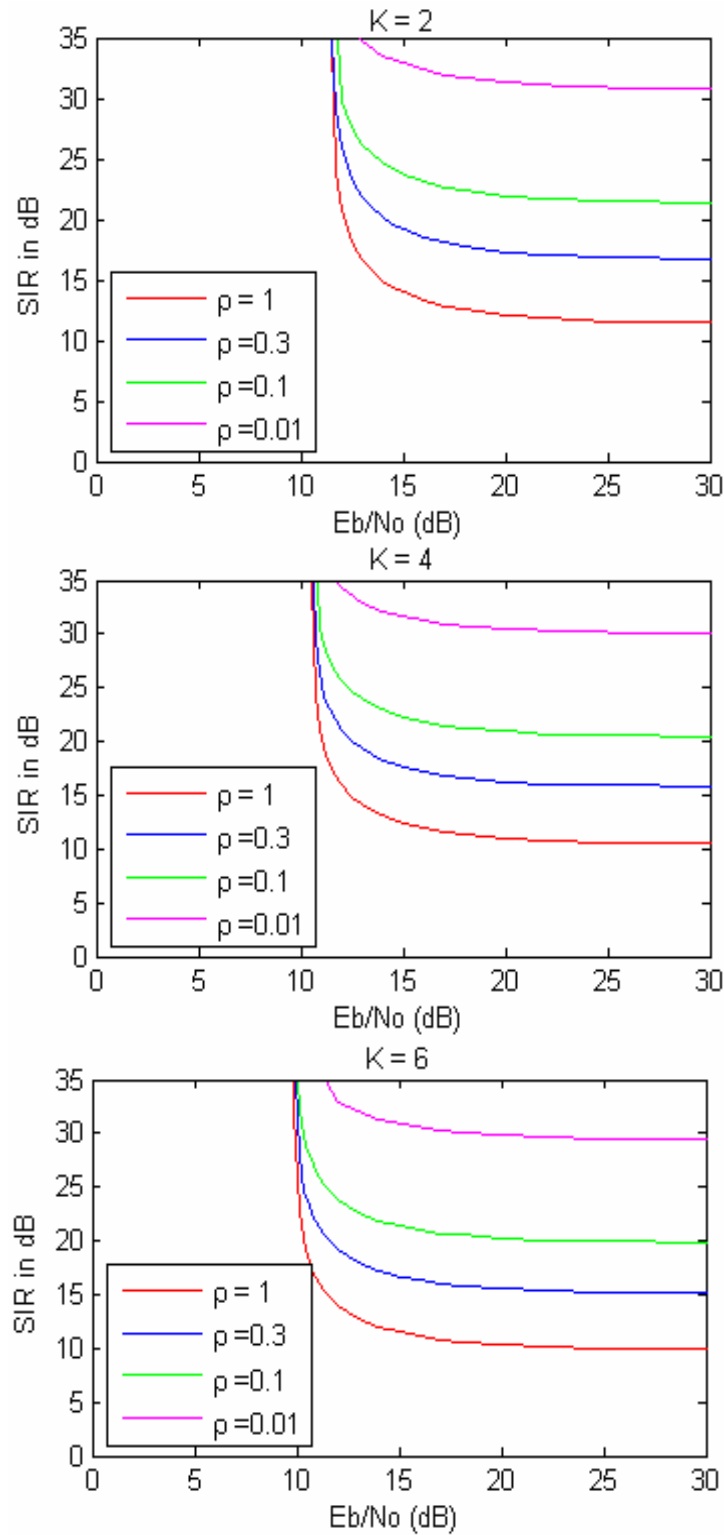


Figure 57. NCBFSK with FEC and SDD combined with linear combining receiver when $r = 1/3$.

The SIR vs. E_b/N_o obtained with a convolutional encoder for a code rate of 1/2 and various number of memory elements in a non-fading channel but a jammed environment with different duty cycles is illustrated in Figure 58.

From Figure 58, we conclude that the interference with $\rho = 0.01$ is the most efficient regardless of the number of memory elements. The performance only improves slightly as the number of memory elements increases for small ρ .

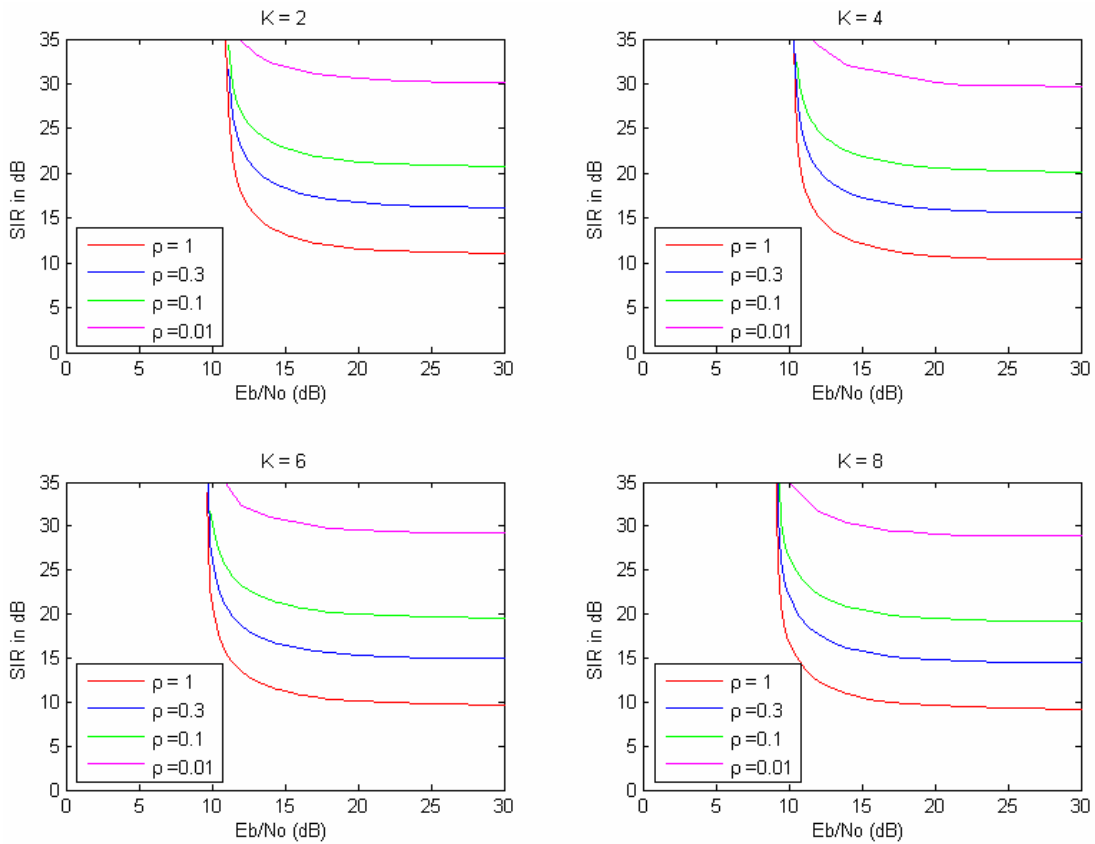


Figure 58. NCBFSK with FEC and SDD combined with linear combining receiver when $r = 1/2$.

The SIR vs. E_b/N_o obtained with a convolutional encoder for a code rate of 2/3 and various number of memory elements in a non-fading channel but a jammed environment with different duty cycles is illustrated in Figure 59.

From Figure 59, we reach the same conclusions as those obtained for the rate 1/2 code. The interference with $\rho = 0.01$ is the most efficient regardless of the number of memory elements, and the performance only improves slightly as the number of memory elements increases for small ρ .

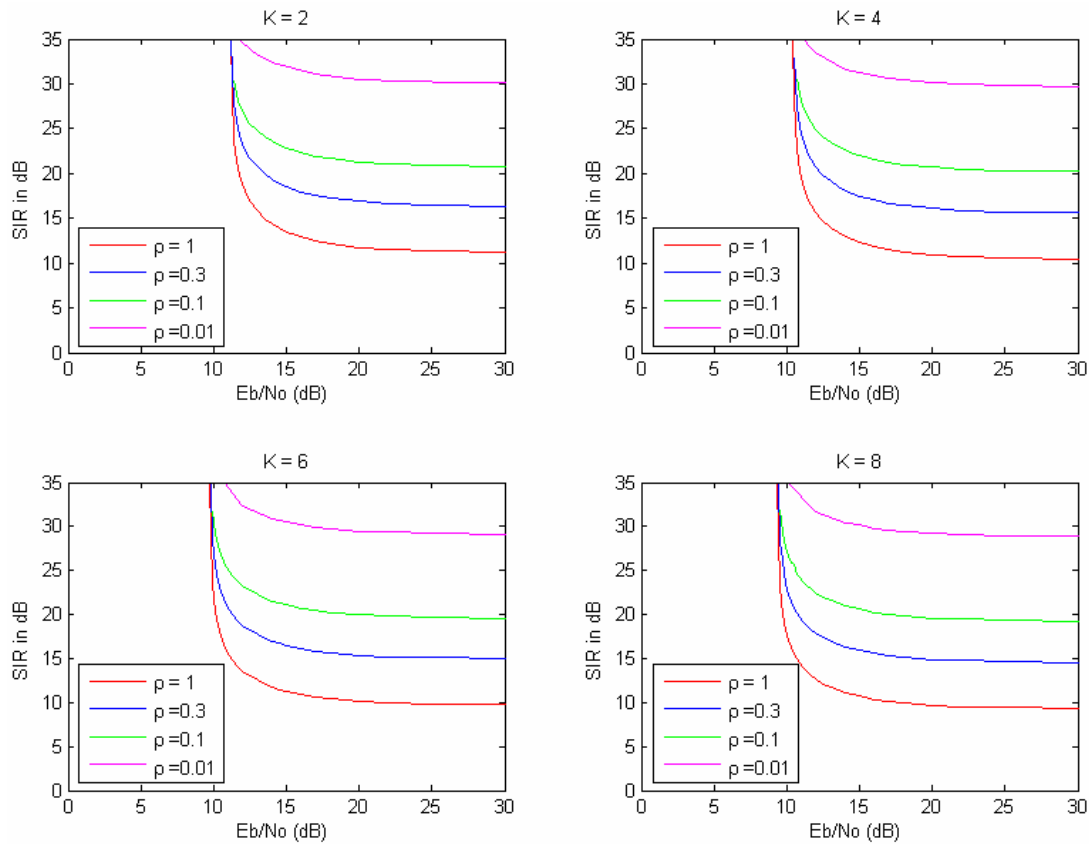


Figure 59. NCBFSK with FEC and SDD combined with linear combining receiver when $r = 2/3$.

The SIR vs. E_b/N_o obtained with a convolutional encoder for a code rate of 3/4 and various number of memory elements in a non-fading channel but a jammed environment with different duty cycles is illustrated in Figure 60.

From Figure 60, we reach the same conclusions as those obtained for the lower code rates. The interference with $\rho = 0.01$ is the most efficient regardless of the number

of memory elements, and the performance only improves slightly as the number of memory elements increases for small ρ .

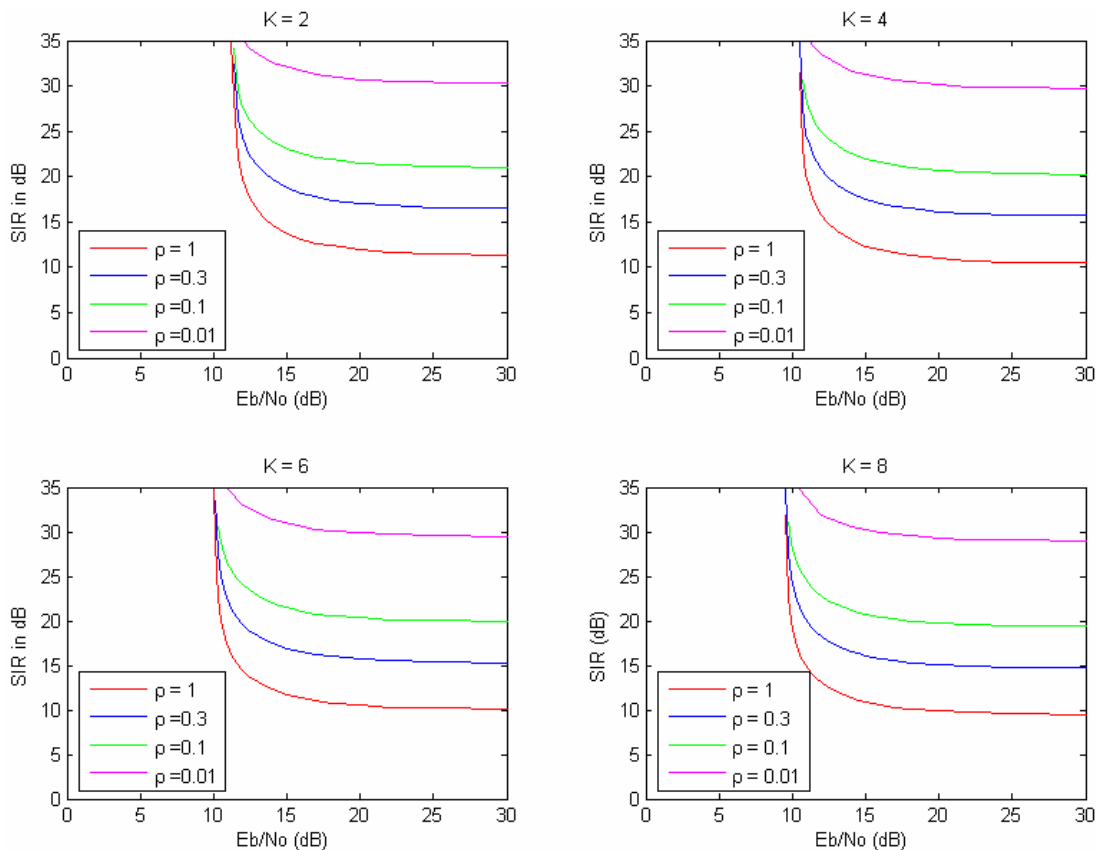


Figure 60. NCBFSK with FEC and SDD combined with linear combining receiver when $r = 3/4$.

From Figures 57, 58, 59, and 60, we conclude that for NCBFSK with FEC and SDD in a jammed environment but without fading when using a linear combining receiver, the performance degrades as ρ decreases and that interference with $\rho = 0.01$ is the most efficient.

2. Using a Linear Combining Receiver in a Rayleigh Fading Channel

This section determines the performance of NCBFSK transmitted over a Rayleigh fading channel with FEC and SDD in an AWGN plus continuous jamming environment

when using a linear combining receiver. The probability of bit error is upper-bounded by (2.3), where P_d is obtained by replacing $N_o \rightarrow N_o + N_I$ in (4.5) and with $\zeta = 0$.

The SIR vs. E_b/N_o obtained with a convolutional encoder for different code rates and various numbers of memory elements in a Rayleigh fading channel and a continuous jammed environment is illustrated in Figure 61.

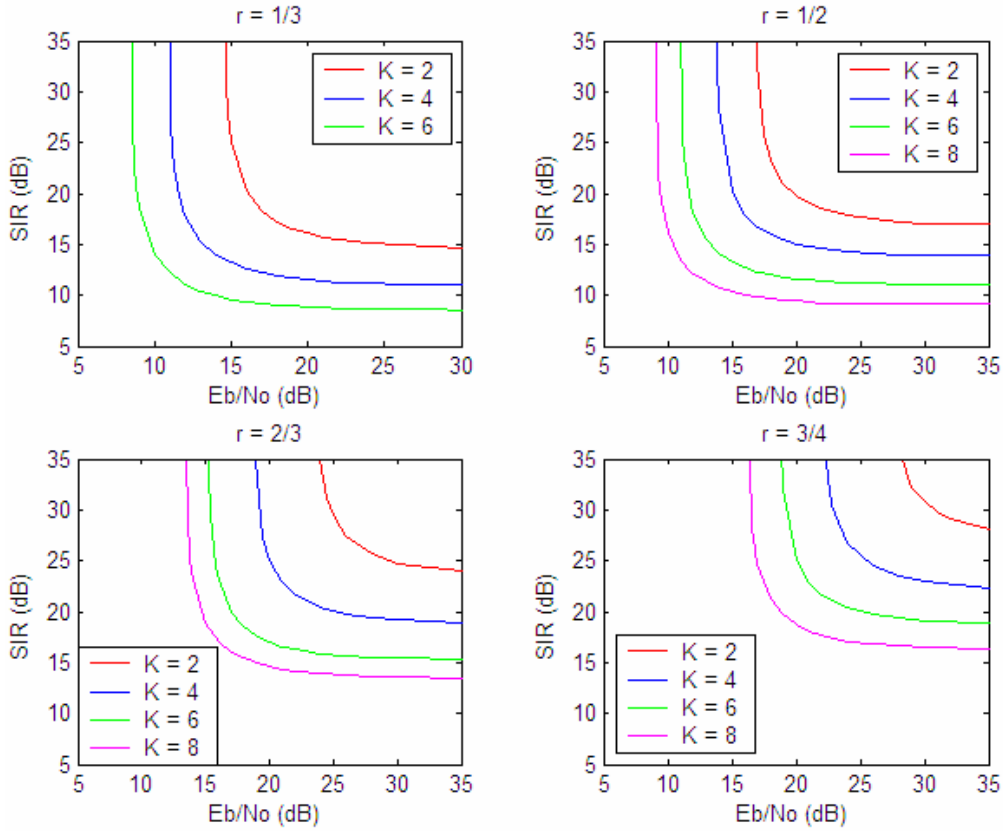


Figure 61. NCBFSK with FEC and SDD combined with linear combining receiver in Rayleigh fading

From Figure 61, we conclude that for NCBFSK transmitted over a Rayleigh fading channel with FEC, SDD, and continuous jamming, performance is improved as the number of memory elements increases and/or as the code rate decreases. Also, it is clear that the nature of the fading channel makes communications more difficult since a much stronger signal is needed to achieve the desired performance.

3. Using a Noise-Normalized Receiver in a Non-Fading Channel

The performance of NCBFSK transmitted over a non-fading channel with convolutional coding and SDD with different code rates in a jammed environment with different duty cycles and a noise-normalized receiver is examined in this section.

In this case, the probability of bit error is upper-bounded by (2.3), where P_d is given by (3.5), and $P_d(i)$ is expressed as [7]

$$P_d(i) = \frac{1}{2^{2^{d-1}}} \exp \left[\frac{-rE_b}{2} \left(\frac{i}{N_o + \frac{N_I}{\rho}} + \frac{d-i}{N_o} \right) \right] \sum_{n=0}^{d-1} c_n \left[\frac{rE_b}{2} \left(\frac{i}{N_o + \frac{N_I}{\rho}} + \frac{d-i}{N_o} \right) \right]^n \quad (5.4)$$

where c_n is given by (4.3).

The SIR vs. E_b/N_o for NCBFSK obtained when using a noise-normalized receiver, when the jammer uses different duty cycles, and when convolutional coding is used with SDD with different code rates and different numbers of memory elements at the target P_b of 10^{-5} are illustrated in Figures 62, 63, 64, and 65.

The SIR vs. E_b/N_o obtained with a convolutional encoder for a code rate of 1/3 and the various number of memory elements in a non-fading channel but a jammed environment with different duty cycles is illustrated in Figure 62.

From Figure 62, we conclude that for NCBFSK transmitted over a non-fading channel with FEC and SDD for a code rate of 1/3 when using a noise-normalized receiver, the performance improves as the number of memory elements increases or as the duty cycle decreases. For all cases, the worst performance obtained is for $\rho = 1$. Recall that for the same conditions but with a linear combining receiver that the interference with $\rho = 0.01$ is the most efficient. The use of the noise-normalized receiver negates the effect of the pulse-noise interference.

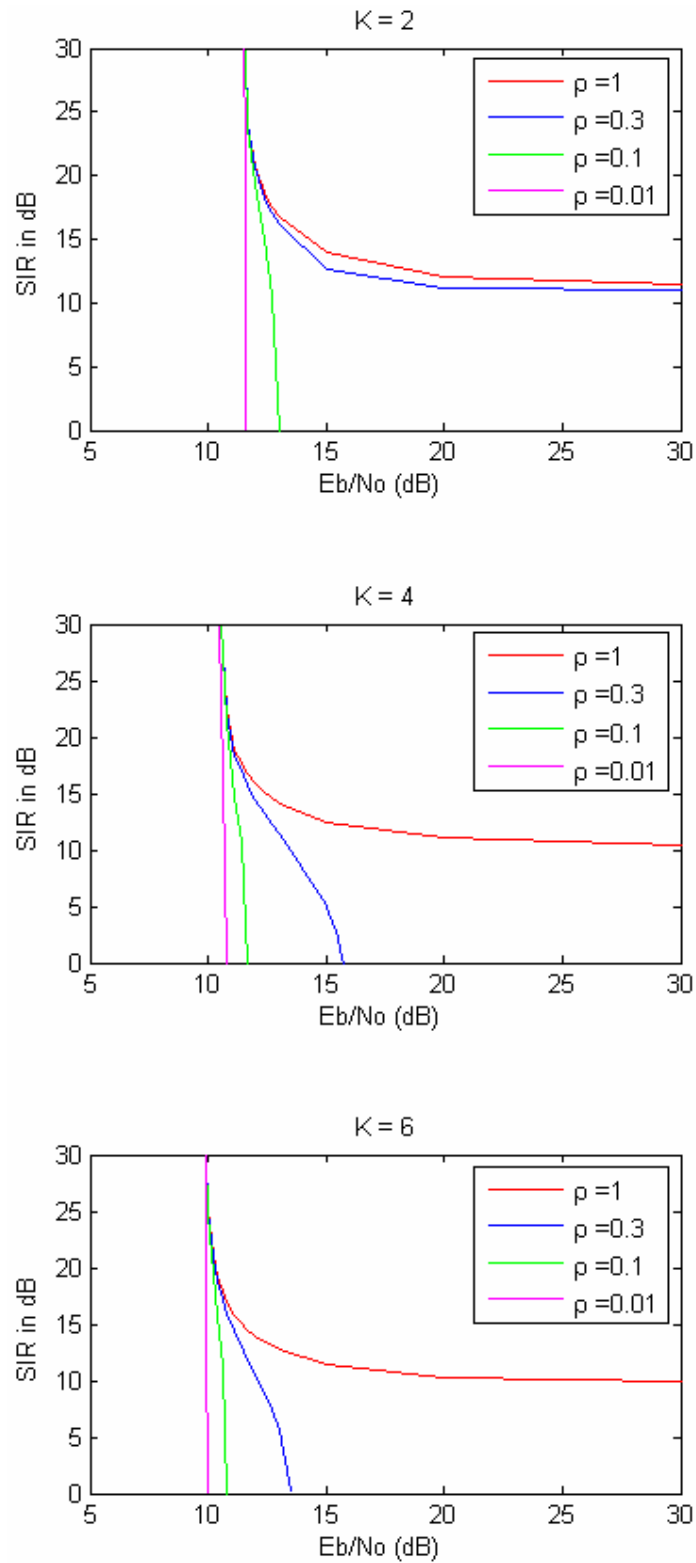


Figure 62. NCBFSK with FEC and SDD combined with noise-normalized receiver when $r = 1/3$.

The SIR vs. E_b/N_o obtained with a convolutional encoder for a code rate of 1/2 and the various number of memory elements in a non-fading channel but a jammed environment with different duty cycles is illustrated in Figure 63.

From Figure 63, we conclude that for NCBFSK transmitted over a non-fading channel with FEC and SDD for a code rate of 1/2 when using a noise-normalized receiver that the interference with $\rho = 0.1$ and $\rho = 0.01$ are not efficient regardless of the number of memory elements. For $K = 2$ and $K = 4$, the interference with $\rho = 0.3$ is the most effective case; while for $K = 6$ and $K = 8$, the interference with $\rho = 1$ is the most effective case.

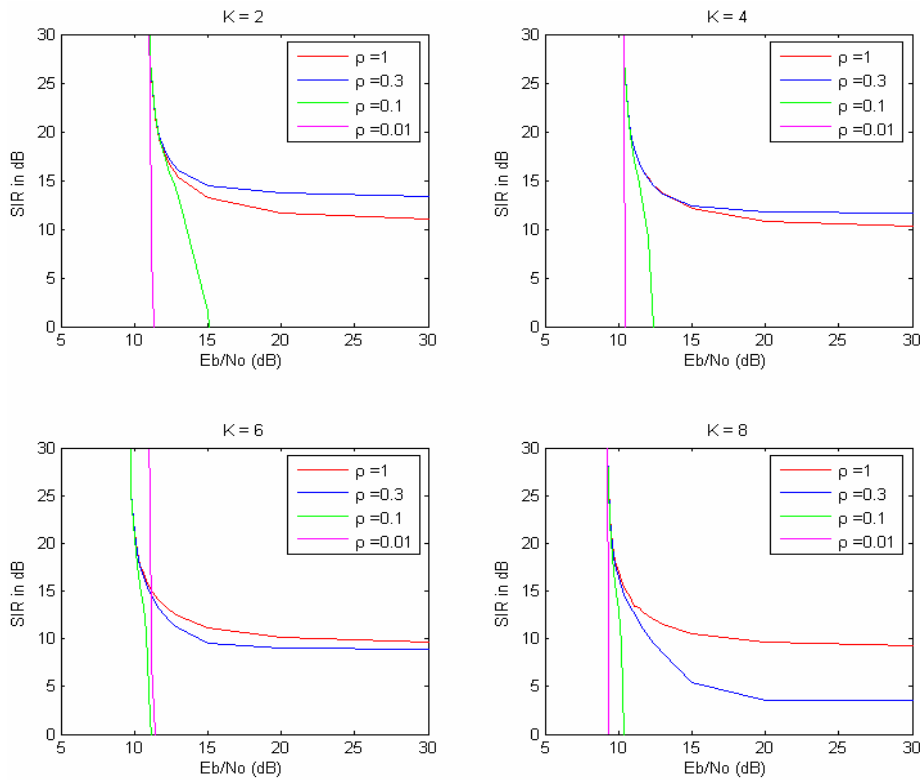


Figure 63. NCBFSK with FEC and SDD combined with noise-normalized receiver when $r = 1/2$.

The SIR vs. E_b/N_o obtained with a convolutional encoder for a code rate of 2/3 and the various number of memory elements in a non-fading channel but a jammed environment with different duty cycles is illustrated in Figure 64.

From Figure 64, we conclude that for NCBFSK transmitted over a non-fading channel with FEC and SDD for a code rate of $2/3$ when using a noise-normalized receiver that the interference with $\rho = 0.01$ is not efficient regardless of the number of memory elements, and that $\rho = 0.1$ is not efficient for $K = 6$ and $K = 8$. Also, the interference with $\rho = 0.1$ is the most effective for $K = 2$; while for $K = 4$, $K = 6$ and $K = 8$, the interference with $\rho = 0.3$ is the most effective.

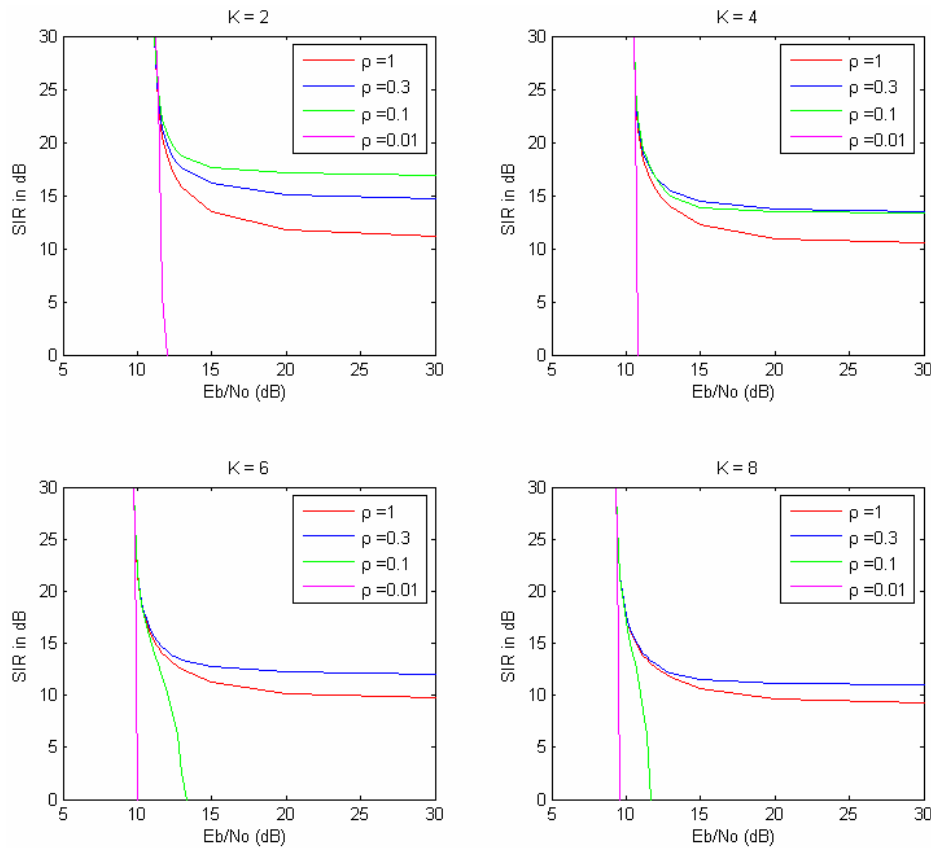


Figure 64. NCBFSK with FEC and SDD combined with noise-normalized receiver when $r = 2/3$.

The SIR vs. E_b/N_o obtained with a convolutional encoder for a code rate of $3/4$ and the various number of memory elements in a non-fading channel but a jammed environment with different duty cycles is illustrated in Figure 65.

From Figure 65, we conclude that for NCBFSK transmitted over a non-fading channel with FEC and SDD for a code rate of $3/4$ when using a noise-normalized receiver

that the interference with $\rho = 0.01$ is not efficient regardless of the number of memory elements. Also, the interference with $\rho = 0.1$ is the most effective for $K = 2$, $K = 4$ and $K = 6$; while for $K = 8$, the interference with $\rho = 0.3$ is the most effective.

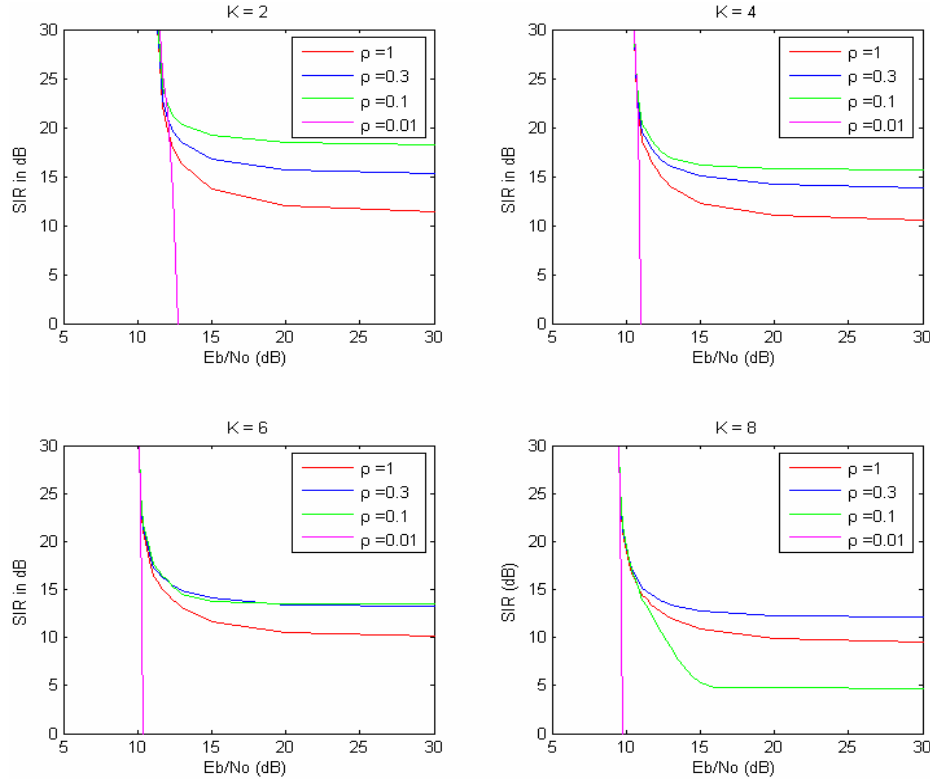


Figure 65. NCBFSK with FEC and SDD combined with noise-normalized receiver when $r = 3/4$.

In general, as can be seen from Figures 62, 63, 64, and 65, as the code rate decreases, the effect of pulse-noise interference decreases (i.e., pulse-noise interference becomes inefficient). This fact is more evident for large K . Also, as the number of memory elements increases for a fixed code rate, pulse-noise jamming with low duty cycle (smaller than 0.1) becomes inefficient. As a result, the worst case performance for $K = 6$ and $K = 8$ occurs either for continuous jamming or for pulse-noise interference with $\rho = 0.3$, depending on the code rate. For the lower code rates with K large, the effects of pulse-noise interference are essentially negated.

D. CHAPTER CONCLUSION

The performance of NCBFSK modulation in an AWGN plus pulse-noise interference environment transmitted over different types of channels was examined in this chapter. First, NCBFSK with FEC and HDD for both a non-fading channel with different duty cycles as well as worst case as well as the effect of a Rayleigh fading channel in a continuous jamming environment was examined. Next, NCBFSK with FEC and SDD using a linear combining receiver in a non-fading channel and in a Rayleigh fading channel was examined. Lastly, the effect of the noise-normalized receiver in the case of FEC and SDD in a non-fading channel was studied.

THIS PAGE INTENTIONALLY LEFT BLANK

VI. CONCLUSIONS

A. INTRODUCTION

The performance of BPSK and NCBFSK modulated signals transmitted over frequency-nonselctive, slowly fading channels in a worst case, pulse-noise interference environment was examined in this thesis. After developing the basic theoretical concepts related to fading channels and error correction coding, the analysis started with the case of only AWGN. The signals were assumed to be transmitted over different types of channels (non-fading, Ricean fading, and Rayleigh fading) combined with either hard or soft decision Viterbi decoding. The performance of convolutional codes for different code rates and different constraint lengths was evaluated. Next, the analysis was extended to an environment where AWGN and noise-like pulse interference were both present. The SIR vs. E_b/N_o obtained for the different cases at a target P_b of 10^{-5} (which is considered the practical limit for successful digital communications) were shown. The plots are an illustration of where communications are successful ($P_b < 10^{-5}$), located in the upper right areas of the curves. In this case, the analysis involved either a non-fading or a Rayleigh fading channel. In the non-fading case, the interference with different duty cycles and the worst case were evaluated; while in the Rayleigh fading case, only continuous jamming was examined. Also, the effect of the noise-normalized receiver in a jammed environment and non-fading channel was evaluated.

B. FINDINGS

The results revealed some general trends for some receiver configurations, but for others, general trends were not evident. The key findings from this work are as follows:

- In general, the performance of communications improves as the code rates decreases and/or as the number of memory elements increases. The exception is for NCBFSK in a non-fading channel where the optimum code rate is $r = 1/2$.
- Generally, for a non-fading channel, the coding gain obtained by implementing SDD is higher than that obtained by implementing HDD for the same conditions when only AWGN is present.
- For a non-fading channel, the coding gain obtained with BPSK is higher than that obtained with NCBFSK for the same conditions.

- The general trend for both BPSK and NCBFSK combined with HDD in an AWGN plus pulse-noise interference, non-fading channel is that the difference between the worst case and $\rho = 1$ decreases, and the value of ρ leading to the worst case performance increases, approaching unity as the code rate decreases and/or as K increases.
- For both BPSK and NCBFSK combined with SDD in a non-fading channel but a jammed environment, the performance was obtained with two different receivers, the linear combining and the noise-normalized receiver. When using a linear combining receiver, the interference with small ρ is the most efficient regardless of the number of memory elements or code rate. However, when using a noise-normalized receiver, the worst performance was obtained for a duty cycle approaching unity. In other words, the use of a noise-normalized receiver negates the effect of the pulse-noise interference.

C. FUTURE WORK

Some areas are recommended for follow-on research. The performance of BPSK and NCBFSK schemes in a pulse-noise interference environment with Ricean fading could be analyzed in future work. The performance for both the noncoherent linear combining receiver and the noncoherent noise-normalized receiver using SDD for fading channels and jammed environments could be analyzed as well. Finally, in some cases for this research, we used approximate formulas. For follow-on research, it will be useful to derive exact formulas for those cases. For example, for NCBFSK combined with SDD, an exact result should be developed for the linear combining receiver in an pulse-noise interference environment and compared with the bound developed in this thesis in order to determine how tight this bound is.

LIST OF REFERENCES

1. Cosa, Irfan, "Performance of *IEEE 802.11a* Wireless LAN Standard over Frequency-Selective, Slowly Fading Nakagami Channels in a Pulsed Jamming Environment," Master's Thesis, Naval Postgraduate School, Monterey, California.
2. Tsoumanis, Andreas and Robertson, R. Clark, "Performance Analysis of the Effect of Pulse-Noise Interference on WLAN Signals Transmitted over a Nakagami Fading Channel," *Proc. of MILCOM 2004 IEEE* vol. 2, pp. 593-597, 31 October - 3 November 2004.
3. Kalogrias, Christos & Robertson, R. Clark, "Performance Analysis of the *IEEE 802.11a* WLAN Standard Optimum and Sub-Optimum Receiver in Frequency-Selective, Slowly Fading Nakagami Channels with AWGN and Pulse-Noise Interference," *Proc. of MILCOM 2004 IEEE* vol. 2, pp. 736-743, 31 October - 3 November 2004.
4. Spyrou, Evangelos, "Performance Analysis of Wireless LAN Signals Transmitted over a Ricean Fading Channel in a Pulsed-Noise Interference," Master's Thesis, Naval Postgraduate School, Monterey, California.
5. Lin, S., and Costello, D.J., *Error Control Coding: Fundamental and Applications*, 2nd edition, Prentice Hall, Upper Saddle River, New Jersey, 2004.
6. Sklar, B., *Digital Communications: Fundamental and Applications*, 2nd edition, Prentice Hall, Upper Saddle River, New Jersey, 2001.
7. Proakis, J.G., *Digital Communications*, 4th edition, McGraw Hill, New York, New York, 2001.
8. Robertson, R. Clark, and Beltz, Nathan, "Digital Communications over Fading Channels," Technical Report NPS-EC-05-002, November 15, 2004.
9. Robertson, R. Clark, Lecture Notes for EC4560 (Spread Spectrum Communications), Naval Postgraduate School, Monterey, California, 2005 (unpublished).
10. Robertson, R. Clark, Notes for EC4550 (Digital Communications), Naval Postgraduate School, Monterey, California, 2005 (unpublished).
11. Robertson, R. Clark, Notes for EC4580 (Coding and Information Theory), Naval Postgraduate School, Monterey, California, 2005 (unpublished).
12. Ziemer, R.E., and Peterson, R.L., *Introduction to Digital Communication*, 2nd edition, Prentice Hall, Upper Saddle River, New Jersey, 2001.

13. Proakis, J.G. and Manolakis, D.G., *Digital Signal Processing: Principles, Algorithms, and Applications*, 3rd edition, Prentice Hall, Upper Saddle River, New Jersey, 1996.
14. Wicker, S.B., *Error Control Systems for Digital Communication and Storage*. Prentice Hall, Upper Saddle River, New Jersey, 1995.
15. Leon-Garcia, A., *Probability and Random Processes for Electrical Engineering*, 2nd edition, Addison Wesley, Reading, Massachusetts, 1994.
16. Clark, G.C., Jr. and Cain, J.B., *Error-Correction Coding for Digital Communications*. Plenum Press, New York, New York, 1981.
17. May, T. Rohling, H., and Engels, V., "Performance Analysis of Viterbi Decoding for 64-DAPSK and 64-QAM Modulated OFDM Signals." *IEEE Transactions on Communications*, vol. 46, no. 2, pp. 182-190, February 1998.

INITIAL DISTRIBUTION LIST

1. Defense Technical Information Center
Ft. Belvoir, Virginia
2. Dudley Knox Library
Naval Postgraduate School
Monterey, California
3. Chairman, Code EC/KO
Department of Electrical and Computer Engineering
Naval Postgraduate School
Monterey, California
4. Professor R. Clark Robertson EC/Rc
Department of Electrical and Computer Engineering
Naval Postgraduate School
Monterey, California
5. Assistant Professor Frank Kragh EC/Kh
Department of Electrical and Computer Engineering
Naval Postgraduate School
Monterey, California
6. Shih, Wan-Chun
No. 190, Sanyuan 1st St., Tashi,
Taoyuan, Taiwan 335